MULTIPLE ISOFORMS OF ADAM12 IN BREAST CANCER: DIFFERENTIAL REGULATION OF EXPRESSION AND UNIQUE ROLES IN CANCER PROGRESSION

by

SARA DUHACHEK MUGGY

B.S., University of Nebraska-Lincoln, 2007
B.A., University of Nebraska-Lincoln, 2007

AN ABSTRACT OF A DISSERTATION

submitted in partial fulfillment of the requirements for the degree

DOCTOR OF PHILOSOPHY

Biochemistry and Molecular Biophysics Graduate Group

KANSAS STATE UNIVERSITY
Manhattan, Kansas

2014

Abstract

The ADAM (A Disintegrin and Metalloprotease) family of multi-domain proteins modulates a number of cellular signaling pathways in both normal and cancerous cells. ADAM12 has been shown to be a candidate cancer gene for breast cancer and its expression is up-regulated in breast tumors. The human *ADAM12* transcript is alternatively spliced. One of these splice variants encodes a transmembrane ADAM12 isoform, ADAM12-L, which has been demonstrated to release cell signaling molecules from the cell surface. Another variant encodes a secreted protease, ADAM12-S, which cleaves extracellular matrix proteins and other secreted proteins. Although these variants are expressed from the same promoter, their relative expression levels are highly discordant. Here, I demonstrate variant-specific regulation of *ADAM12* transcripts by microRNAs. Members of the microRNA-29 and microRNA-200 families target the unique 3'UTR of the *ADAM12-L* transcript and cause transcript degradation. Additionally, I show the presence of a novel *ADAM12* splicing event in which 9 additional nucleotides are inserted in the region encoding the autoinhibitory pro-domain. I demonstrate that this novel variant is expressed in breast epithelial cells and breast cancer cell lines. The resulting protein isoform does not undergo proteolytic processing to activate the protease. Additionally, trafficking of the novel isoform to the cell surface is impaired and this isoform is localized to the endoplasmic reticulum. Finally, I determined a role for ADAM12-L in the progression of triple negative breast cancers (TNBCs). These tumors are lacking expression of hormone receptors and the HER2 receptor. HER2 is a member of the epidermal growth factor receptor (EGFR) family and the loss of the HER2 receptor causes tumors to rely on EGFR for propagating pro-growth signals. I show here that, in TNBC tumors, ADAM12-L expression is strongly correlated with poor patient prognosis and increased activation of EGFR. These data suggest that in TNBCs, ADAM12-L enhances tumor growth via EGFR activation. Collectively, the data presented here demonstrate (a) transcript-specific regulation of *ADAM12* in breast cancer, (b) the existence of a novel splice variant and protein isoform with impaired cellular trafficking, and (c) an important role of the ADAM12-L isoform in EGFR activation in TNBC.

MULTIPLE ISOFORMS OF ADAM12 IN BREAST CANCER: DIFFERENTIAL REGULATION OF EXPRESSION AND UNIQUE ROLES IN CANCER PROGRESSION

by

SARA DUHACHEK MUGGY

B.S., University of Nebraska-Lincoln, 2007
B.A., University of Nebraska-Lincoln, 2007

A DISSERTATION

submitted in partial fulfillment of the requirements for the degree

DOCTOR OF PHILOSOPHY

Biochemistry and Molecular Biophysics Graduate Group

KANSAS STATE UNIVERSITY
Manhattan, Kansas

2014

Approved by:

Major Professor
Anna Zolkiewska

Copyright

Abstract

The ADAM (A Disintegrin and Metalloprotease) family of multi-domain proteins modulates a number of cellular signaling pathways in both normal and cancerous cells. ADAM12 has been shown to be a candidate cancer gene for breast cancer and its expression is up-regulated in breast tumors. The human *ADAM12* transcript is alternatively spliced. One of these splice variants encodes a transmembrane ADAM12 isoform, ADAM12-L, which has been demonstrated to release cell signaling molecules from the cell surface. Another variant encodes a secreted protease, ADAM12-S, which cleaves extracellular matrix proteins and other secreted proteins. Although these variants are expressed from the same promoter, their relative expression levels are highly discordant. Here, I demonstrate variant-specific regulation of *ADAM12* transcripts by microRNAs. Members of the microRNA-29 and microRNA-200 families target the unique 3'UTR of the *ADAM12-L* transcript and cause transcript degradation. Additionally, I show the presence of a novel *ADAM12* splicing event in which 9 additional nucleotides are inserted in the region encoding the autoinhibitory pro-domain. I demonstrate that this novel variant is expressed in breast epithelial cells and breast cancer cell lines. The resulting protein isoform does not undergo proteolytic processing to activate the protease. Additionally, trafficking of the novel isoform to the cell surface is impaired and this isoform is localized to the endoplasmic reticulum. Finally, I determined a role for ADAM12-L in the progression of triple negative breast cancers (TNBCs). These tumors are lacking expression of hormone receptors and the HER2 receptor. HER2 is a member of the epidermal growth factor receptor (EGFR) family and the loss of the HER2 receptor causes tumors to rely on EGFR for propagating pro-growth signals. I show here that, in TNBC tumors, ADAM12-L expression is strongly correlated with poor patient prognosis and increased activation of EGFR. These data suggest that in TNBCs, ADAM12-L enhances tumor growth via EGFR activation. Collectively, the data presented here demonstrate (a) transcript-specific regulation of *ADAM12* in breast cancer, (b) the existence of a novel splice variant and protein isoform with impaired cellular trafficking, and (c) an important role of the ADAM12-L isoform in EGFR activation in TNBC.

Table of Contents

List of Figures

List of Tables

List of Abbreviations

ADAM	a disintegrin and metalloprotease
ADAMTS	ADAM with thrombospondin motifs
ADC	antibody-drug conjugate
AEBSF	4-(2-Aminoethyl) benzenesulfonyl fluoride hydrochloride
AI	Aromatase Inhibitors
APC	allophycocyanin
AREG	amphiregulin
BRCA1/2	breast cancer susceptibility protein 1/2
BSA	bovine serum albumin
BTC	betacellulin
BTIC	breast tumor initiating cell
CI	confidence interval
CMV	cytomegalovirus
DAB	3,3'-Diaminobenzidine
DAPI	4',6-diamidino-2-phenylindole
DLL1	delta-like ligand 1
DMEM	Dulbecco’s modified Eagle medium
DMFS	distant metastasis free survival
DPBS	Dulbecco’s phosphate buffered saline
EDTA	Ethylenediaminetetraacetic acid
EEA1	early endosomal antigen 1
EGF	epidermal growth factor
EGFR	epidermal growth factor receptor
EMT	epithelial-mesenchymal transition
Endo H	endoglycosidase H
EnR	endoplasmic reticulum
EPGN	epigen
ER	estrogen receptor
ERAD	endoplasmic reticulum associated degradation

EREG	epiregulin
ESE	exonic splicing enhancer
ESR1	estrogen receptor gene
ESS	exonic splicing silencer
FBS	fetal bovine serum
FGFR2	fibroblast growth factor receptor 2
FITC	Fluorescein isothiocyanate
GEO	Gene Expression Omnibus
GLuc	*Gaussia* luciferase
HB-EGF	heparin binding epidermal growth factor
HEPES	4-(2-hydroxyethyl)-1-piperazineethanesulfonic acid
hnRNP	heterogeneous nuclear ribonucleoprotein
HR	hazard ratio
HoR	hormone receptor
IGF	insulin-like growth factor
IGFBP	IGF binding protein
IHC	immunohistochemistry
ILK	integrin-linked kinase
ISE	intronic splicing enhancer
ISS	intronic splicing silencer
KLF4	Krüppel-like factor 4
LGI1	Leucine-rich glioma inactivated protein 1
mAb	monoclonal antibody
MAPK	mitogen-associated protein kinase
MIND	mouse intraductal
miRNA	microRNA
MMP	matrix metalloprotease
mTOR	mammalian target of rapamycin
NF-κB	nuclear factor κB
NOD-SCID	non-obese diabetic severe combined immunodeficient (mouse strain)
NSG	NOD-SCID IL2 receptor γ knockout (mouse strain)

nt	nucleotide
PAGE	polyacrylamide gel electrophoresis
PARP	poly (ADP-ribose) polymerase
PGR	progesterone receptor gene
PI	propidium iodide
PI3K	phosphoinositide-3 kinase
PR	progesterone receptor
PyMT	polyoma virus middle T antigen
qRT-PCR	quantitative real time PCR
ROI	region of interest
SDS	sodium dodecyl sulfate
SEAP	secreted alkaline phosphatase
SEM	standard error of the mean
SERM	selective estrogen receptor modulator
SMI	small molecule inhibitor
SNP	single nucleotide polymorphism
SR	serine-arginine rich proteins
SRE	splicing regulatory elements
TACE	TNFα converting enzyme
TAE	Tris-Acetate-EDTA buffer
TCGA	The Cancer Genome Atlas
TGFα	transforming growth factor α
TGFβ	transforming growth factor β
TIMP	tissue inhibitor of metalloproteases
TNBC	triple negative breast cancer
TNFα	tissue necrosis factor α
Tris	2-Amino-2-hydroxymethyl-propane-1,3-diol
TSS	translation start site
UTR	untranslated region

Acknowledgements

I would first like to thank my mentor, Dr. Anna Zolkiewska, for her support, guidance, and training. She taught me how to read journal articles, how to culture cells, and, most importantly, how to approach problems scientifically. She answered countless questions and engaged in numerous theoretical discussions, sharing her knowledge, experience, and enthusiasm. Ultimately, she molded me into the researcher I am today.

I would also like to thank my committee members: Dr. Larry Davis, Dr. Annelise Nguyen, and Dr. Stella Lee. Their thoughtful questions and suggestions have been valuable. I thank Dr. Brian Lindshield for his willingness to serve as an external chair during my defense.

Additionally, I would also like to thank my current and former lab mates/colleagues: Dr. Hui Li, Yue Qi, Linda Alyaha, and Randi Wise. Hui was a constant source of information and training during my early years and was always willing to share her skills, passion and experience. Yue and I discussed many scientific theories and approaches, took classes together and, occasionally, ate dinner at our desks together. She is a valued friend and colleague. Linda and Randi extended patience and support as I wrote my dissertation.

Lastly, I thank my husband, Luke; throughout this entire process he was my rock, my tech support, and my cheerleader.

Dedication

I dedicate this work to my amazing family whose love and encouragement made this endeavor possible.

Chapter 1 - Literature Review

The ability to classify tumors into subtypes with similar characteristics, such as stage of disease, prognosis and susceptibility to certain treatments, is critical in order to provide the most effective therapy. In addition to determining the cell type in which the tumor originated, pathologists use a staging scale that incorporates information about tumor size, lymph node involvement and the presence of any metastatic lesions as well as a grading scheme that determines the degree of differentiation the cancer cells exhibit [1, 2]. This information has proven to be valuable in determining overall prognosis, as the tumors with lower stage and grade values, or smaller-sized and more differentiated tumors, tend to have a better overall prognosis [1, 2]. However, these metrics offer no information about aberrant metabolic pathways that are operating within the cancer cells that may be targetable for therapeutic intervention.

Clinical Subtypes of Breast Cancer

Additional analysis for the presence of certain important drivers of tumor growth is now done routinely at diagnosis. Breast cancer patient biopsies are tested using immunohistochemistry for 3 major proteins markers; the estrogen receptor (ER), progesterone receptor (PR) and the overexpression of the HER2 receptor, a member of the Epithelial Growth Factor Receptor family. Clinically, the tumors are categorized based on the presence or absence of each of these markers and the optimal course of treatment is determined, whether it will be targeted therapy, conventional chemotherapy or a combination of the two.

Hormone Receptor Positive Subtype

ER is encoded by the *ESR1* gene and generates the major estrogen receptor isoform, ERα. The receptor itself is a 67-kDa protein that, in response to estrogen binding, undergoes a conformational change, translocates to the nucleus and acts as a transcription factor [3–6]. One of the many proteins whose expression is activated by ER activity is PR [7]. PR is encoded by the *PGR* gene and the receptor works in a very similar manner to ER; in response to progesterone binding, the receptor changes conformation and gains transcription factor activity [8]. The ER and PR hormone receptors are so strongly linked that only 5% of PR+ tumors are ER-, and therefore these two markers are often listed together as hormone receptor positive or

HoR+ [4]. Typically, tumors in this class are lacking overexpression of the HER2 receptor, as those tumors which are positive for all 3 major immunohistochemical markers are usually classified as HER2+ rather than HoR+ [9]. HoR+ tumors are the most common type of breast carcinomas and represent ~60-70% of all cases [10].

In general, HoR+ tumors are poorly proliferative and usually have good prognoses, especially when both receptors are present [4, 11]. However, there is some variability within the HoR+ group and a smaller subset has a higher proliferation index [4, 10, 11]. Interestingly, despite the overall good prognosis for patients, HoR+ tumors respond poorly to conventional cytotoxic chemotherapy [12–14]. The good prognosis is due to the widespread use of anti-estrogen therapies alone or in addition to chemotherapy. There are 3 major types of anti-estrogens: selective estrogen receptor modulators (SERMs), aromatase inhibitors (AIs) and fulvestrant [6, 14]. Each of these compounds works to prevent the action of the ER, but by different mechanisms. SERMs, like tamoxifen, work by binding to the ER in the ligand binding site and causing a conformational change in the protein; however, the resulting structure is an inhibited receptor that lacks transcription factor activity [3]. Fulvestrant also binds directly to the ER but, in this case, binding causes degradation of the protein [4]. AIs inhibit the enzymes responsible for estrogen production, thereby limiting ER activity by reducing ligand concentrations [3]. Most HoR+ tumors are treated only with anti-estrogen therapy, however, if the tumor is advanced or assessed as being highly proliferative, chemotherapy may be added to the treatment plan [15]. Overall, the anti-estrogen therapies are quite effective and have greatly improved prognosis for patients with HoR+ tumors.

HER2-Amplified (HER2+) Subtype

HER2-amplified or HER2+ tumors are tumors in which the HER2 protein is overexpressed. Approximately 20% of all patients present with these types of tumors [16]. HER2 is the product of the *ERBB2* gene which is found on chromosome 17. Overexpression usually occurs due to amplification of this region of the chromosome and can be identified at the protein level by immunohistochemistry or at the DNA level by *in situ* hybridization. Additionally, overexpression can occur without gene duplication by aberrant transcriptional up-regulation and therefore can only be detected by the immunohistochemical method [16].

HER2 is a member of the Epidermal Growth Factor Receptor (EGFR) family. The EGFR family consists of 4 receptor tyrosine kinases, EGFR/HER1, HER2, HER3 and HER4, which are activated by Epidermal Growth Factor (EGF) and EGF-like ligands. The ligands are synthesized as transmembrane proteins and activated via proteolytic cleavage; this cleavage event is a source of pathway regulation [17]. Upon binding of the ligand to the receptor, the receptor forms a homo- or heterodimer with other HER family members and the cytosolic kinase domains are activated. The kinase domains perform multiple phosphorylation events on the cytoplasmic tails which creates binding sites for proteins like Ras, mitogen-activated protein kinases (MAPK), Src tyrosine kinase, and phosphoinositide-3 kinase (PI3K) [18]. The activation of these signaling proteins by the EGFR family of receptors promotes cell growth. HER2 is the only member of this family that does not require ligand binding for activation and therefore a major regulatory step is lost. In tumors where HER2 is overexpressed, it dimerizes readily which results in strong, sustained activation of the pro-growth signaling pathways and little negative regulation of this pathway activation [18, 19].

Not surprisingly, HER2+ tumors are highly proliferative. Before the advent of anti-HER2 therapy, patients with HER2+ tumors had higher rates of recurrence and poorer overall survival [16, 19, 20]. These patients are now typically treated with trastuzumab, a monoclonal antibody specific for the extracellular portion of HER2, and a cytotoxic chemotherapy which has dramatically improved survival for these patients [15, 16, 20–22]. Since the success of trastuzumab, other anti-HER2 therapies have been developed including the small molecule inhibitor lapatinib [16, 20]. Lapatinib blocks the tyrosine kinase activity of both EGFR and HER2 and has been shown to improve the response to chemotherapy in patients whose tumors progressed after trastuzumab treatment [20]. Additional anti-HER2 therapies are now available including pertuzumab, which is an antibody that inhibits HER2 receptor dimerization, and other small molecule inhibitors of the tyrosine kinase domain [20]. The success of targeting the HER2 receptor has yielded a variety of treatment options and has improved overall prognosis for patients with HER2+ tumors.

Triple Negative Subtype

Triple negative breast cancers (TNBC) are defined as tumors that lack expression of ER and PR and do not overexpress HER2. Approximately 10-20% of breast tumors are triple

negative [23]. Typically, these tumors are poorly differentiated and patients with TNBCs have a poor 5 year prognosis compared to patients with HoR+ tumors. However, TNBC patients are less likely to recur more than 5 years post-diagnosis [23, 24]. These tumors are found disproportionately more often in younger women, women with oncogenic mutations of breast cancer susceptibility proteins 1 and 2, *BRCA1* or *BRCA2,* and women of African or Hispanic descent [13, 23, 24].

TNBCs are clearly unable to be treated with the targeted anti-estrogen or anti-HER2 therapies that have been so successful in improving survival for patients with HoR+ and HER2+ tumors. As a result, the only available options for these patients are radiotherapy and systemic cytotoxic chemotherapy [15, 25]. Interestingly, triple negative tumors are much more responsive to chemotherapy than HoR+ and HER2+ tumors, 85% of TNBC patients experience partial or complete response to chemotherapy, meaning that the tumor is decreased in size or eliminated by chemotherapy [13]. In comparison, only 47% of HoR+ patients and 64% of HER2+ patients show the same response. Despite early success of treatment, TNBCs are more likely to recur than HoR+ cancers and are much more comparable to HER2+ tumors in this respect [13]. TNBCs preferentially metastasize to the lungs and the brain which diverges from the typical pattern of bone and liver metastasis in non-TNBC patients [23]. There is a need for more effective, targeted therapies for TNBCs. Researchers have been working to identify required genes in these tumors that may make effective drug targets, but thus far there has not been enough evidence of additional benefit to patients and the recommended standard treatment is still traditional chemotherapy only [6, 15].

Molecular Subtypes of Breast Cancer

In response to this need for more druggable targets and with the development of rapid, inexpensive methods to survey global gene expression, researchers began studying gene expression differences between breast tumors. Early studies utilized microarrays to identify transcriptomic differences and, more recently, next generation RNA sequencing has been used [26, 27]. The results of these investigations revealed 5 unique subtypes of breast cancer that vary in incidence, prognosis, and treatment [27–29]. These studies use the expression of ~1900 "intrinsic" genes, which are defined as genes whose expression differs substantially between tumors but rarely change in duplicate samples from the same tumor or its metastases [27, 30, 31].

It should be noted that these classifications are less commonly used clinically due to the cost of analysis, the requirement for larger amounts of raw tumor tissue and the complexity of the post-analysis computations [32]. However, a subset of 50 genes, known as PAM50, was shown to adequately classify tumors into 4 of the 5 known subtypes as well as offer value in determining patient prognosis without therapy and response to therapy [31, 33].

Luminal A and Luminal B Tumors

The luminal subtypes were identified early due to the high prevalence of these tumors; they represent an estimated 60-70% of new diagnoses [10, 27]. Both subtypes express the hormone receptors, ER and PR, and luminal markers such as cytokeratins -8 and -18 [10, 27, 29].

Luminal A tumors express higher levels of transcription factors such as FOXA1 and GATA3 than luminal B tumors [10, 27, 30]. These transcription factors, in combination with the hormone receptors, drive expression of luminal genes and are responsible for the maintenance of the luminal phenotype. In fact, expression of FOXA1 and GATA3 correlate strongly with ER expression [34]. It has also been suggested that FOXA1 is a marker of improved prognosis because this transcription factor, in combination with BRCA1, activates expression of $p27^{Kip1}$, the cyclin-dependent kinase inhibitor that prevents the cell from entering the cell cycle [35]. Additionally, FOXA1 has been shown to activate transcription of E-cadherin, an important protein involved in epithelial cell-cell interactions [36]. Down-regulation of E-cadherin induces cells to become more migratory and invasive [37], therefore maintenance of E-cadherin expression in the breast tumor improves the patient's overall prognosis. It has been shown that GATA3 expression is also correlated with more differentiated, less metastatic tumors [34, 38]. Additionally, GATA3 correlates with ER expression and is associated with longer survival; however specific molecular mechanisms that explain this activity are only beginning to be elucidated. One such mechanism suggests that GATA3 induces the expression of microRNA-29b, which is responsible for down-regulating numerous proteins involved in angiogenesis, remodeling of surrounding collagens, and metastasis [38].

Overall, luminal A tumors are less proliferative and less invasive, therefore this subtype of tumors has the best prognosis of the major subtypes, and the course of treatment is more clearly defined. Similarly to HoR+ tumors determined by immunohistochemistry, luminal A tumors are often treated with SERMs or AIs [15]. These treatments provide the best rate of

success for luminal A tumors, since only 7% of these tumors respond well to cytotoxic chemotherapy [10]. However, current convention states that patients with luminal A tumor should be treated with chemotherapy if the disease is advanced or present in multiple lymph nodes at the time of diagnosis [15].

Luminal B tumors express many of the luminal genes including ER and PR but the level of expression of these receptors is typically lower than in luminal A tumors [39]. Additionally, expression of FOXA1 and GATA3 is lower in luminal B tumors and the beneficial effects of these genes are absent [10, 40]. The major difference between the luminal A and B subtypes is that luminal B tumors have much higher expression of proliferation genes [10, 28, 39]. Luminal B tumors are often being assigned by a more clinically accessible, surrogate assay involving immunohistochemistry, where they are HoR+, HER2- and scored as highly proliferative by the Ki67 marker [41]. Patients with luminal B tumors have less favorable prognoses than patients with luminal A tumors. Luminal B tumors are more likely to recur and, therefore, more aggressive therapy is recommended. These tumors are often treated with AIs in addition to conventional chemotherapies [10, 15]. In general, luminal tumors do not respond well to chemotherapy, however, luminal B tumors respond better than luminal A tumors, with ~17% of patients exhibiting a favorable response [10].

HER2-Enriched Tumors

Similar to HER2+ tumors identified by immunohistochemistry, the tumors in this subtype are identified by strong expression of the HER2 receptor and/or several co-regulated genes [27]. HER2-enriched tumors exhibit high levels of proliferation markers and are characterized by having low expression of luminal markers and virtually no expression of basal markers [42]. These tumors represent ~10-20% of all breast carcinomas and usually have poor patient prognosis; however, the development of anti-HER2 therapy has greatly improved the treatment [10]. Patients with HER2-enriched tumors also have a higher risk of recurrence and breast cancer-related death than those with luminal A tumors [43]. As with HER2+ cancers, HER2-enriched tumors are treated with trastuzumab, the anti-HER2 monoclonal antibody, and concurrent chemotherapy [15]. Interestingly, patients with HER2-enriched tumors respond better to anti-HER2 therapy than patients with clinically HER2+ tumors [44], presumably due to the dependence on HER2-related pathways observed in these tumors. Additionally, HER2-

enriched tumors respond quite well to chemotherapy, with 43% of patients exhibiting pathologic complete response, comparing to 7% and 17% of luminal A and luminal B tumors, respectively [10].

HER2-enriched tumors do not perfectly align with the HER2+ tumors, in fact almost one third of the HER2-enriched tumors are classified as HER2- by immunohistochemistry [42]. A recent analysis of over 2000 tumor samples showed that among clinically HER2+ tumors, only 47% have the HER2-enriched intrinsic subtype [44]. This is especially important since the tumors that are ER-/HER2+ by immunohistochemistry are often roughly categorized as HER2-enriched [42]. It is also worth noting that HER2 overexpression is observed in all major molecular subtypes of breast cancer [45], therefore identifying tumors of this molecular subtype is more complicated than the name suggests.

HER2-enriched tumors typically exhibit overexpression of HER2, due to gene amplification, and many of the neighboring genes are also markers of this amplification event. Since the HER2-enriched subtype is determined by the high expression of multiple genes related to the HER2 signaling pathway rather than just the overexpression of HER2, more information about the metabolic demands of these tumors can be extracted than from HER2+ tumors alone. The 17q12-21 amplicon contains genes encoding HER2, STARD3, and the SH2 adapter protein GRB7 [46–48]. Many of these co-amplified genes are thought to be involved in tumor progression and even in acquired resistance to anti-HER2 therapy [49]. The non-oncogene addiction theory suggests that tumors become dependent on the actions of certain gene products that are often co-regulated with HER2 which helps explain the discrepancies observed between the HER2+ tumors and the HER2-enriched tumors.

Basal Tumors

Basal tumors represent approximately 10-20% of all invasive breast carcinomas and are characterized by expression of so-called “basal” genes [10, 27, 50]. These tumors have high expression of basal cytokeratins like cytokeratins-5, -6 and -17, while having low expression of ER, GATA3, HER2 and the luminal cytokeratins -8 and -18 [10, 42]. Additionally, basal tumors have increased expression of P-cadherin, CD44 and EGFR [10]. P-cadherin has a role in normal mammary duct formation, however, its expression is restricted to the terminal end bud and in the myoepithelium of the mature breast [51]. In breast tumors, expression of P-cadherin has been

associated with poorer prognosis in patients and increased cell migration *in vitro* [51]. CD44 is a hyaluronan receptor, however, it also interacts with a variety of extracellular matrix components such as laminin, collagens, and fibronectin [52]. CD44 has been shown to be strongly relevant in normal breast and breast cancer biology. Breast cancer cells with high CD44 expression are enriched in mammary stem cells and initiate tumors more readily in mouse xenograft experiments [53, 54]. EGFR is related to HER2, however, this receptor requires ligand to initiate pro-growth signals, which means that activation of this pathway is regulated by the availability of ligand. In addition to these gene expression alterations, basal tumors also have a high rate of mutation of the p53 oncogene and patients with germ-line mutations of *BRCA1* and *BRCA2* typically develop tumors that are basal in nature [10].

Basal tumors most strongly resemble the triple-negative tumors identified by clinical subtyping, in fact, ~80% of basal tumors are triple-negative [10, 15]. Accordingly, patients with these tumors also have poor prognoses. One study showed that the risk of death due to breast cancer was 6-8 times greater for basal tumors than luminal A tumors in the first 5 years after diagnosis [43]. The same study showed that the risk of relapse is significantly greater for patients with basal tumors than those with luminal A tumors. Basal tumors express high levels of proliferation markers and are quite aggressive [10]. At the time of diagnosis, these tumors are more likely to have larger tumor volumes, lymph node involvement and higher histologic grade, or less cellular differentiation [10]. The current treatment recommendations are surgery and chemotherapy [15]. These tumors respond better to chemotherapy than the luminal tumors, in fact, basal tumors show the best response to chemotherapy of all subtypes [10, 28]. However, like TNBCs, these tumors have a high rate of relapse in the first 5 years [10, 42]. The lack of any therapies beyond conventional chemotherapy presents a real challenge to the treatment of these patients and there is a strong need to develop more targeted therapies for basal tumors.

Claudin-low Tumors

Claudin-low tumors represent ~10% of all breast cancers [10]. This subtype was identified more recently [29] and it cannot be recognized using the common PAM50 test [28]. Claudin-low tumors cluster near the basal subtype, because both subtypes express low levels of luminal genes and HER2-related genes [10, 28, 29]. Similar to basal tumors, claudin-low tumors are usually triple negative [42]. As the name suggests, these tumors have strongly down-

regulated genes involved in cell-cell contacts, like the claudins, occludin and E-cadherin [10, 28]. Furthermore, these tumors have high expression of immune response genes, which may be accounted for by the high level of lymphoid infiltration [28]. Claudin-low tumors are also very undifferentiated and therefore express many genes associated with mammary stem cells [28, 55]. These tumors have been shown to express both markers of epithelial cells, like the breast tissue in which they originate, and markers of mesenchymal cells [28]. The percentage of cells that are positive for both sets of markers is significantly higher in claudin-low tumors than in luminal subtypes.

Patients with claudin-low tumors have poor prognoses compared to luminal A tumors and comparable to patients with basal, luminal B or HER2-enriched tumors [42]. Interestingly, claudin-low tumors express lower amounts of proliferation genes than basal, HER2-enriched and luminal B tumors [28]. Claudin-low tumors are moderately responsive to chemotherapy, but the response rate is lower than for basal tumors, 39% versus 73%, presumably because many cytotoxic agents target replicating cells [28, 42]. Interestingly, analysis of other subtypes of tumors prior to therapy and the residual tumors after treatment with hormone or chemotherapy has shown that claudin-low features are increased during treatment [56]. There is less clinical information for this subtype, as it is new, rarer, and is usually mis-diagnosed as basal by the PAM50 test or the use of surrogate immunohistochemical tests. However, there is interest in studying claudin-low tumors because these tumors are particularly enriched in breast tumor initiating cells (BTICs) [56]. BTICs are proposed to be responsible for resistance to therapy and breast tumor recurrence [57].

The ADAM Metalloproteases

A Disintegin And Metalloproteases (ADAMs) are multi-domain proteins that are widely observed in eukaryotic organisms [58]. Canonical ADAMs contain a signal sequence, pro-domain, metalloprotease domain, disintegrin domain, cysteine-rich region, EGF-like motif, a transmembrane helix, and a cytoplasmic domain (Figure 1.1). The pro-domain exerts an autoinhibitory effect over the catalytic metalloprotease domain [59, 60]. The metalloprotease domain of ADAMs can be either active or inactive and this is determined by the presence of the HEXGHXXGXXHD motif, in which the histidine residues coordinate a zinc ion and the glutamate is the catalytic residue [59]. The disintegrin and cysteine-rich domains are involved in

protein-protein interactions with substrate molecules and in cell adhesion [59, 61]. The role of the EGF-like region is less clear and it may be involved in oligomerization of ADAMs [62]. The cytoplasmic domains of ADAMs contain interaction motifs for several cellular proteins. These interactions have been shown to activate signaling pathways, especially through activation of Src, and even affect localization of the ADAM itself [63–68].

Since ADAMs are integral membrane proteins, they are synthesized and trafficked via the cellular secretory pathway. The signal sequence is removed in the endoplasmic reticulum and the protein is folded and glycosylated in this compartment before being trafficked to the Golgi apparatus [58, 69]. Once inside the Golgi, the pro-domain is proteolytically cleaved by pro-protein convertases, like furin or similar enzymes, at the R-X-K/R-R consensus site between the pro-domain and metalloprotease domain [58, 60, 69]. Additionally, in the Golgi apparatus the polysaccharides are modified to their mature form [70]. From the Golgi, the mature, active ADAM is trafficked to the cell surface.

Patterns of Expression of ADAMs

In vertebrates, ADAMs show variable patterns of expression and a number of ADAMs are expressed only in select tissues. A large number of ADAMs are expressed exclusively in the testes andothers are found predominantly in hematopoetic cells and tissues. However, the majority of ADAMs are expressed in a more global manner. The categorization of the 20 human ADAMs can be seen in Figure 1.2. The expression pattern of each ADAM provides a clue toward the specific biological role(s) for each metalloprotease.

Testis-specific ADAMs

The first two members of the ADAM family, fertilin α and fertilin β (later re-named ADAM1 and ADAM2), were identified from guinea pig testes and were shown to be essential in sperm-egg interaction [71]. Interestingly, although the ADAM family is highly conserved in mammals, the major differences observed between the mouse and human genomes is in the presence and copy number of testis-specific ADAMs [72]. One half of all murine ADAMs and one third of all human ADAMs are testis-specific [58, 72]. Human ADAM2, ADAM18, ADAM20, ADAM21, ADAM29, and ADAM30 are expressed in spermatogenic cells and/or mature sperm cells while ADAM7 is expressed in the epididymus and on mature sperm cells [72]. Not all of the testis-specific ADAMs are proteolytically active, only ADAM20, ADAM21,

and ADAM30 contain the HEXGHXXGXXHD motif while ADAM2, ADAM7, ADAM18, and ADAM29 do not have this motif and are therefore catalytically inactive [58]. Thus far, the best evidence for the function of testicular ADAMs has come from knockout mice studies, which have shown that expression of these ADAMs is required for male fertility [58, 72, 73]. The sperm of knockout mice exhibit problems with egg adhesion and/or migration into the oviduct, resulting in male infertility [58, 72]. The ADAMs on the surface of the sperm cells have been shown to form heterodimers and heterotrimers that are involved in protein stabilization, cleavage of the extracellular matrix surrounding the egg, and interaction with integrins on the surface of the ovum [72]. However, less is known about the exact physiological roles for the individual human testicular ADAMs due to the poor evolutionary conservation of this subgroup of ADAMs.

Hematopoetic ADAMs

This is a small subgroup of ADAMs, comprised only of ADAM8 and ADAM28, both of which are catalytically active metalloproteases [58]. Interestingly, ADAM8 and ADAM28 are the only two ADAMs capable of auto-activation, meaning that their own metalloprotease activity is responsible for cleavage of the pro-domain and they do not require pro-protein convertases [74, 75]. The expression of ADAM8 occurs primarily in myeloid and lymphoid cells of the blood and bone marrow and other lymphatic tissues, but it is also observed in osteoclasts and cells of the central nervous system [76, 77]. ADAM8 is thought to be involved in inflammatory processes due to its transcriptional induction by multiple inflammatory stimuli such as lipopolysaccharide, tumor necrosis factor α, interferon γ, and certain prostaglandins [78]. ADAM8 is also up-regulated in asthma, Parkinson's Disease, rheumatoid arthritis and cancers of the brain, lung, pancreas, prostate, and breast [79–82], indicating roles in numerous disease processes. However, the knockout mouse revealed that the presence of ADAM8 is not necessary for normal murine growth and development [83].

Human ADAM28 protein is found primarily in lymphocytes, monocytes, and neutraphils but it is also expressed in the lymph nodes, intestines, spleen, and the epididymus [73, 84, 85]. In rodents, the epididymal expression is much higher than expression in other tissues and for this reason, ADAM28 is often included in the testicular ADAM subgroup. However, unlike the other testicular ADAMs, the expression of ADAM28 is not restricted to the testes. ADAM28 was

shown to be highly expressed in lymphocytes and is thought to mediate lymphocyte-leukocyte interactions through its interaction with the α4β1-integrin heterodimer [86, 87].

Globally Expressed ADAMs

The globally expressed group of ADAMs is the largest and most diverse group. It includes most of the catalytically active ADAMs: ADAM9, ADAM10, ADAM12, ADAM15, ADAM17, ADAM19, and ADAM33. It also includes ADAM11, ADAM22, ADAM23, and ADAM32, which are all catalytically inactive. The two most heavily studied ADAMs, ADAM10 and ADAM17, belong to this group.

Both ADAM10 and ADAM17 are globally expressed and are critically important in development, as evidenced by embryonic lethality of the knockout mice [88, 89]. ADAM10 is expressed in a variety of tissues including bone, brain, and hematological cells [58, 90]. The knockout mouse model exhibited early lethality due to severe defects in cardiovascular development [88]. ADAM10 is very widely studied due to the large number of known substrates and the importance of these substrates in pathologies. For example, a substantial amount of data supports a role for ADAM10 in prevention of amyloid β formation and Alzheimer's Disease [91]. ADAM17 is widely expressed and its pattern of expression varies from fetal development to the adult organism [92]. In adults, it is expressed in cardiac and skeletal muscles as well as pancreas, spleen, small intestine, ovaries, testes, and prostate; however, in fetal development, ADAM17 is predominantly expressed in the brain, lungs, liver and kidneys. ADAM17 is best known for cleaving tumor necrosis factor α (TNFα), and is often called TNFα converting enzyme, or TACE, instead of the ADAM nomenclature. Similar to ADAM10, ADAM17 is very heavily studied and has a large list of known substrates. As an interesting note, the embryonic lethality observed in early mouse studies was a result of metalloprotease deletion by mutating the zinc binding sites, indicating that the major functions of ADAM17 are due to its metalloprotease activity [89].

ADAM9 and ADAM12 are both predominantly expressed in adult stem cells, mesenchymal stem cells, and placental tissues [58]. ADAM9 knockout mice exhibited no major defects in growth and development [93], whereas ADAM12 knockout mice exhibited 30% embryonic lethality and some brown fat abnormalities [58]. ADAM15 and ADAM19 are expressed rather widely, but they also show strong expression in mesenchymal stem cells. ADAM15 knockout mice exhibited no gross differences from their wild type littermates in

behavior, growth, and development [94]. However, despite normal vascular development, the knockout mice showed decreased ability to form vascular systems in models of retinal pathology and tumor development, suggesting a possible role for ADAM15 in pathology-specific angiogenesis. ADAM19 knockout mice exhibited a strong perinatal lethality due to cardiovascular defects [58, 95] All four of these ADAMs have been implicated in disease processes, particularly in cancers of the brain, breast, lung, stomach, and kidney [96].

ADAM33 is strongly expressed in the urinary, respiratory, gastrointestinal, and endocrine systems [58]. However, despite this strong expression in a variety of important tissues, the ADAM33 knockout mouse showed no phenotype [58]. Recently, polymorphisms in the *ADAM33* gene have been shown to be good markers for asthma [97, 98]. The catalytically inactive ADAM, ADAM11, is primarily expressed in the nervous system, erythrocytes, and the liver. The ADAM11 knockout mice exhibit alterations in pain response and spatial learning [99, 100]. ADAM22 and ADAM23 are also predominantly expressed in the nervous system. The ADAM22 knockout mouse showed signs of severe ataxia and all mice died due to convulsions within the first few weeks of life [101]. ADAM11, ADAM22 and ADAM23 have all been shown to interact with the neuronal protein leucine-rich glioma-inactivated protein 1, LGI1, which is involved in expression of neurotransmitter receptors and in regulating the voltage-gated channels in neurons, and the LGI1-ADAM interactions seem to be critical to these activities [102]. ADAM32 is highly expressed blood lymphoid cells and little else is known about its role in humans or in mice.

Activity of the ADAM Metalloproteases

The expression patterns for each ADAM hinted at possible roles for each protease and many of the early studies of ADAMs began by analyzing roles in the area of maximal expression or in the areas most affected by gene deletion studies. More recently, researchers have begun to identify novel roles for these proteins in disease conditions due to the abundance of transcriptomic data that is publicly available through databases like the Gene Expression Omnibus and The Cancer Genome Atlas. Additionally, proteomic analyses of the degradomes of each protease are providing a wealth of information about the potential substrates of the catalytically active ADAMs. It is important to note that due to the multi-domain structure of the ADAMs, the activity may be related to protein-protein interactions mediated by the disintegrin,

cysteine-rich, EGF-like, or cytoplasmic domains or through proteolytic activity in the cases of active metalloproteases, or some combination of the two. Here, I will focus on the proteolytic functions of the ADAMs.

Shedding Membrane Proteins

Much of the known information about the function of ADAMs relates to their activity as sheddases. A sheddase is a protein responsible for cleaving membrane proteins near the membrane bilayer to "shed" an ectodomain into the surrounding space [69]. These shed proteins may be transmembrane precursors to soluble growth factors, membrane-anchored ligands, or membrane receptors. The ultimate effect of shedding is the activation or deactivation of the signaling pathway downstream of the ADAM activity. ADAMs, in particular, have been linked to shedding molecules involved in the EGFR, TNFα, and Notch signaling pathways.

Notch Signaling

The Notch signaling pathway is an evolutionarily conserved pathway that is critically important in regulating cell proliferation, differentiation and death [103, 104]. Notch ligands are integral membrane proteins that interact in a *trans* manner with Notch receptors on a neighboring cell (Figure 1.3B). In response to this interaction, the Notch receptor is cleaved near the membrane by ADAM10. After this cleavage event, γ-secretase cleaves the receptor at an intramembrane site, thereby releasing the intracellular domain into the cytosol. This domain translocates to the nucleus where it acts as a transcription factor [103–105]. ADAM10 is critical to the activation of the Notch pathway, and Notch signaling is necessary for stem cell maintenance as well as normal organismal growth and development. Consistently, the loss of Notch receptors in mice phenocopies the ADAM10 knockout indicating that the most important role for ADAM10 in fetal development is related to Notch activation [58]. Alternatively, ADAM17 has also been shown to be capable of cleaving the Notch receptors [106]. The difference between the phenotypes of the knockout mice suggests that ADAM10 and not ADAM17 is the primary protease responsible for Notch activation during embryonic development. However, ADAM17 cleavage of Notch may be specific to certain cell types, developmental stages or even disease processes [91]. In addition to cleavage of the Notch receptors, the ligands themselves are cleaved as well, and ligand cleavage inhibits Notch signaling. Several ADAMs have been shown to cleave the ligand Delta-like 1 (DLL1),

including ADAM9, ADAM10, ADAM12 and ADAM17. Due to the requirement for proteolysis in Notch activation, the ADAMs are critically important in the propagation of signals through the Notch pathway.

EGFR Signaling

The ADAMs are also vital to signaling through the EGFR pathway. As previously mentioned, the EGFR pathway involves four receptor tyrosine kinases, EGFR/HER1, HER2, HER3 and HER4 and a number of ligands. HER2 is constitutively active and has no known ligand-binding ability, whereas EGFR, HER3 and HER4 all bind EGF-like ligands. However, HER3 is kinase-defective and must be phosphorylated by dimerization with another HER family receptor. HER4 seems to be unique among the HER family of receptors in that activated HER4 has been shown to reduce cell proliferation and promote apoptosis in breast cancer cells [107]. Therefore, in breast cancer studies, EGFR and HER2 are the receptors that most critically mediate EGFR signaling and the downstream pro-growth signals.

There are eleven EGFR ligands; amphiregulin, epiregulin, epigen, betacellulin, EGF, heparin-binding EGF, transforming growth factor α, and neureglins 1-4 [17]. Each of these ligands is synthesized as membrane-anchored precursor and must be shed by an ADAM in order to be functional (Figure 1.3A). A large number of ADAMs have been shown to cleave the EGF ligands and a degree of redundancy exists, with the same ligand being cleaved by multiple ADAMs [17, 108]. Cleavage of EGF ligands can be performed by ADAM9, ADAM10, ADAM12, ADAM15, ADAM17, or ADAM19 [17]. Each ADAM shows some selectivity and will only shed a subset of EGF ligands [109]. Once the ligand is cleaved, the soluble ectodomain is free to interact with the ligand-dependent members of the HER family of receptors and initiate pro-survival signals within the receiving cell.

TNFα Signaling

Similar to EGF ligands, TNFα is synthesized as a transmembrane precurser and must be activated by being released from the cell surface [58]. TNFα is a pro-inflammatory cytokine that can induce cell survival and expression of other pro-inflammatory signals or induce apoptosis in the receiving cell [110]. TNFα shedding is predominantly mediated by ADAM17 and this ADAM is central to regulating inflammation through its role in TNFα activation. As a result,

ADAM17 is being investigated as a possible therapeutic in a number of inflammatory diseases [111].

Other Proteolytic Activities

In addition to shedding members of the aforementioned signaling pathways, ADAMs are known to cleave a number of adhesion and cell-cell interacting proteins like L-selectin, N-cadherin, E-cadherin, VE-cadherin, L1 cell adhesion molecule (L1-CAM), V-CAM-1, and N-CAM [58, 111]. These cleavage activities reduce cell-cell contacts and have been hypothesized to play vital roles in cancer metastasis [112]. In addition to decreasing cell-cell interactions, cleavage of E-cadherin stimulates proliferation in some cancer cells [113]. Furthermore, the cleavage of cell-cell contact proteins specific to endothelial cells enables migratory cells to enter or exit a blood vessel, which are required steps in tumor metastasis [112].

Regulation of the Catalytic Activity

The proteolytic activity of ADAMs is responsible for activating numerous signaling pathways, so it follows that the activity of the metalloprotease domain is regulated. The primary method of protease activity regulation is via interactions with the pro-domain. The pro-domain blocks the active site through a "cysteine switch" mechanism, where a conserved cysteine residue in the pro-domain interacts with the zinc ion bound to the metalloprotease domain and as a result, excludes water from the active site [60]. In this state, the metalloprotease is inactive. Upon removal of the pro-domain, the active site is open and functional. Pro-domain removal occurs in the Golgi apparatus and the ADAM is considered active once this has occurred. ADAM activity can also be modulated through interactions with a small class of proteins known as the tissue inhibitors of metalloproteases, TIMPs [58]. There are four TIMPs in the human genome, TIMP1-4. These inhibitors have been shown to inhibit the activity of many, but not all, ADAMs, with TIMP3 showing the broadest range of the inhibitory activity [58, 96]. The TIMPs bind non-covalently in a 1:1 stoichiometry to the ADAM protease [96]. Finally, re-localization of the ADAM itself is an efficient method of modulating its activity [108]. For example, ADAM17 is often located in vesicles or in the Golgi apparatus until a signaling event (in this case, activation of protein kinase C) induces its transport to the cell surface. Similarly, ADAM10 is re-localized to the surface in response to calcium ion influx [96, 108].

The ADAMs in Breast Cancer

Many of the activities of ADAM proteases involve activating pro-survival or pro-growth signaling pathways, which are important for normal growth and development. However, aberrant activation of these same pathways can prove beneficial to cancer cells. Many of the pathways discussed here are being actively studied as potential targets for anti-tumor therapies. Consistently, many ADAMs are up-regulated in tumors when compared to normal tissues. Analysis of ADAM expression across the molecular subtypes of breast cancer revealed that ADAMs are most highly expressed in claudin-low tumors compared to the other molecular subtypes (Figure 1.4), and may therefore represent effective druggable targets in the treatment of these therapy-resistant tumors. ADAM8, ADAM12, ADAM15 and ADAM17 have been shown to be involved in breast tumor growth and progression [82, 114–120].

ADAM8

ADAM8 was previously demonstrated to have a role in both brain and lung cancers and its level of expression was indicative of overall survival [121, 122]. Recently, a new study revealed strong up-regulation of ADAM8 in breast carcinomas and a poorer prognosis for patients with high ADAM8 expression [82]. Knockdown of ADAM8 inhibited cell migration and invasion *in vitro* and prevented tumor growth in an orthotopic xenograft model. Additionally, mice implanted with ADAM8-depleted cells exhibited fewer metastatic lesions and fewer circulating tumor cells, consistent with the *in vitro* decrease in cell invasion and migration. Mechanistically, ADAM8 is up-regulated by the hypoxic conditions in early tumor development and functions to ameliorate the low oxygen environment by inducing neovascularization. ADAM8 knockdown cells shed fewer pro-angiogenic factors into the cell culture media and produced fewer tumors with decreased blood vessel density upon transplantation. Additionally, these cells had a decreased ability to adhere to endothelial cells and transmigrate through the endothelial layer, which supports the observation of reduced metastasis of tumors formed by these cells. An antibody raised against the ADAM8 metalloprotease and disintegrin domains mimicked the effect of ADAM8 knockout, causing reduced tumor volume, decreased vascularization and less metastasis in mice. This report provides strong evidence of a pro-tumorigenic role for ADAM8 in breast cancer and suggests a potential therapy for patients with tumors that highly express ADAM8.

ADAM15

The *ADAM15* gene was shown to have a large increase in copy number in breast cancer cell lines, with 70% of cell lines having 5 or more copies [116]. ADAM15 was shown to be overexpressed at the mRNA and protein levels in breast tumors and related to increased angio-invasion into the tumor [115]. ADAM15 was also shown to activate non-canonical EGFR signaling via shedding of E-cadherin [123]. The shed E-cadherin ectodomain interacts with a HER2-HER3 heterodimer and leads to receptor activation and increased proliferation and cell migration.

The region of the *ADAM15* mRNA that encodes the cytoplasmic tail is extensively alternatively spliced [116, 124]. The novel splice variants were initially discovered in breast cancer cells, yet, they were later shown to be the result of normal splicing events and are also present in non-cancerous tissues. However, two of these variants, *ADAM15B* and *ADAM15C*, are up-regulated specifically in breast tumors and *ADAM15B* is associated with poor prognosis in patients with lymph node-negative disease [125]. The ADAM15B isoform contains an inserted Src binding site in the cytoplasmic domain [125]. ADAM15 also sheds fibroblast growth factor receptor 2 (FGFR2) and this activity may be involved in breast cancer development. ADAM15B sheds FGFR2 more efficiently than other ADAM15 isoforms and in a Src-dependent manner [126]. Thus, ADAM15 has been shown to promote breast tumor progression through multiple mechanisms and may represent a potential druggable target.

ADAM17

ADAM17 is overexpressed in many breast tumors [114, 120, 127, 128] and, consistent with its critical roles in a number of key pro-survival, pro-growth signaling pathways, aberrant expression of ADAM17 has been linked to tumors with poorer prognoses [129]. Overexpression of ADAM17 increased cell proliferation and invasion in cell based assays, while in tumors, ADAM17 expression correlates with expression of the proliferating cell nuclear antigen (PCNA), a proliferation marker, and the serine protease uPA which has been implicated in cancer metastasis [128]. Another study demonstrated that invasive breast cancer cells showed increased EGFR signaling when compared to pre-invasive cells and that this is due to transcriptional up-regulation of the ligands amphiregulin and TGFα and increased shedding of these EGFR ligands [114]. Non-specific metalloprotease inhibitors reverted the more aggressive cells to a less aggressive phenotype with respect to proliferation and invasive capabilities. ADAM17 was

shown to be the primary protease responsible for EGFR ligand shedding. In patients, expression of ADAM17 and TGFα were significantly correlated to each other and both were associated with poor prognosis. Another study further investigated the downstream modulators of this EGFR signaling and found that inhibition of the PI3K/Akt pathways also abolished the deleterious effects of ADAM17 overexpression [130]. Additionally, this study demonstrated that ADAM17 is capable of inducing expression of pro-angiogenic factors and increased tube formation, an *in vitro* assay for neovascularization. Anti-ADAM17 antibodies were previously shown to inhibit growth of breast cancer cell lines *in vitro* [127], indicating that targeting ADAM17 may yield therapeutic benefit. However, I will show here that in patients with TNBC, ADAM17 expression does not correlate with poor prognosis (See Chapter 4). However, high ADAM12 expression does significantly associate with poor prognosis, indicating that the identity of the ADAM responsible for EGF ligand shedding is dependent upon the tumor subtype.

ADAM12

ADAM12 was shown to be up-regulated in breast tumors and breast cancer cell lines [119, 120, 127, 131]. When ADAM12 was overexpressed in the polyoma middle T antigen (PyMT) model of breast cancer, the mice formed breast tumors more rapidly than control littermates and exhibited more metastatic lesions [131]. Conversely, knocking down ADAM12 in this mouse model delayed tumor onset and resulted in less proliferative and less metastatic tumors [117]. This study also confirmed that ADAM12 expression by the tumor, rather than the surrounding stroma, was related to these effects. Interestingly, the catalytic activity of ADAM12 was not required for accelerated tumor formation and increased metastasis. In the PyMT model, EGFR phosphorylation was unchanged between control mice, wild-type ADAM12 and inactive ADAM12 overexpressing mice. However, *in vitro* studies have shown dramatic differences in EGFR activation and cellular migration in response to ADAM12 overexpression that are dependent upon the ADAM12 proteolytic activity [132]. The PyMT model produces luminal tumors whereas the *in vitro* studies utilized basal cell lines and therefore, shedding of EGFR ligands by ADAM12 may be specific to the basal subtype. In patients, *ADAM12* is somatically mutated more frequently than any other *ADAM* gene and it is the only *ADAM* identified as a candidate cancer gene by a global analysis [132–134]. Deactivating mutations in the *ADAM12* gene appear to be excluded from triple negative breast cancers, which rely upon EGFR signaling. Although this finding appears to contrast with the data from the mouse model [132], I show here

that, in triple negative breast cancer patients, ADAM12 expression is correlated with activated EGFR and high ADAM12 expression is associated with increased risk of relapse in patients with early stage tumors [135]. The apparent discrepancy between patient data and the PyMT mouse model is eliminated when the molecular subtype of the tumor is considered. ADAM12 overexpression has also been shown to promote orthotopic growth of poorly tumorigenic cell lines and induce greater degrees of metastasis [119]. Additionally, ADAM12 has been demonstrated to confer estrogen-independence to HoR+ cells through activation of the EGFR pathway [136], which is consistent with the observation that expression of ADAM12 is increased in residual tumors after estrogen-targeted therapy [118]. An abundance of clinical and pre-clinical data suggest that ADAM12 is an important modulator of tumor growth and progression and that ADAM12 represents a promising potential target in the treatment of breast cancer.

The Major Isoforms of ADAM12

ADAM12 is one of the small number of ADAMs that is alternatively spliced and produces more than one major protein isoform. These different isoforms have distinct points of regulation at the mRNA and protein level, unique cellular localizations and, therefore, varying substrates and biological roles.

Alternative Splicing of the ADAM12 *Transcript*

In humans, *ADAM12* exists as two major splice variants, *ADAM12-var1* and *ADAM12-var2* [137]. The *ADAM12-var1* variant contains exons 1-18 and 20-24, while *ADAM12-var2* contains exons 1-19 (Figure 1.5a). This splicing results in variants with two very different 3' untranslated regions (3'UTRs). The *ADAM12-var1* 3'UTR is approximately 5 kb long while the *ADAM12-var2* 3'UTR is only around 800 nucleotides in length. Due to these large variable regions, the two splice variants are easily distinguished in molecular assays such as Northern blots, PCR, and microarrays. It is currently unknown what factors regulate this splicing event and if the relative levels of *ADAM12-var1* and *ADAM12-var2* are altered due to cellular signals or during certain diseases or pathogenic processes.

In addition to the major splicing event that results in generating *ADAM12-var1* and *ADAM12-var2*, there is a previously uncharacterized alternative splicing site near exon 4 that will be described here [138]. This alternative splice site involves the inclusion of a nine nucleotide extension at the end of exon 4. Exon 4 is therefore designated as having two forms,

exon 4a and exon 4b, and the transcripts containing these exons are denoted *ADAM12-var1a/ADAM12-var2a* and *ADAM12-var1b/ADAM12-var2b*, respectively. The four variants resulting from this splicing event currently cannot be differentiated by qRT-PCR or by existing microarray platforms. Here, I show the occurrence of *ADAM12-var1b* in breast epithelial and carcinoma cells and I characterize the phenotypic effect of this insertion on protein localization and function (See Chapter 3).

ADAM12-L

ADAM12-L is the protein isoform encoded by *ADAM12-var1* and is consistent with the canonical ADAM structure (Figure 1.5b). ADAM12-L is the transmembrane isoform with a large cytoplasmic domain; therefore, this isoform is localized to the cell membrane. Because of the membrane localization, the ADAM12-L metalloprotease domain is ideally positioned for the juxtamembrane cleavage events that are typically associated with ADAM activities. ADAM12-L has been shown to shed the EGFR ligands EGF, heparin-binding EGF, and betacellulin as well as a Notch ligand DLL1, Sonic hedgehog protein, the endothelial receptor tyrosine kinases Tie-2 and Flk-1, and the endothelial cell adhesion proteins VE-cadherin, and VCAM-1 [109, 139–142].

Additionally, ADAM12-L contains the large cytosolic domain that has been shown to interact with Src tyrosine kinase, integrin-linked kinase (ILK), and α-actinin-1 [66–68]. The interaction with α-actinin-1 has been shown to direct ADAM12-L to focal adhesions, where it may play a role in cell-cell contacts [67]. The interaction with ILK also recruits ADAM12-L to focal adhesions in response to integrin activation [66]. Once localized to focal adhesions, ADAM12-L is involved in cell adhesion to the extracellular matrix and in activation of the pro-survival PI3K/Akt pathway. The interaction with Src has been shown to activate Src and to induce invadopodia formation in cancer cells [68, 143]. Invadopodia are cellular projections that are involved in cancer cell invasion into the surrounding tissues, and ADAM12-L-mediated shedding of heparin-binding EGF has been shown to further increase invadopodia formation [139].

ADAM12-S

ADAM12-S is a shorter, secreted isoform of ADAM12 which is encoded by the *ADAM12-var2* variant (Figure 1.5) [137] . This isoform lacks the transmembrane and cytoplasmic domains and includes a 34-residue C-terminal sequence unique to ADAM12-S.

This isoform is secreted into the extracellular space and is not in the correct orientation to shed molecules from the cell surface. ADAM12-S has been shown to cleave insulin-like growth factor binding proteins 3 and 5 (IGFBP-3 and IGFBP-5) [144]. This cleavage releases insulin-like growth factor (IGF) and increases its bioavailability, thereby increasing signaling through the IGF receptor.

Elevated levels of ADAM12-S were found in the urine of breast cancer patients and higher levels were correlated with more advanced disease [145]. However, this view has been challenged recently, when another study indicated that the levels of urinary ADAM12-S are not significantly different between control participants and pre-operative cancer patients [146]. Interestingly, the elevated urinary ADAM12-S levels detected in patients with advanced disease may be related to the more radical surgical procedures utilized when treating these patients [146]. Despite this contradiction, it has been demonstrated that ADAM12-S expression by the cancer cells is important in breast tumor invasion and metastasis [119]. The increased number of metastases was reportedly dependent upon the catalytic activity of ADAM12-S and might have been related to the ability of this isoform to degrade extracellular matrix components, like type IV collagens and fibronectin [145]. Surprisingly, in these studies, overexpression of ADAM12-L did not show increased invasion or metastasis [119]. The difference between the two isoforms may, in fact, be related to the model system used in the referenced study, i.e. HoR+ cancer cells. I will show here that high expression of ADAM12-L or ADAM12-S does not affect patient prognosis in patients with HoR+ tumors but, in TNBC, ADAM12-L, and not ADAM12-S, is associated with poor prognosis (See Chapter 4).

Regulation of Expression of ADAM12

Since ADAM12 has been demonstrated to be involved in the development and metastasis of breast tumors, it is important to understand what factors influence its expression. The *ADAM12* gene is regulated by a number of signaling pathways that are also implicated in cancer development, metastasis, and recurrence. The ADAM12 mRNA and protein are also subjected to regulatory mechanisms that govern the rate of translation and protein turnover. Additionally, the two major splice variants/isoforms are differentially regulated at the mRNA and protein levels, which will be more thoroughly investigated in this dissertation.

Induction by Transforming Growth Factor β Signaling

Transforming growth factor β (TGFβ) is particularly interesting to cancer researchers because of its role in a global cellular transdifferentiation program known as epithelial-mesenchymal transition (EMT). EMT is a normal developmental process that has been shown to also occur in tumors, where it modulates tumor growth and progression. Cells that undergo EMT lose cell-cell contacts and cell polarity, becoming more elongated in appearance, more motile and more resistant to apoptosis than the original cell [147]. EMT is clearly observed by studying cell morphology and the presence of epithelial or mesenchymal markers. Epithelial markers are often cell-cell contact proteins like ZO-1 and E-cadherin, while mesenchymal markers are α-smooth muscle actin, vimentin, and a number of transcription factors, including ETS1, ZEB1, ZEB2, Twist, Snail, and Slug, which are drivers of EMT. Tumor cells that have undergone EMT are more migratory, and are, therefore, hypothesized to be more likely to metastasize. This hypothesis is strongly supported by the studies showing that EMT increases cell migration *in vitro* and induces characteristics of tumor-initiating cells [148], and that tumor cells circulating in the bloodstream of cancer patients are more mesenchymal [149].

ADAM12 was demonstrated to be transcriptionally induced in cultured cells by treatment with TGFβ. Initially, this induction was discovered in hepatic stellate cells and analyzed in the context of liver carcinomas [150], however, it was also observed in murine fibroblasts, murine mammary epithelial cells, and human breast cancer cell lines [151], suggesting that the effect is not cell-type specific. A mechanism involving TGFβ-dependent degradation of the SnoN transcriptional repressor was described [151]. However, a site that responds to TGFβ was not identified in the mouse [151] or human *ADAM12* promoters (my unpublished work). This could mean that the site of regulation is further upstream of the transcription initiation site or is actually located in the first intron of the *ADAM12* gene. Another study determined that TGFβ activated transcription of the *ADAM12* gene indirectly and demonstrated strong up-regulation of an *ADAM12* promoter reporter [152]. However, the reporter used in this study lacked a known negative regulatory element and the absence of this element may explain the difference observed between our work [ref.151 and my unpublished data] and this study where a strong induction of the *ADAM12* promoter by TGFβ was observed [152]. In addition to being transcriptionally induced by TGFβ signaling, ADAM12-L also enhanced TGFβ signaling forming a positive feedback loop [153]. ADAM12-L protein stabilized the TGFβ receptor and modulated

intracellular localization of the receptor. Interestingly, this activity was not dependent on the proteolytic activity of ADAM12-L and a catalytically inactive mutant was capable of inducing the same effects. Given this positive feedback loop with TGFβ, it follows that ADAM12-L is also strongly correlated with features of EMT and tumor-initiating cells [118].

Induction by HER2 Signaling

Recently, *ADAM12* expression has been shown to be modulated by HER2 signaling in squamous cell carcinomas [154, 155]. Expression of HER2 correlated with ADAM12 expression in cell lines and overexpression of HER2 resulted in a several fold increases in the levels of *ADAM12-L* and *ADAM12-S* transcripts [154]. This induction was dependent upon HER2 tyrosine kinase activity. Topical application of a small molecule tyrosine kinase inhibitor dramatically reduced the expression levels of *ADAM12* compared to control-treated mice. In the proposed model, the HER2 receptor activates PI3K, which is upstream of Akt and mammalian target of rapamycin (mTOR), and ultimately this is responsible for the up-regulation of *ADAM12*. It was not specifically determined whether this up-regulation occurred at the transcriptional level, and no promoter analyses or treatments with transcriptional inhibitors were performed. Additionally, ADAM12 and HER2 were shown to form a positive feedback loop, where, in a squamous cell carcinoma cell line, overexpression of either isoform of ADAM12 induced transcriptional up-regulation of HER2 through the action of the ETS1 transcription factor [154]. A more complete mechanism, detailing the manner in which ADAM12 might up-regulate ETS1, has not be determined.

Induction by Nuclear Factor κB Signaling

Nuclear factor κB (NFκB) belongs to a superfamily of evolutionarily conserved transcription factors. These transcription factors activate genes involved in cell survival, proliferation, and cytokine production. Highlighting the importance of NFκB in tumor development, constitutive activation of this pathway has been observed in breast cancers [156]. NFκB signaling has also been linked to ADAM12 expression. Studies have demonstrated that activation of TGFβ and Notch pathways ultimately result in NFκB activation [152, 157], and that an active NFκB pathway is critical for induction of *ADAM12*. An NFκB responsive element was identified in the human *ADAM12* promoter and was demonstrated to interact with NFκB transcription factors only in the context of cancer cells, whereas non-transformed cells did not

exhibit binding of NFκB to the *ADAM12* promoter [152]. This study showed that TGFβ activates NFκB, which then induces *ADAM12* expression in breast cancer cell lines, however, it did not rule out direct activation of the *ADAM12* promoter by the canonical TGFβ pathway. For example, it was demonstrated that NFκB is important for up-regulation of *ADAM12* by TGFβ. However, while *ADAM12* expression is dramatically induced by TGFβ in MCF10A non-cancerous cells, NFκB does not bind to the *ADAM12* promoter in these cells. This suggests that, in the context of tumor cells, TGFβ may act to activate *ADAM12* transcription both directly and indirectly through NFκB.

Post-transcriptional Regulation

ADAM12 is also regulated post-transcriptionally. Regulation at the mRNA level is mediated by the action of microRNAs (miRNAs) that interact with the *ADAM12* mRNA and cause decreased translation or degradation of the mRNA. miRNAs typically interact with the 3'UTRs of transcripts and therefore this mechanism allows for differential regulation of the long and short variants of *ADAM12* mRNA since the 3'UTRs are dissimilar. Currently, little is known about miRNA regulation of the *ADAM12* transcripts. In Chapter 2, I will investigate the roles of three miRNA families to selectively regulate *ADAM12-L* expression in breast cancer cells.

One known mechanism of *ADAM12* regulation by miRNAs involves the Notch signaling pathway. ADAM12 is up-regulated by Notch, however, this induction is indirect and does not seem to affect the transcription of the *ADAM12* gene itself. Rather, Notch increases *ADAM12* mRNA stability [157]. In murine fibroblast cells, Notch activation was shown to decrease the transcription of microRNA-29a (miR-29a), which targets the 3'UTR of murine *Adam12* mRNA and causes its degradation. This mechanism requires a functional NFκB pathway, since NFκB acts as a repressor inhibiting transcription of miR-29a. In human cells, miR-29a targets the *ADAM12-L* 3'UTR specifically, causing mRNA degradation. When Notch is activated, cells therefore selectively up-regulate *ADAM12-L* but not *ADAM12-S* as its 3'UTR is not targeted by miR-29a. The miRNA-29 family has also been shown to target *ADAM12* in trabecular meshwork cells [158] and in renal fibrosis [159], however, the stimuli modulating miR-29 levels were not related to Notch signaling in these studies.

At the protein level, ADAM12 is regulated primarily by turnover and altering protein localization. Mature, cell-surface ADAM12-L protein is internalized rapidly via clathrin-mediated endocytosis and knockdown of clathrin heavy chain mRNA decreases the amount of ADAM12-L internalization [160]. After endocytosis, ADAM12-L co-localizes with markers of early and recycling endosomes but not late endosomes that are targeted towards the lysosomes. Consistently, the authors observed recycling of ADAM12-L proteins in which internalized molecules are re-directed to the cell surface. A proline-rich region in the cytoplasmic tail of ADAM12-L seems to be responsible for the internalization. This region interacts with the adapter protein Grb2 and the ADAM12-L/Grb2 interaction is required for clathrin-mediated endocytosis of ADAM12-L. Interestingly, the proline-rich region in ADAM12-L involved interactions with Grb2 is also responsible for binding Src, which has been demonstrated to localize ADAM12-L to focal adhesions [143]. A model in which Src and Grb2 compete for the same binding site, where Src mediates trafficking of ADAM12-L to the cell surface and Grb2/clathrin mediate ADAM12-L internalization, has been proposed [160].

Main Goals of This Study

Since the major isoforms of ADAM12 are significantly different in terms of membrane association and cellular localization and, therefore, may cleave a different group of substrate molecules, these isoforms should have unique physiological roles. In this dissertation, I aimed to study the differential regulation of the *ADAM12* mRNA variants and the role of each variant in breast tumor biology.

- I sought to investigate the cellular mechanisms for isoform/variant-specific regulation. I focused on miRNA regulation of the *ADAM12-L* 3'UTR by three miRNA families. I selected the miRNA families that are specific to the claudin-low molecular subtype of breast cancer since *ADAM12*, and particularly *ADAM12-L*, is strongly up-regulated in these tumors (Figure 1.4 and 2.1a,b).
- I also discovered a novel splice variant of *ADAM12* expressed in several breast cancer cell lines. My goal was to express the new variant and characterize the resulting protein isoform in terms of proteolytic activation and cellular localization.
- Finally, I wanted to investigate the effect of each ADAM12 isoform on breast tumor progression. Specifically, I determined a role for ADAM12-L in the biology of triple

negative breast cancers.

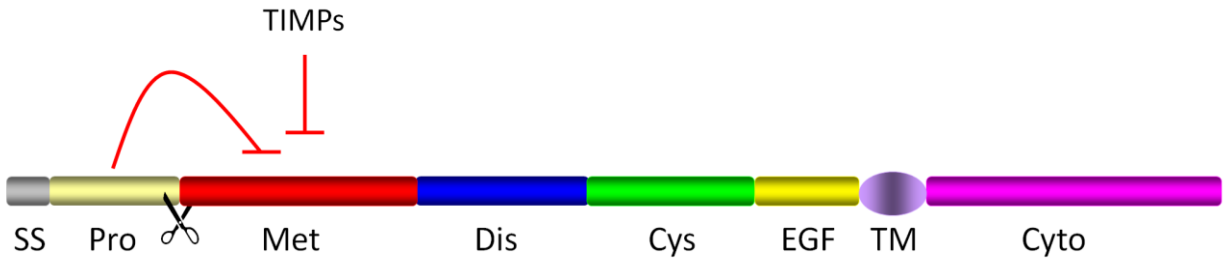

Figure 1.1 Domain organization of the ADAM metalloproteases

ADAM domain organization diagram. SS, signal sequence; Pro, pro-domain; Met, metalloprotease; Dis, disintegrin; Cys, cysteine-rich; EGF, EGF-like; TM, transmembrane; Cyto, cytoplasmic. The scissors represent the site of pro-protein convertase cleavage. In the case of active metalloprotease domains, the inhibitory effects of the pro-domain and the TIMPs are indicated.

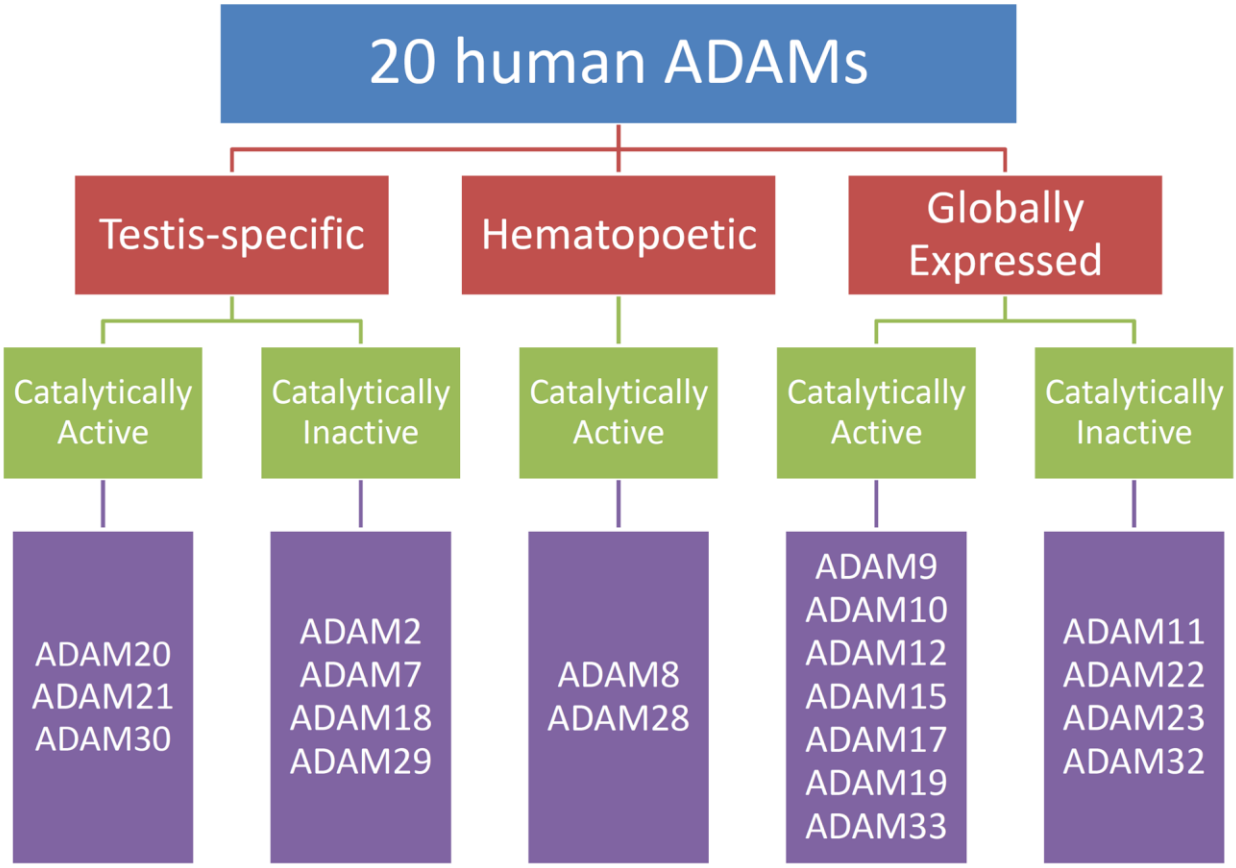

Figure 1.2 The human ADAM proteins grouped by site of expression and catalytic activity

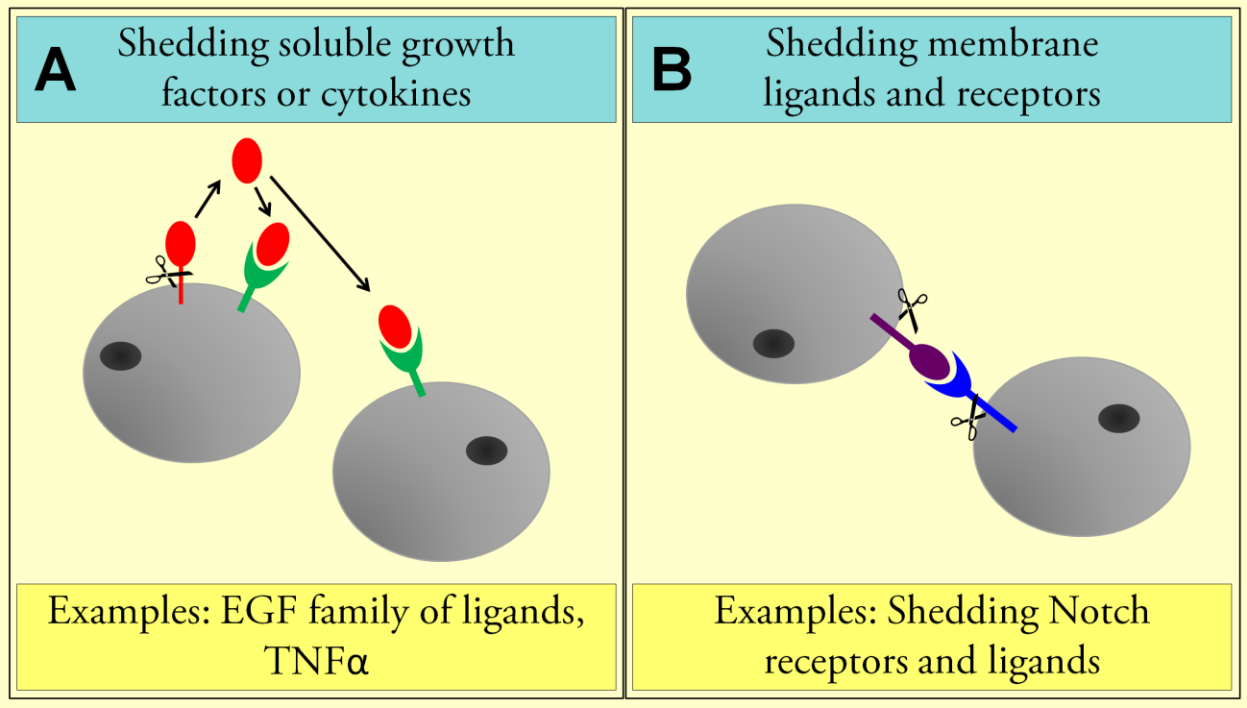

Figure 1.3 The roles of ADAM-mediated proteolysis in selected cellular signaling pathways

Schematic diagram illustrating the membrane proximal events in the cellular signaling pathways discussed in this dissertation and the roles for ADAM activity within these pathways. The scissors represent a catalytically active ADAM. The red objects represent transmembrane proforms of soluble growth factors or cytokines, such as members of the EGF family or TNFα. The green objects represent the membrane receptors for these growth factors. ADAM cleavage of the growth factor or cytokine proform sheds a soluble molecule. The released factor interacts with its receptor to activate cellular signaling either in the same cell or a nearby cell. The purple object represents a membrane-bound ligand, such as DLL-1, while the blue object represents the receptor for membrane-bound ligands, such as the Notch receptors. ADAM cleavage of the Notch receptor is required for pathway activation in the cell that expresses the receptor; however, ADAM cleavage of the ligand inhibits Notch signaling in neighboring cells since ligand availability is reduced.

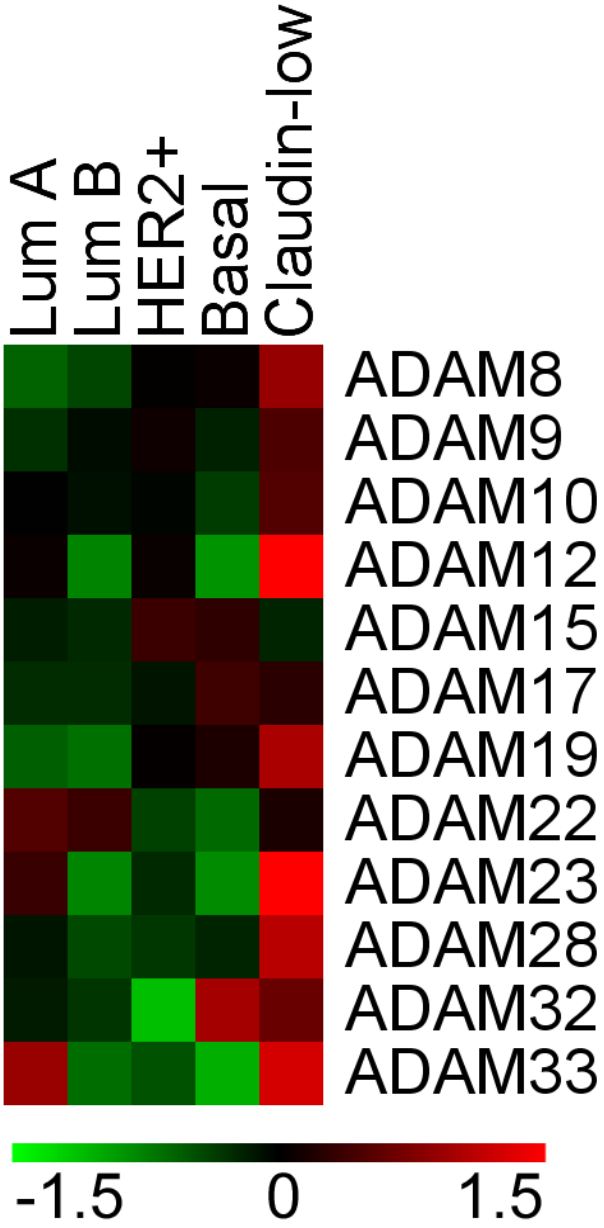

Figure 1.4 Expression of ADAM proteases across the molecular subtypes of breast cancer

The majority of ADAMs are most strongly expressed in tumors of the claudin-low molecular subtype. Raw RNA-Seq expression values for all human ADAMs were downloaded from The Cancer Genome Atlas Breast Invasive Carcinoma provisional dataset via the cBioPortal for Cancer Genomics (n=507 complete records at the time of analysis). ADAMs with mean expression values <10 were eliminated, which included all the testes-specific ADAMs and ADAM11. The remaining values were $\log_2$-transformed and an average value for each molecular subtype was calculated. The values were mean-centered and then used to generate a heat map. Each square represents the relative abundance of the transcript, with red squares indicating that expression is greater than the mean value for all subtypes and green squares indicating expression lower than the mean value.

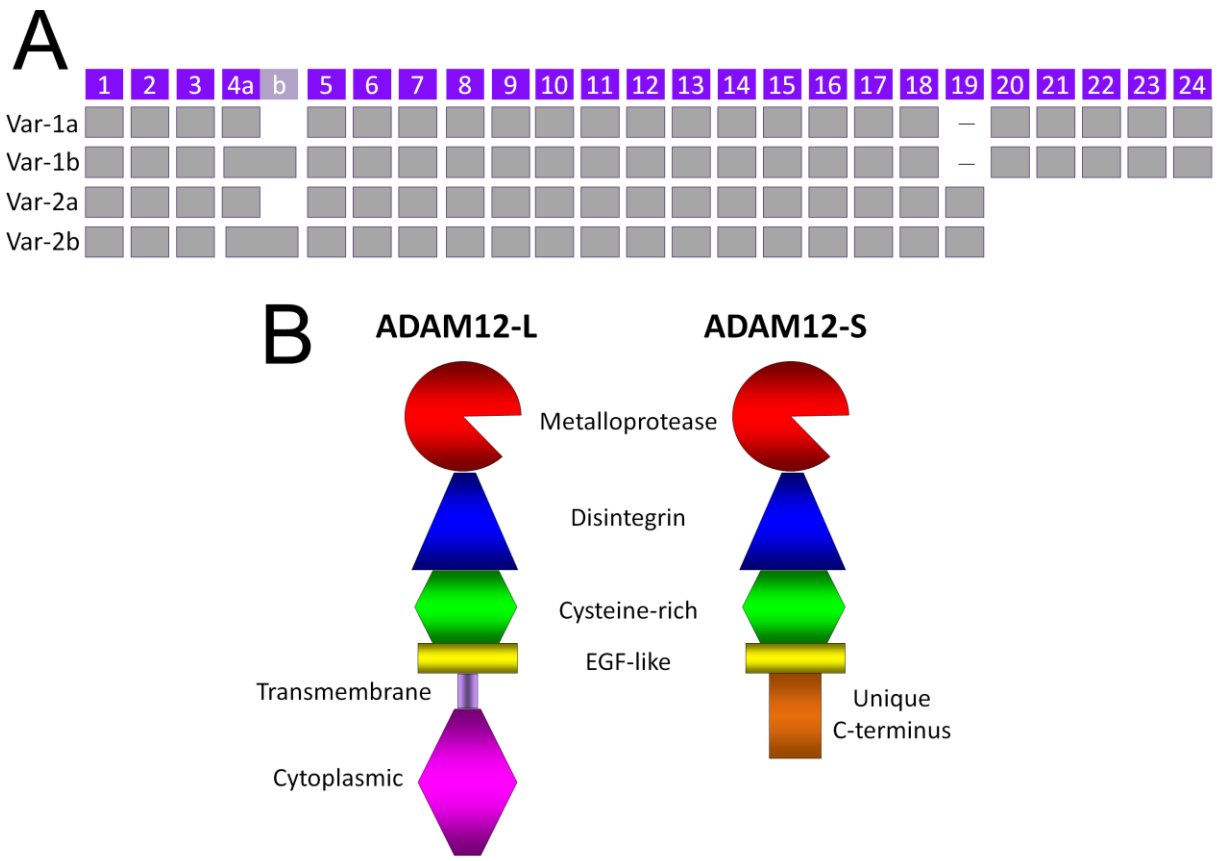

Figure 1.5 The major splice variants and protein isoforms of human ADAM12

(A) Schematic diagram of the exons included in the four splice variants of human *ADAM12*. The 9-nucleotide extension that is unique to exon 4b is shown in lavender. Exons are not drawn to scale. This panel was reproduced from the following journal article: Duhachek-Muggy, S., Li, H., Qi, Y., and Zolkiewska, A. (2013). PLoS ONE 8(10):e75730 (See Chapter 3). (B) Cartoon diagram of the two major ADAM12 protein isoforms in their activated states after pro-domain removal. The ADAM12-L and ADAM12-S isoforms both contain the metalloprotease, disintegrin, cysteine-rich, and EGF-like domains. In the transmembrane isoform, ADAM12-L, the EGF-like domain is followed by a transmembrane helix and the cytoplasmic tail. In the secreted isoform, ADAM12-S, the EGF-like domain is followed by a unique 34-residue C-terminus.

References

1. Elston CW, Ellis IO (1991) Pathological prognostic factors in breast cancer. I. The value of histological grade in breast cancer: experience from a large study with long-term follow-up. Histopathology 19:403–410.
2. Singletary SE (2002) Revision of the American Joint Committee on Cancer Staging System for Breast Cancer. J Clin Oncol 20:3628–3636. doi: 10.1200/JCO.2002.02.026
3. Deroo BJ, Korach KS (2006) Estrogen receptors and human disease. 116:561–570. doi: 10.1172/JCI27987.Review
4. Badve S, Nakshatri H (2009) Oestrogen-receptor-positive breast cancer: towards bridging histopathological and molecular classifications. J Clin Pathol 62:6–12. doi: 10.1136/jcp.2008.059899
5. Levin ER (2005) Integration of the extranuclear and nuclear actions of estrogen. Mol Endocrinol 19:1951–1959. doi: 10.1210/me.2004-0390
6. Mohamed A, Krajewski K, Cakar B, Ma CX (2013) Targeted therapy for breast cancer. Am J Pathol 183:1096–1112. doi: 10.1016/j.ajpath.2013.07.005
7. Laidlaw IJ, Clarke RB, Howell A, et al. (1995) The proliferation of normal human breast tissue implanted into athymic nude mice is stimulated by estrogen but not progesterone. Endocrinology 136:164–171. doi: 10.1210/endo.136.1.7828527
8. Hagan CR, Lange CA (2014) Molecular determinants of context-dependent progesterone receptor action in breast cancer. BMC Med 12:32. doi: 10.1186/1741-7015-12-32
9. Lamy P-J, Fina F, Bascoul-Mollevi C, et al. (2011) Quantification and clinical relevance of gene amplification at chromosome 17q12-q21 in human epidermal growth factor receptor 2-amplified breast cancers. Breast Cancer Res 13:R15. doi: 10.1186/bcr2824
10. Eroles P, Bosch A, Pérez-Fidalgo JA, Lluch A (2012) Molecular biology in breast cancer: intrinsic subtypes and signaling pathways. Cancer Treat Rev 38:698–707. doi: 10.1016/j.ctrv.2011.11.005
11. Dunnwald LK, Rossing MA, Li CI (2007) Hormone receptor status, tumor characteristics, and prognosis: a prospective cohort of breast cancer patients. Breast Cancer Res 9:R6. doi: 10.1186/bcr1639

12. Paik S, Tang G, Shak S, et al. (2006) Gene expression and benefit of chemotherapy in women with node-negative, estrogen receptor-positive breast cancer. J Clin Oncol 24:3726–3734. doi: 10.1200/JCO.2005.04.7985
13. Carey LA, Dees EC, Sawyer L, et al. (2007) The triple negative paradox: primary tumor chemosensitivity of breast cancer subtypes. Clin Cancer Res 13:2329–34. doi: 10.1158/1078-0432.CCR-06-1109
14. Barrios CH, Sampaio C, Vinholes J, Caponero R (2009) What is the role of chemotherapy in estrogen receptor-positive, advanced breast cancer? Ann Oncol 20:1157–1162. doi: 10.1093/annonc/mdn756
15. Goldhirsch A, Winer EP, Coates AS, et al. (2013) Personalizing the treatment of women with early breast cancer: highlights of the St Gallen International Expert Consensus on the Primary Therapy of Early Breast Cancer 2013. Ann Oncol 24:2206–2223. doi: 10.1093/annonc/mdt303
16. Arteaga CL, Sliwkowski MX, Osborne CK, et al. (2012) Treatment of HER2-positive breast cancer: current status and future perspectives. Nat Rev Clin Oncol 9:16–32. doi: 10.1038/nrclinonc.2011.177
17. Kataoka H (2009) EGFR ligands and their signaling scissors, ADAMs, as new molecular targets for anticancer treatments. J Dermatol Sci 56:148–153. doi: 10.1016/j.jdermsci.2009.10.002
18. Foley J, Nickerson NK, Nam S, et al. (2010) EGFR signaling in breast cancer: bad to the bone. Semin Cell Dev Biol 21:951–960. doi: 10.1016/j.semcdb.2010.08.009
19. Montemurro F, Di Cosimo S, Arpino G (2013) Human epidermal growth factor receptor 2 (HER2)-positive and hormone receptor-positive breast cancer: new insights into molecular interactions and clinical implications. Ann Oncol 24:2715–2724. doi: 10.1093/annonc/mdt287
20. Incorvati J a, Shah S, Mu Y, Lu J (2013) Targeted therapy for HER2 positive breast cancer. J Hematol Oncol 6:38. doi: 10.1186/1756-8722-6-38
21. Slamon DJ, Leyland-Jones B, Shak S, et al. (2001) Use of chemotherapy plus a monoclonal antibody against HER2. N Engl J Med 344:783–792.
22. Buzdar AU, Ibrahim NK, Francis D, et al. (2005) Significantly higher pathologic complete remission rate after neoadjuvant therapy with trastuzumab, paclitaxel, and epirubicin

chemotherapy: results of a randomized trial in human epidermal growth factor receptor 2-positive operable breast cancer. J Clin Oncol 23:3676–3685. doi: 10.1200/JCO.2005.07.032

23. Foulkes WD, Smith IE, Reis-Filho JS (2010) Triple-Negative Breast Cancer. N Engl J Med 363:1938–1948.
24. Carey LA, Winer E, Viale G, et al. (2010) Triple-negative breast cancer: disease entity of title of convenience? Nat Rev Clin Oncol 7:683–692.
25. Engebraaten O, Vollan HKM, Børresen-Dale A-L (2013) Triple-negative breast cancer and the need for new therapeutic targets. Am J Pathol 183:1064–1074. doi: 10.1016/j.ajpath.2013.05.033
26. The Cancer Genome Atlas Network (2012) Comprehensive molecular portraits of human breast tumours. Nature 490:61–70. doi: 10.1038/nature11412
27. Perou CM, Sørlie T, Eisen MB, et al. (2000) Molecular portraits of human breast tumours. Nature 406:747–752. doi: 10.1038/35021093
28. Prat A, Parker JS, Karginova O, et al. (2010) Phenotypic and molecular characterization of the claudin-low intrinsic subtype of breast cancer. Breast Cancer Res 12:R68. doi: 10.1186/bcr2635
29. Herschkowitz JI, Simin K, Weigman VJ, et al. (2007) Identification of conserved gene expression features between murine mammary carcinoma models and human breast tumors. Genome Biol 8:R76. doi: 10.1186/gb-2007-8-5-r76
30. Ross DT, Perou CM (2001) A comparison of gene expression signatures from breast tumors and breast tissue derived cell lines. Dis Markers 17:99–109.
31. Parker JS, Mullins M, Cheang MCU, et al. (2009) Supervised risk predictor of breast cancer based on intrinsic subtypes. J Clin Oncol 27:1160–1167. doi: 10.1200/JCO.2008.18.1370
32. Guiu S, Michiels S, André F, et al. (2012) Molecular subclasses of breast cancer: how do we define them? The IMPAKT 2012 Working Group Statement. Ann Oncol 23:2997–3006. doi: 10.1093/annonc/mds586
33. Prat A, Ellis MJ, Perou CM (2012) Practical implications of gene-expression-based assays for breast oncologists. Nat Rev Clin Oncol 9:48–57. doi: 10.1038/nrclinonc.2011.178
34. Albergaria A, Paredes J, Sousa B, et al. (2009) Expression of FOXA1 and GATA-3 in breast cancer: the prognostic significance in hormone receptor-negative tumours. Breast Cancer Res 11:R40. doi: 10.1186/bcr2327

35. Williamson EA, Wolf I, O'Kelly J, et al. (2006) BRCA1 and FOXA1 proteins coregulate the expression of the cell cycle-dependent kinase inhibitor p27(Kip1). Oncogene 25:1391–1399. doi: 10.1038/sj.onc.1209170

36. Liu Y-N, Lee W-W, Wang C-Y, et al. (2005) Regulatory mechanisms controlling human E-cadherin gene expression. Oncogene 24:8277–8290. doi: 10.1038/sj.onc.1208991

37. Onder TT, Gupta PB, Mani S a, et al. (2008) Loss of E-cadherin promotes metastasis via multiple downstream transcriptional pathways. Cancer Res 68:3645–3654. doi: 10.1158/0008-5472.CAN-07-2938

38. Chou J, Lin JH, Brenot A, et al. (2013) GATA3 suppresses metastasis and modulates the tumour microenvironment by regulating microRNA-29b expression. Nat Cell Biol 15:201–213. doi: 10.1038/ncb2672

39. Ades F, Zardavas D, Bozovic-Spasojevic I, et al. (2014) Luminal B Breast Cancer: Molecular Characterization, Clinical Management, and Future Perspectives. J Clin Oncol 1–12. doi: 10.1200/JCO.2013.54.1870

40. Badve S, Turbin D, Thorat M a, et al. (2007) FOXA1 expression in breast cancer--correlation with luminal subtype A and survival. Clin Cancer Res 13:4415–4421. doi: 10.1158/1078-0432.CCR-07-0122

41. Cheang MCU, Chia SK, Voduc D, et al. (2009) Ki67 index, HER2 status, and prognosis of patients with luminal B breast cancer. J Natl Cancer Inst 101:736–750. doi: 10.1093/jnci/djp082

42. Prat A, Perou CM (2011) Deconstructing the molecular portraits of breast cancer. Mol Oncol 5:5–23. doi: 10.1016/j.molonc.2010.11.003

43. Caan BJ, Sweeney C, Habel L a, et al. (2014) Intrinsic subtypes from the PAM50 gene expression assay in a population-based breast cancer survivor cohort: prognostication of short- and long-term outcomes. Cancer Epidemiol Biomarkers Prev 23:725–734. doi: 10.1158/1055-9965.EPI-13-1017

44. Prat A, Carey LA, Adamo B, et al. (2014) Molecular Features and Survival Outcomes of the Intrinsic Subtypes Within HER2-Positive Breast Cancer. J Natl Cancer Inst 106:1–8. doi: 10.1093/jnci/dju152

45. Ellis MJ (2014) HER2-Positive Breast Cancer, Intrinsic Subtypes, and Tailoring Therapy. J Natl Cancer Inst 106:14–15. doi: 10.1093/jnci/dju212

46. Saito M, Kato Y, Ito E, et al. (2012) Expression screening of 17q12-21 amplicon reveals GRB7 as an ERBB2-dependent oncogene. FEBS Lett 586:1708–1714. doi: 10.1016/j.febslet.2012.05.003
47. Sahlberg KK, Hongisto V, Edgren H, et al. (2013) The HER2 amplicon includes several genes required for the growth and survival of HER2 positive breast cancer cells. Mol Oncol 7:392–401. doi: 10.1016/j.molonc.2012.10.012
48. Sørlie T, Perou CM, Tibshirani R, et al. (2001) Gene expression patterns of breast carcinomas distinguish tumor subclasses with clinical implications. Proc Natl Acad Sci U S A 98:10869–10874. doi: 10.1073/pnas.191367098
49. Luo J, Solimini NL, Elledge SJ (2009) Principles of cancer therapy: oncogene and non-oncogene addiction. Cell 136:823–837. doi: 10.1016/j.cell.2009.02.024
50. Prat A, Karginova O, Parker JS, et al. (2013) Characterization of cell lines derived from breast cancers and normal mammary tissues for the study of the intrinsic molecular subtypes. Breast Cancer Res Treat 142:237–55. doi: 10.1007/s10549-013-2743-3
51. Albergaria A, Ribeiro A-S, Vieira A-F, et al. (2011) P-cadherin role in normal breast development and cancer. Int J Dev Biol 55:811–822. doi: 10.1387/ijdb.113382aa
52. Louderbough JM V, Schroeder JA (2011) Understanding the dual nature of CD44 in breast cancer progression. Mol Cancer Res 9:1573–1586. doi: 10.1158/1541-7786.MCR-11-0156
53. Dontu G, Abdallah WM, Foley JM, et al. (2003) In vitro propagation and transcriptional profiling of human mammary stem/progenitor cells. Genes Dev 17:1253–1270. doi: 10.1101/gad.1061803
54. Al-Hajj M, Wicha MS, Benito-Hernandez A, et al. (2003) Prospective identification of tumorigenic breast cancer cells. Proc Natl Acad Sci U S A 100:3983–3988. doi: 10.1073/pnas.0530291100
55. Lim E, Vaillant F, Wu D, et al. (2009) Aberrant luminal progenitors as the candidate target population for basal tumor development in BRCA1 mutation carriers. Nat Med 15:907–913. doi: 10.1038/nm.2000
56. Creighton CJ, Li X, Landis M, et al. (2009) Residual breast cancers after conventional therapy display mesenchymal as well as tumor-initiating features. Proc Natl Acad Sci U S A 106:13820–13825. doi: 10.1073/pnas.0905718106

57. Ghaffari S (2011) Cancer, stem cells and cancer stem cells: old ideas, new developments. F1000 Med Rep 3:23. doi: 10.3410/M3-23
58. Edwards DR, Handsley MM, Pennington CJ (2008) The ADAM metalloproteinases. Mol Aspects Med 29:258–289. doi: 10.1016/j.mam.2008.08.001
59. Gomis-Rüth FX (2009) Catalytic domain architecture of metzincin metalloproteases. J Biol Chem 284:15353–15357. doi: 10.1074/jbc.R800069200
60. Van Wart HE, Birkedal-Hansen H (1990) The cysteine switch: a principle of regulation of metalloproteinase activity with potential applicability to the entire matrix metalloproteinase gene family. Proc Natl Acad Sci U S A 87:5578–5582.
61. Nyren-Erickson EK, Jones JM, Srivastava DK, Mallik S (2013) A disintegrin and metalloproteinase-12 (ADAM12): function, roles in disease progression, and clinical implications. Biochim Biophys Acta 1830:4445–4455. doi: 10.1016/j.bbagen.2013.05.011
62. Lorenzen I, Trad A, Grötzinger J (2011) Multimerisation of A disintegrin and metalloprotease protein-17 (ADAM17) is mediated by its EGF-like domain. Biochem Biophys Res Commun 415:330–336. doi: 10.1016/j.bbrc.2011.10.056
63. Cousin H, Gaultier A, Bleux C, et al. (2000) PACSIN2 is a regulator of the metalloprotease/disintegrin ADAM13. Dev Biol 227:197–210. doi: 10.1006/dbio.2000.9871
64. Weskamp G, Krätzschmar J, Reid MS, Blobel CP (1996) MDC9, a widely expressed cellular disintegrin containing cytoplasmic SH3 ligand domains. J Cell Biol 132:717–726.
65. Ebsen H, Lettau M, Kabelitz D, Janssen O (2014) Identification of SH3 domain proteins interacting with the cytoplasmic tail of the a disintegrin and metalloprotease 10 (ADAM10). PLoS One 9:e102899. doi: 10.1371/journal.pone.0102899
66. Leyme A, Bourd-Boittin K, Bonnier D, et al. (2012) Identification of ILK as a new partner of the ADAM12 disintegrin and metalloprotease in cell adhesion and survival. Mol Biol Cell 23:3461–3472. doi: 10.1091/mbc.E11-11-0918
67. Cao Y, Kang Q, Zolkiewska A (2001) Metalloprotease-disintegrin ADAM 12 interacts with alpha-actinin-1. Biochem J 357:353–361.
68. Kang Q, Cao Y, Zolkiewska A (2000) Metalloprotease-disintegrin ADAM 12 binds to the SH3 domain of Src and activates Src tyrosine kinase in C2C12 cells. Biochem J 352 Pt 3:883–892.

69. Reiss K, Saftig P (2009) The “a disintegrin and metalloprotease” (ADAM) family of sheddases: physiological and cellular functions. Semin Cell Dev Biol 20:126–137. doi: 10.1016/j.semcdb.2008.11.002
70. Cao Y, Kang Q, Zhao Z, Zolkiewska A (2002) Intracellular processing of metalloprotease disintegrin ADAM12. J Biol Chem 277:26403–26411. doi: 10.1074/jbc.M110814200
71. Blobel CP, Wolfsberg TG, Turck CW, et al. (1992) A potential fusion peptide and an integrin ligand domain in a protein active in sperm-egg fusion. Nature 356:248–252.
72. Cho C (2012) Testicular and epididymal ADAMs: expression and function during fertilization. Nat Rev Urol 9:550–560.
73. Cho C (2005) Mammalian ADAMs with testis-specific or -predominant expression: Testicular ADAMs. In: Hooper NM, Lendeckel U (eds) ADAM Fam. Proteases. Springer, pp 239–259
74. Howard L, Maciewicz RA, Blobel CP (2000) Cloning and characterization of ADAM28: evidence for autocatalytic pro-domain removal and for cell surface localization of mature ADAM28. Biochem J 348:21–27.
75. Schlomann U, Wildeboer D, Webster A, et al. (2002) The metalloprotease disintegrin ADAM8. Processing by autocatalysis is required for proteolytic activity and cell adhesion. J Biol Chem 277:48210–48219. doi: 10.1074/jbc.M203355200
76. Hoiruchi K, Blobel CP (2005) Studies from ADAM knockout mice. In: Hooper NM, Lendeckel U (eds) ADAM Fam. Proteases. Springer, pp 29–64
77. Hall T, Leone JW, Wiese JF, et al. (2009) Autoactivation of human ADAM8: a novel pre-processing step is required for catalytic activity. Biosci Rep 29:217–228. doi: 10.1042/BSR20080145
78. Bartsch JW, Naus S, Rittger A, Schlomann U (2005) ADAM8/MS2/CD156a: A metalloprotease-disintegrin involved in immune responses. In: Hooper NM, Lendeckel U (eds) ADAM Fam. Proteases. Springer, pp 65–73
79. Koller G, Schlomann U, Golfi P, et al. (2009) ADAM8/MS2/CD156, an emerging drug target in the treatment of inflammatory and invasive pathologies. Curr Pharm Des 15:2272–2281.
80. Chen J, Jiang X, Duan Y, et al. (2013) ADAM8 in Asthma: Friend or Foe to Airway Inflammation? Am J Respir Cell Mol Biol 49:875–884. doi: 10.1165/rcmb2013-0168TR

81. Gómez-Gaviro M, Domínguez-Luis M, Canchado J, et al. (2007) Expression and regulation of the metalloproteinase ADAM-8 during human neutrophil pathophysiological activation and its catalytic activity on L-selectin shedding. J Immunol 178:8053–8063.
82. Romagnoli M, Mineva ND, Polmear M, et al. (2014) ADAM8 expression in invasive breast cancer promotes tumor dissemination and metastasis. EMBO Mol Med 6:278–294. doi: 10.1002/emmm.201303373
83. Kelly K, Hutchinson G, Nebenius-Oosthuizen D, et al. (2005) Metalloprotease-disintegrin ADAM8: expression analysis and targeted deletion in mice. Dev Dyn 232:221–231. doi: 10.1002/dvdy.20221
84. Fourie AM (2005) ADAM28. In: Hooper NM, Lendeckel U (eds) ADAM Fam. Proteases. Springer, pp 223–238
85. Howard L, Zheng Y, Horrocks M, et al. (2001) Catalytic activity of ADAM28. FEBS Lett 498:82–86.
86. Bridges LC, Tani PH, Hanson KR, et al. (2002) The lymphocyte metalloprotease MDC-L (ADAM 28) is a ligand for the integrin alpha4beta1. J Biol Chem 277:3784–3792. doi: 10.1074/jbc.M109538200
87. McGinn OJ, English WR, Roberts S, et al. (2011) Modulation of integrin α4β1 by ADAM28 promotes lymphocyte adhesion and transendothelial migration. Cell Biol Int 35:1043–1053. doi: 10.1042/CBI20100885
88. Hartmann D, de Strooper B, Serneels L, et al. (2002) The disintegrin/metalloprotease ADAM 10 is essential for Notch signalling but not for alpha-secretase activity in fibroblasts. Hum Mol Genet 11:2615–2624.
89. Peschon JJ, Slack JL, Reddy P, et al. (1998) An Essential Role for Ectodomain Shedding in Mammalian Development. Science 282:1281–1284. doi: 10.1126/science.282.5392.1281
90. Van der Vorst EPC, Keijbeck AA, de Winther MPJ, Donners MMPC (2012) A disintegrin and metalloproteases: Molecular scissors in angiogenesis, inflammation and atherosclerosis. Atherosclerosis 224:302–308. doi: 10.1016/j.atherosclerosis.2012.04.023
91. Saftig P, Hartmann D (2005) ADAM10. In: Hooper NM, Lendeckel U (eds) ADAM Fam. Proteases. Springer US, Boston, MA, pp 85–121
92. Arribas J, Ruiz-Paz S (2005) ADAM17: Regulation of ectodomain shedding. In: Hooper NM, Lendeckel U (eds) ADAM Fam. Proteases. Springer, pp 171–197

93. Ishiura S (2005) ADAM9. In: Hooper NM, Lendeckel U (eds) ADAM Fam. Proteases. Springer, pp 75–83
94. Horiuchi K, Weskamp G, Lum L, et al. (2003) Potential role for ADAM15 in pathological neovascularization in mice. Mol Cell Biol 23:5614–5624.
95. Kang T, Newcomer RG, Zhao Y-G, Sang Q-XA (2005) ADAM19: Domain structure, regulation, processing and functions. In: Hooper NM, Lendeckel U (eds) ADAM Fam. Proteases. Springer, pp 199–221
96. Mochizuki S, Okada Y (2007) ADAMs in cancer cell proliferation and progression. Cancer Sci 98:621–628. doi: 10.1111/j.1349-7006.2007.00434.x
97. Liu Y, Wang Z-H, Zhen W, et al. (2014) Association Between Genetic Polymorphisms in the ADAM33 Gene and Asthma Risk: A Meta-Analysis. DNA Cell Biol 33:1–9. doi: 10.1089/dna.2013.2284
98. Liang S, Wei X, Gong C, et al. (2013) A disintegrin and metalloprotease 33 (ADAM33) gene polymorphisms and the risk of asthma: a meta-analysis. Hum Immunol 74:648–657. doi: 10.1016/j.humimm.2013.01.025
99. Takahashi E, Sagane K, Oki T, et al. (2006) Deficits in spatial learning and motor coordination in ADAM11-deficient mice. BMC Neurosci 7:19. doi: 10.1186/1471-2202-7-19
100. Takahashi E, Sagane K, Nagasu T, Kuromitsu J (2006) Altered nociceptive response in ADAM11-deficient mice. Brain Res 1097:39–42. doi: 10.1016/j.brainres.2006.04.043
101. Sagane K, Hayakawa K, Kai J, et al. (2005) Ataxia and peripheral nerve hypomyelination in ADAM22-deficient mice. BMC Neurosci 6:33. doi: 10.1186/1471-2202-6-33
102. Kegel L, Aunin E, Meijer D, Bermingham JR (2013) LGI proteins in the nervous system. ASN Neuro 5:167–181. doi: 10.1042/AN20120095
103. Kopan R (2012) Notch signaling. Cold Spring Harb Perspect Biol 4:a011213. doi: 10.1101/cshperspect.a011213
104. Kopan R, Ilagan MXG (2009) The canonical Notch signaling pathway: unfolding the activation mechanism. Cell 137:216–233. doi: 10.1016/j.cell.2009.03.045
105. Hori K, Sen A, Artavanis-Tsakonas S (2013) Notch signaling at a glance. J Cell Sci 126:2135–2140. doi: 10.1242/jcs.127308

106. Brou C, Logeat F, Gupta N, et al. (2000) A Novel Proteolytic Cleavage Involved in Notch Signaling. Mol Cell 5:207–216. doi: 10.1016/S1097-2765(00)80417-7
107. Koutras AK, Fountzilas G, Kalogeras KT, et al. (2010) The upgraded role of HER3 and HER4 receptors in breast cancer. Crit Rev Oncol Hematol 74:73–78. doi: 10.1016/j.critrevonc.2009.04.011
108. Murphy G (2008) The ADAMs: signalling scissors in the tumour microenvironment. Nat Rev Cancer 8:929–941. doi: 10.1038/nrc2459
109. Horiuchi K, Le Gall S, Schulte M, et al. (2007) Substrate selectivity of epidermal growth factor-receptor ligand sheddases and their regulation by phorbol esters and calcium influx. Mol Biol Cell 18:176–188. doi: 10.1091/mbc.E06-01-0014
110. Zelová H, Hošek J (2013) TNF-α signalling and inflammation: interactions between old acquaintances. Inflamm Res 62:641–651. doi: 10.1007/s00011-013-0633-0
111. Arribas J, Esselens C (2009) ADAM17 as a therapeutic target in multiple diseases. Curr Pharm Des 15:2319–2335.
112. Duffy MJ, Mullooly M, O'Donovan N, et al. (2011) The ADAMs family of proteases: new biomarkers and therapeutic targets for cancer? Clin Proteomics 8:9. doi: 10.1186/1559-0275-8-9
113. Maretzky T, Reiss K, Ludwig A, et al. (2005) ADAM10 mediates E-cadherin shedding and regulates epithelial cell-cell adhesion, migration, and beta-catenin translocation. Proc Natl Acad Sci U S A 102:9182–9187. doi: 10.1073/pnas.0500918102
114. Kenny PA, Bissell MJ (2007) Targeting TACE-dependent EGFR ligand shedding in breast cancer. J Clin Invest 117:337–345. doi: 10.1172/JCI29518
115. Kuefer R, Day KC, Kleer CG, et al. (2006) ADAM15 disintegrin is associated with aggressive prostate and breast cancer disease. Neoplasia 8:319–329. doi: 10.1593/neo.05682
116. Ortiz RM, Kärkkäinen I, Huovila A-PJ (2004) Aberrant alternative exon use and increased copy number of human metalloprotease-disintegrin ADAM15 gene in breast cancer cells. Genes Chromosomes Cancer 41:366–378. doi: 10.1002/gcc.20102
117. Fröhlich C, Nehammer C, Albrechtsen R, et al. (2011) ADAM12 produced by tumor cells rather than stromal cells accelerates breast tumor progression. Mol Cancer Res 9:1449–1461. doi: 10.1158/1541-7786.MCR-11-0100

118. Li H, Duhachek-Muggy S, Dubnicka S, Zolkiewska A (2013) Metalloproteinase-disintegrin ADAM12 is associated with a breast tumor-initiating cell phenotype. Breast Cancer Res Treat 139:691–703.
119. Roy R, Rodig S, Bielenberg D, et al. (2011) ADAM12 transmembrane and secreted isoforms promote breast tumor growth: a distinct role for ADAM12-S protein in tumor metastasis. J Biol Chem 286:20758–20768. doi: 10.1074/jbc.M110.216036
120. Narita D, Seclaman E, Ursoniu S, Anghel A (2012) Increased expression of ADAM12 and ADAM17 genes in laser-capture microdissected breast cancers and correlations with clinical and pathological characteristics. Acta Histochem 114:131–139. doi: 10.1016/j.acthis.2011.03.009
121. Ishikawa N, Daigo Y, Yasui W, et al. (2004) ADAM8 as a novel serological and histochemical marker for lung cancer. Clin Cancer Res 10:8363–8370. doi: 10.1158/1078-0432.CCR-04-1436
122. Wildeboer D, Naus S, Sang Q-XA, et al. (2006) Metalloproteinase Disintegrins ADAM8 and ADAM19 Are Highly Regulated in Human Primary Brain Tumors and their Expression Levels and Activities Are Associated with Invasiveness. J Neuropathol Exp Neurol 65:516–527.
123. Najy AJ, Day KC, Day ML (2008) The ectodomain shedding of E-cadherin by ADAM15 supports ErbB receptor activation. J Biol Chem 283:18393–18401. doi: 10.1074/jbc.M801329200
124. Kleino I, Ortiz RM, Huovila A-PJ (2007) ADAM15 gene structure and differential alternative exon use in human tissues. BMC Mol Biol 8:90. doi: 10.1186/1471-2199-8-90
125. Zhong JL, Poghosyan Z, Pennington CJ, et al. (2008) Distinct functions of natural ADAM-15 cytoplasmic domain variants in human mammary carcinoma. Mol Cancer Res 6:383–394. doi: 10.1158/1541-7786.MCR-07-2028
126. Maretzky T, Le Gall SM, Worpenberg-Pietruk S, et al. (2009) Src stimulates fibroblast growth factor receptor-2 shedding by an ADAM15 splice variant linked to breast cancer. Cancer Res 69:4573–4576. doi: 10.1158/0008-5472.CAN-08-4766
127. Lendeckel U, Kohl J, Arndt M, et al. (2005) Increased expression of ADAM family members in human breast cancer and breast cancer cell lines. J Cancer Res Clin Oncol 131:41–48. doi: 10.1007/s00432-004-0619-y

128. McGowan PM, Ryan BM, Hill ADK, et al. (2007) ADAM-17 expression in breast cancer correlates with variables of tumor progression. Clin Cancer Res 13:2335–2343. doi: 10.1158/1078-0432.CCR-06-2092
129. McGowan PM, McKiernan E, Bolster F, et al. (2008) ADAM-17 predicts adverse outcome in patients with breast cancer. Ann Oncol 19:1075–1081. doi: 10.1093/annonc/mdm609
130. Zheng X, Jiang F, Katakowski M, et al. (2009) ADAM17 promotes breast cancer cell malignant phenotype through EGFR-PI3K-AKT activation. Cancer Biol Ther 8:1045–1054.
131. Kveiborg M, Fröhlich C, Albrechtsen R, et al. (2005) A role for ADAM12 in breast tumor progression and stromal cell apoptosis. Cancer Res 65:4754–4761. doi: 10.1158/0008-5472.CAN-05-0262
132. Qi Y, Duhachek-Muggy S, Li H, Zolkiewska A (2014) Phenotypic diversity of breast cancer-related mutations in metalloproteinase-disintegrin ADAM12. PLoS One 9:e92536. doi: 10.1371/journal.pone.0092536
133. Sjöblom T, Jones S, Wood LD, et al. (2006) The consensus coding sequences of human breast and colorectal cancers. Science 314:268–274. doi: 10.1126/science.1133427
134. Wood LD, Parsons DW, Jones S, et al. (2007) The genomic landscapes of human breast and colorectal cancers. Science 318:1108–1113. doi: 10.1126/science.1145720
135. Li H, Duhachek-Muggy S, Qi Y, et al. (2012) An essential role of metalloprotease-disintegrin ADAM12 in triple-negative breast cancer. Breast Cancer Res Treat 135:759–769.
136. Roy R, Moses MA (2012) ADAM12 induces estrogen-independence in breast cancer cells. Breast Cancer Res Treat 131:731–741. doi: 10.1007/s10549-011-1431-4
137. Gilpin BJ, Loechel F, Mattei MG, et al. (1998) A novel, secreted form of human ADAM 12 (meltrin alpha) provokes myogenesis in vivo. J Biol Chem 273:157–166.
138. Duhachek-Muggy S, Li H, Qi Y, Zolkiewska A (2013) Alternative mRNA Splicing Generates Two Distinct ADAM12 Prodomain Variants. PLoS One 8:e75730. doi: 10.1371/journal.pone.0075730
139. Díaz B, Yuen A, Iizuka S, et al. (2013) Notch increases the shedding of HB-EGF by ADAM12 to potentiate invadopodia formation in hypoxia. J Cell Biol 201:279–292. doi: 10.1083/jcb.201209151

140. Ohlig S, Farshi P, Pickhinke U, et al. (2011) Sonic hedgehog shedding results in functional activation of the solubilized protein. Dev Cell 20:764–774. doi: 10.1016/j.devcel.2011.05.010
141. Dyczynska E, Sun D, Yi H, et al. (2007) Proteolytic processing of delta-like 1 by ADAM proteases. J Biol Chem 282:436–444. doi: 10.1074/jbc.M605451200
142. Fröhlich C, Klitgaard M, Noer JB, et al. (2013) ADAM12 is expressed in the tumour vasculature and mediates ectodomain shedding of several membrane-anchored endothelial proteins. Biochem J 452:97–109. doi: 10.1042/BJ20121558
143. Albrechtsen R, Stautz D, Sanjay A, et al. (2011) Extracellular engagement of ADAM12 induces clusters of invadopodia with localized ectodomain shedding activity. Exp Cell Res 317:195–209. doi: 10.1016/j.yexcr.2010.10.003
144. Loechel F, Fox JW, Murphy G, et al. (2000) ADAM 12-S cleaves IGFB- 3 and IGFBP-5 and is inhibited by TIMP-3. Biochem Biophys Res Commun 278:511–515.
145. Roy R, Wewer UM, Zurakowski D, et al. (2004) ADAM 12 cleaves extracellular matrix proteins and correlates with cancer status and stage. J Biol Chem 279:51323–51330. doi: 10.1074/jbc.M409565200
146. Nyren-Erickson EK, Bouton M, Raval M, et al. (2014) Urinary concentrations of ADAM 12 from breast cancer patients pre- and post-surgery vs. cancer-free controls: a clinical study for biomarker validation. J Negat Results Biomed 13:5. doi: 10.1186/1477-5751-13-5
147. Kalluri R, Weinberg RA (2009) The basics of epithelial-mesenchymal transition. J Clin Invest 119:1420–1428. doi: 10.1172/JCI39104.1420
148. Mani S a, Guo W, Liao M-J, et al. (2008) The epithelial-mesenchymal transition generates cells with properties of stem cells. Cell 133:704–715. doi: 10.1016/j.cell.2008.03.027
149. Yu M, Bardia A, Wittner BS, et al. (2013) Circulating breast tumor cells exhibit dynamic changes in epithelial and mesenchymal composition. Science 339:580–584. doi: 10.1126/science.1228522
150. Le Pabic H, Bonnier D, Wewer UM, et al. (2003) ADAM12 in human liver cancers: TGF-beta-regulated expression in stellate cells is associated with matrix remodeling. Hepatology 37:1056–1066. doi: 10.1053/jhep.2003.50205

151. Solomon E, Li H, Duhachek Muggy S, et al. (2010) The role of SnoN in transforming growth factor beta1-induced expression of metalloprotease-disintegrin ADAM12. J Biol Chem 285:21969–21977.
152. Ray A, Dhar S, Ray BK (2010) Transforming growth factor-beta1-mediated activation of NF-kappaB contributes to enhanced ADAM-12 expression in mammary carcinoma cells. Mol Cancer Res 8:1261–70. doi: 10.1158/1541-7786.MCR-10-0212
153. Atfi A, Dumont E, Colland F, et al. (2007) The disintegrin and metalloproteinase ADAM12 contributes to TGF-beta signaling through interaction with the type II receptor. J Cell Biol 178:201–208. doi: 10.1083/jcb.200612046
154. Rao VH, Kandel A, Lynch D, et al. (2012) A positive feedback loop between HER2 and ADAM12 in human head and neck cancer cells increases migration and invasion. Oncogene 31:2888–2898. doi: 10.1038/onc.2011.460
155. Rao VH, Vogel K, Yanagida JK, et al. (2014) Erbb2 up-regulation of ADAM12 expression accelerates skin cancer progression. Mol Carcinog 1–11. doi: 10.1002/mc.22171
156. Shostak K, Chariot A (2011) NF-κB, stem cells and breast cancer: the links get stronger. Breast Cancer Res 13:214. doi: 10.1186/bcr2886
157. Li H, Solomon E, Duhachek Muggy S, et al. (2011) Metalloprotease-disintegrin ADAM12 expression is regulated by Notch signaling via microRNA-29. J Biol Chem 286:21500–21510.
158. Luna C, Li G, Qiu J, et al. (2009) Role of miR-29b on the regulation of the extracellular matrix in human trabecular meshwork cells under chronic oxidative stress. Mol Vis 15:2488–2497.
159. Ramdas V, McBride M, Denby L, Baker AH (2013) Canonical transforming growth factor-β signaling regulates disintegrin metalloprotease expression in experimental renal fibrosis via miR-29. Am J Pathol 183:1885–1896. doi: 10.1016/j.ajpath.2013.08.027
160. Stautz D, Leyme A, Grandal MV, et al. (2012) Cell-surface metalloprotease ADAM12 is internalized by a clathrin- and Grb2-dependent mechanism. Traffic 13:1532–46. doi: 10.1111/j.1600-0854.2012.01405.x

Chapter 2 - ADAM12-L is a direct target of the miR-29 and miR-200 families in breast cancer

This chapter has been submitted for publication as a journal article:

Duhachek-Muggy, S and Zolkiewska, A.

ADAM12-L is a direct target of the miR-29 and miR-200 families in breast cancer.

Abstract

Background *ADAM12-L* and *ADAM12-S* represent two major splice variants of human metalloproteinase-disintegrin 12 (*ADAM12*) mRNA, which differ in their 3'-untranslated regions (3'UTRs). *ADAM12-L*, but not *ADAM12-S*, has prognostic and chemopredictive values in breast cancer. The expression levels of the two *ADAM12* splice variants in clinical samples are highly discordant, suggesting post-transcriptional regulation of the *ADAM12* gene. The miR-29, miR-30, and miR-200 families have potential target sites in the *ADAM12-L* 3'UTR and thus they may negatively regulate *ADAM12-L* expression.

Methods miR-29b/c, miR-30b/d, and miR-200b/c mimics or control miRNA mimic were transfected into SUM159PT and SUM1315MO2 breast cancer cells. The levels of ADAM12-L protein in transfected cells were measured by Western blotting. ADAM12-L and ADAM12-S mRNA levels were measured by qRT-PCR. Direct targeting of the ADAM12-L 3'UTR by miRNA-29b/c, miR-30b/d, and miR-200b/c was tested by using a luciferase reporter vector containing the wild-type or mutated ADAM12-L 3'UTR. Indirect effect of miR-29b/c, miR-30b/d, and miR-200b/c on transcription of the *ADAM12* gene was investigated by using an ADAM12 promoter reporter construct. Possible correlations between *ADAM12*, miR-29b/c, miR-30b/d, and miR-200b/c were examined for 284 breast tumors from The Cancer Genome Atlas (TCGA) database.

Results Transfection of miR-29b/c and miR-200b/c mimics strongly decreased the level of ADAM12-L protein, while miR-30b/d mimics had a more modest, although noticeable, effect. miR-29b/c and miR-200b/c significantly decreased *ADAM12-L* mRNA levels, whereas *ADAM12-S* levels were not changed. miR-29b/c and miR-200b/c also significantly diminished the activity of an *ADAM12-L* 3'UTR reporter, and this effect was abolished when miR-29b/c and

miR-200b/c target sequences were mutated. In addition, miR-200b/c significantly decreased the activity of the *ADAM12* promoter, most likely through down-regulation of transcription factors that are essential for expression of the *ADAM12* gene. Furthermore, we found a significant negative correlation between all miRNAs tested here and *ADAM12* in breast invasive carcinomas from the TCGA database.

Conclusions The *ADAM12-L* 3'UTR is a direct target of the miR-29 and miR-200 families. As miR-29 and miR-200 play important roles in breast cancer progression, these results may help explain the different prognostic and chemopredictive values of *ADAM12-L* and *ADAM12-S* in breast cancer.

Background

Deregulated expression and activity of ADAM12 (A Disintegrin And Metalloproteinase 12) have been frequently observed in human breast cancer [1, 2]. Overexpression of ADAM12 in the Polyoma virus middle T antigen (PyMT) mouse model of breast cancer accelerates tumor progression, and ADAM12 deficiency delays PyMT-induced mammary tumorigenesis [3, 4]. The human *ADAM12* gene is the most frequently somatically mutated *ADAM* in breast cancer, and four missense mutations, D301H, G479E, T596A, and G668A, have a significant impact on protein functionality in cancer cells [5-7].

Human *ADAM12* mRNA is alternatively spliced, with several different transcript variants giving rise to distinct ADAM12 protein isoforms. Transcript variant 1 (exons 1-18 and 20-24, ~ 8,000 nt, RefSeq NM_003474) encodes a long, transmembrane protein isoform ADAM12-L. Transcript variant 2 (exons 1-19, ~3,400 nt, RefSeq NM_021641) gives rise to a short, secreted protein isoform ADAM12-S [8]. *ADAM12-L* and *ADAM12-S* mRNAs contain entirely different 3' untranslated regions (3'UTRs) and are readily distinguishable by variant-specific probe-sets in several microarray platforms. Each of these two variants can further exist as an "a" or "b" form, which differ by a 9-nt extension at the end of exon 4. The "a" and "b" variants are not distinguishable in microarray profiling experiments [9].

There is a striking difference in the prognostic value of *ADAM12-L* and *ADAM12-S,* and the expression levels of these two *ADAM12* splice variants in clinical samples are highly discordant. *ADAM12-L,* but not *ADAM12-S,* is significantly elevated in the claudin-low

molecular subtype of breast cancer, which has features of epithelial-mesenchymal transition (EMT), high expression of immune and endothelial genes, and gene expression signature reminiscent of mammary stem cells [10-12]. *ADAM12-L* is also induced during EMT in mammary epithelial cells [12-16], is enriched in mammary epithelial cells or breast cancer cells grown in suspension as mammospheres [12, 17, 18], is up-regulated in residual tumors remaining after endocrine therapy for estrogen receptor (ER)-positive disease [12, 18, 19], and the level of *ADAM12-L* expression predicts resistance to chemotherapy in ER-negative breast tumors [12, 20-22]. In patients with lymph node-negative breast tumors who did not receive systemic treatment, *ADAM12-L* expression level is significantly associated with decreased distant metastasis-free survival times [23-26]. In contrast, *ADAM12-S* is not related to any of these characteristics [12, 26].

The discrepancy between expression patterns of *ADAM12-L* and *ADAM12-S* in breast cancer clinical samples suggests that *ADAM12-L* expression may be regulated at the post-transcriptional level, through microRNAs targeting the unique 3'UTR present in this variant. Of particular interest are the miR-200, miR-29, and miR-30 families, which all have been linked to the mesenchymal phenotype, invasion, or metastasis in breast cancer [27, 28], and which all have predicted target sites in the *ADAM12-L* 3'UTR, but not in the *ADAM12-S* 3'UTR. The miR-200 family, by forming a double-negative feedback loop with transcription factors of ZEB1 and ZEB2, is a key negative regulator of EMT and is down-regulated in breast cancer stem-like cells and in normal mammary stem/progenitor cells [28-32]. The miR-29 family, in particular miR-29b, is enriched in luminal breast cancers and inhibits metastasis by repressing regulators of angiogenesis, collagen remodeling, and tumor microenvironment [33]. Loss of miR-29b promotes a mesenchymal phenotype and increases metastasis. Furthermore, the miR-29 family members directly target Krüppel-like factor 4 (KLF4), a transcription factor required for the maintenance of breast cancer stem cells, and down-regulation of miR-29 family members results in increased stem-like properties *in vitro* and *in vivo* [34]. The miR-30 family appears to modulate the stem-like properties of breast cancer cells as well. Reduction of miR-30 levels was reported to promote self-renewal and to inhibit apoptosis in breast tumor-initiating cells [35]. Down-regulation of miR-30 family members was observed in non-adherent mammospheres compared to breast cancer cells under adherent conditions [36].

In this report, we asked whether ADAM12-L expression in breast cancer cells is regulated by members of the miR-200, miR-29, and miR-30 families. We established that transfection of miR-29b/c and miR-200b/c mimics strongly decreased the level of ADAM12-L protein in claudin-low SUM159PT and SUM1315MO2 cells, while miR-30b/d mimics had a more modest, although noticeable, effect. Down-regulation of *ADAM12-L* by miR-29b/c occurred at the post-transcriptional level and was mediated through direct targeting of the *ADAM12-L* 3'UTR. The decrease in ADAM12-L in response to miR-200b/c involved both direct targeting of the *ADAM12-L* 3'UTR and indirect targeting of the *ADAM12* promoter, most likely through down-regulation of transcription factors that are essential for expression of the *ADAM12* gene. Importantly, we found a significant negative correlation between miR-29b/c, miR-30b/d, and miR-200b/c and *ADAM12* in breast invasive carcinomas, for which gene expression profiles are available at The Cancer Genome Atlas (TCGA) database [37]. These results underscore a novel post-transcriptional mode of regulation of ADAM12 expression and help explain the different prognostic and chemopredictive value of *ADAM12-L* and *ADAM12-S* in breast cancer.

Methods

Reagents

MiRIDIAN microRNA mimics and mimic negative control were obtained from Dharmacon. The *ADAM12-L* 3'UTR luciferase reporter construct containing nt 3097-6065 from the *ADAM12-L* transcript was obtained from Origene. The *ADAM12* promoter reporter vector, containing 2599 nt upstream of the translation start site and the complete 5'UTR cloned into the pEZX-PG04 vector, was custom-synthesized by GeneCopoeia. Anti-ADAM12-L rabbit polyclonal antibody (#3394), raised against the cytoplasmic domain of human ADAM12-L, was generated in our laboratory, as previously described [26]. This antibody was used for immunoblotting at a 1:10,000 dilution, with overnight incubation.

Cell culture

SUM159PT and SUM1315MO2 cell lines were obtained from Asterand (Detroit, MI). SUM159PT cells were cultured in Ham's F-12 medium supplemented with 5% fetal bovine serum (FBS), 10 mM HEPES, 5 μg/ml insulin, and 1 μg/ml hydrocortisone. SUM1315MO2

cells were cultured in Ham's F-12 medium supplemented with 5% FBS, 10 mM HEPES, 10 ng/ml epidermal growth factor, and 5 µg/ml insulin. Cells were maintained at 37° C under humidified atmosphere containing 5% CO_2.

Cell transfections

Cells were seeded onto new plates one day prior to transfection. MicroRNA mimics were resuspended in 1X siRNA buffer (Dharmacon) and transfected at a final concentration of 50 nM using DharmaFECT 1 transfection reagent (Dharmacon) according to the manufacturer's instructions. Transfection complexes were removed after 24 hours and cells were analyzed after an additional 48-72 hours. Plasmid transfection was performed using 0.1 µg DNA per well of a 24-well plate and X-tremeGENE HP transfection reagent (Roche), at a 2:1 reagent:DNA ratio. For cells transfected with both miRNA and plasmid DNA, the transfections were performed sequentially, with the miRNA mimics introduced first and the plasmid introduced the following day.

Western blotting

Cells were treated with lysis buffer (50 mM Tris-HCl pH 7.4, 150 mM NaCl, 1% Triton X-100, 0.5% sodium deoxycholate, 0.1% sodium dodecylsulfate (SDS), 5 mM EDTA, 1 mM 4-(2-Aminoethyl) benzenesulfonyl fluoride hydrochloride (AEBSF), 5 µg/mL pepstatin, 5 µg/mL leupeptin, 5 µg/mL aprotinin, and 10 mM 1,10-phenanthroline). Extracts were centrifuged for 15 minutes at 16,000g at 4°C. After centrifugation, the supernatants were incubated with concanavalin A agarose (Sigma; 50 µl resin per 1 ml cell lysate) for 2 hours at 4°C to enrich for glycoproteins. The resin was washed three times and the glycoproteins were eluted with 3X SDS gel loading buffer. Proteins were resolved using SDS-PAGE (8% gel) and were transferred to a nitrocellulose membrane. The membrane was stained with Ponceau S and an image was saved. The membrane was blocked using 5% milk and 0.3% Tween-20 in Dulbecco's Phosphate Buffered Saline (DPBS). Primary antibody was diluted in blocking buffer and incubated with the membrane. Horseradish peroxidase-conjugated anti-rabbit antibody was used as a secondary antibody. Detection was performed using the SuperSignal West Pico Chemiluminescent Substrate (Pierce).

3'UTR luciferase reporter assays

Cells were sequentially transfected with miRNA mimics and the 3'UTR reporter plasmids as described above. A *Renilla* luciferase vector, pRL-TK (Promega) was co-transfected with the reporter plasmid as a transfection control. Forty eight hours after vector transfection, the cells were washed with DPBS containing calcium and magnesium and then lysed using 1X Passive Lysis Buffer (Promega), according to the manufacturer's instructions. The lysates were analyzed for firefly and *Renilla* luciferase using the Dual Luciferase Reporter Assay System (Promega).

Mutagenesis

The predicted miR-29, miR-30, and two miR-200 target sites in the *ADAM12* 3'UTR reporter plasmid were mutated by site-directed mutagenesis. The primers to mutate the miR-29 site were: 5'-TGC TGT GCT GTG CTA CTT TGC TCT GTC TAC TTG C-3' (F) and the reverse complement. The primers to mutate the miR-30 site were: 5'- TAT ACT ATT AAA AAG TCC TAC AGA ATT TTA TGG-3' (F) and the reverse complement. The primers used to mutate the first miR-200 site were: 5'-TTC CCT TAC AAT ATG GAT CTT ATT AAT CCT TCC AAG A-3' (F) and the reverse complement. The primers used to mutate the second miR-200 site were: 5'-TTA ATC CTT CCA AGA TGT CTT ATT TAT CAA GTG AAG C-3' (F) and the reverse complement. The underlined portions represent the mutated bases. Mutations were confirmed by DNA sequencing.

Promoter reporter assay

Cells were sequentially transfected with miRNA mimics and the promoter reporter plasmids as described above. The *ADAM12* promoter reporter construct contained a secreted *Gaussia* luciferase coding sequence downstream of the *ADAM12* promoter. The same vector encoded secreted alkaline phosphatase (SEAP) driven by the constitutively active CMV promoter. Therefore, SEAP served as an internal transfection control. The control vector lacked the *ADAM12* promoter. Twenty four hours after vector transfection, fresh medium was added and collected for analysis 48 hour later. The medium was centrifuged for 3 minutes at 3,200 rpm and the supernatant was analyzed using the Secrete-Pair Dual Luminescence Assay kit (GeneCopoeia) according to the manufacturer's protocol.

cDNA preparation and qRT-PCR analysis

Total RNA was extracted using the Qiagen RNeasy kit and was subjected to on-column digestion with deoxyribonuclease I (Qiagen). One microgram of the total RNA was reverse-transcribed using the SuperScript III First Strand Synthesis system (Invitrogen) and oligo(dT) primers. Real time quantitative PCR (qRT-PCR) was performed using 15 µl volumes in a 96-well format on a CFX96 cycler. The final reaction mixture contained 7.5 µl iQ SYBRgreen Supermix, 6 µl diluted cDNA (1:10 for *ADAM12* analysis and 1:100 for *ACTIN* analysis) and 0.5 µM primers. The primers used for *ADAM12-L* analysis were 5'-AGC CAC ACC AGG ATA GAG AC-3' (F) and 5'-CGC CTT GAG TGA CAC TAC AG-3' (R). The primers used for the *ADAM12-S* analysis were 5'-TCC ATC CAA GCA AAC TGA AT-3' (F) and 5'-GTT GGT GAC TCT GTG GGT TC-3' (R). The primers used for *ACTIN* analysis were 5'-TTG CCG ACA GGA TGC AGA A-3' (F) and 5'-GCC GAT CCA CAC GGA GTA CT-3' (R). The PCR conditions were: 95°C, 10 s; 60°C, 15 s; 72°C, 30 s. At the conclusion of each run, a melt curve analysis was performed to ensure that a single product had been synthesized. The relative expression of *ADAM12-L* and *ADAM12-S*, normalized to *ACTIN*, was calculated using the $2^{-\Delta\Delta Ct}$ method.

Data mining

ADAM12-L and *ADAM12-S* expression data for a panel of breast cancer cell lines were retrieved from Gene Expression Omnibus (GEO) (http://www.ncbi.nlm.nih.gov/geo/) and ArrayExpress (http://www.ebi.ac.uk/arrayexpress/). Expression data for *ADAM12* and miRNAs were accessed from The Cancer Genome Atlas [37] via the cBioPortal for Cancer Genomics (http://www.cbioportal.org/public-portal/) [38, 39]. The Breast Invasive Carcinoma (TCGA, Provisional) database was searched and all cases with reported expression values were included in the analyses. The Z-score data were downloaded and median-centered prior to analysis.

Statistics

Correlation and *t* test analyses were performed using the GraphPad Prism 6.0 software.

Results

Our previous analysis of a number of gene expression profiles of human breast cancers revealed significant discrepancies between *ADAM12-L* and *ADAM12-S* expression levels [12].

Here, we examined *ADAM12-L* and *ADAM12-S* levels in a panel of breast cancer cell lines, which were previously profiled using two different microarray platforms: an Agilent 4x44K platform (ref. [40], Figure 2.1A) or an Affymetrix HG-U133A platform (ref. [41], Figure 2.1B). In both cases, *ADAM12-L* was strongly up-regulated in claudin-low cell lines, whereas the level of *ADAM12-S* in claudin-low cells did not significantly differ from the rest of the cell lines. This expression pattern of *ADAM12-L* and *ADAM12-S* in cell lines mirrored their expression patterns in clinical tumor samples [12].

Selective up-regulation of *ADAM12-L* in claudin-low samples raised a possibility that *ADAM12-L* expression might be repressed by one or more miRNAs, which are down-regulated in claudin-low tumors/cell lines and which could directly target the sites present in the *ADAM12-L* 3'UTR. We focused on the miR-29, miR-30, and miR-200 families, which act as tumor suppressors in breast cancer. The miR-29 family consists of three members with the same seed sequence, miR-29a-c. The miR-30 family is made up of 5 members, miR-30a-e. The miR-200 family consists of five members: miR-200a-c, miR-141 and miR-429. We have selected to study two representative miRNAs from each family: miR-29b (a potent inhibitor of breast tumor metastasis [33]) and miR-29c (associated with a significantly reduced risk of dying from breast cancer [42]), miR-30b and miR-30d (both significantly down-regulated in ER-negative and progesterone receptor (PR)-negative breast tumors [43]), and miR-200b and miR-200c (both representing key negative regulators of EMT and anoikis resistance [29-31]). The 3'UTR of human *ADAM12-L* contains well conserved potential target sites for miR-29b/c, miR-30b/d, and two poorly conserved potential sites for miR-200b/c (Figure 2.1C). miRNA profiling of 51 breast cancer cell lines has previously established that miR-29b/c, miR-30d, and miR-200b/c are under-expressed in claudin-low breast cancer cell lines (ref. [44], Figure 2.1D; miR-30b was not measured in the referenced study).

To determine whether low levels of miR-29b/c, miR-30b/d, and miR-200b/c are required for high expression of ADAM12-L in claudin-low cell lines, we transfected SUM159PT and SUM1315MO2 cells, two representative claudin-low cell lines, with miR-29b/c, miR-30b/d, miR-200b/c, or control miRNA mimics, and measured the level of ADAM12-L protein expression three days later by immunoblotting. We observed that miR-29b/c and miR-200b/c strongly diminished the level of ADAM12-L protein in both cell lines, whereas miR-30b/d had a more modest effect (Figure 2.2). Testing the effect of miRNAs on the expression level of the

ADAM12-S isoform was not possible, because specific antibodies against ADAM12-S are not currently available. In parallel experiments, we examined the effects of miR-29b/c, miR-30b/d, and miR-200b/c on the levels of *ADAM12-L* and *ADAM12-S* mRNAs by qRT-PCR. We found that miR-29b/c mimics decreased the level of *ADAM12-L* in SUM159PT and SUM1315MO2 cells by ~70%, and this effect was statistically significant (Figure 2.3A,B). miR-200b/c diminished *ADAM12-L* expression by ~20%, and this effect did not reach statistical significance in SUM159PT cells, but it was significant in SUM1315MO2 cells. Finally, miR-30d exerted a ~30%, statistically significant, down-regulation of *ADAM12-L* expression in SUM159PT cells and no apparent inhibition of *ADAM12-L* expression in SUM1315MO2 cells. miR-30b did not diminish *ADAM12-L* levels in either cell line (Figure 2.3A,B). Importantly, none of the tested miRNAs had a significant effect on *ADAM12-S* expression in SUM159PT or SUM1315MO2 cells (Figure 2.3C,D).

Decreased ADAM12-L protein or mRNA levels after transfection of miR-29b/c, miR-30b/d, or miR-200b/c suggested that these miRNAs might be directly targeting the *ADAM12-L* 3'UTR or that they might indirectly target the *ADAM12* promoter, through down-regulation of transcription factors that are essential for expression of the *ADAM12* gene. The latter possibility seemed less likely, because of the lack of the effect of the tested miRNAs on the level of *ADAM12-S* mRNA. Nevertheless, to directly test whether miR-29b/c, miR30b/d, or miR-200b/c regulate *ADAM12* expression at the transcriptional level, we transfected SUM159PT cells with individual miRNA mimics, followed by transfection with an *ADAM12* promoter reporter vector. The *ADAM12* promoter reporter contained the 2.6 kb region upstream of the transcriptional start site in the *ADAM12* gene and the entire 5'UTR of *ADAM12* (Figure 2.4A), cloned upstream of the secreted *Gaussia* luciferase (GLuc) gene. The activity of GLuc in the culture medium was measured two days after transfection of the reporter, and it was normalized to the secreted alkaline phosphatase as the internal control for transfection efficiency. We observed that the activity of the *ADAM12* promoter was significantly down-regulated by miR-200b and miR-200c (Figure 2.4D). The other four miRNAs did not exert any effect on the *ADAM12* promoter (Figure 2.4B,C). As the miR-200 family directly targets ZEB1/2 [30, 31] and the ETS1 transcription factor [45], and both ZEB1/2 and ETS1 transcription factors have potential binding sites in the *ADAM12* promoter (identified with the MatInspector tool of the Genomatix software at www.genomatix.de/matinspector.html), we tested the effect of ZEB1 and ETS1 siRNA on

ADAM12 expression in SUM159PT cells. Despite potent down-regulation of ZEB1 and ETS1, the level of ADAM12-L protein was not diminished (results not shown), indicating that either ZEB1 and ETS1 do not regulate ADAM12 expression or that down-regulation of any these transcription factors alone is not sufficient to elicit a noticeable decrease in ADAM12 expression.

To examine whether miR-29b/c, miR-30b/d, or miR-200b/c regulate *ADAM12-L* at the post-transcriptional level, we performed a miRNA target reporter luciferase assay using the pMirTarget reporter vector comprising a ~3-kb region of the *ADAM12-L* 3'UTR down-stream of the firefly luciferase gene. An approximately 50-60% reduction in the luciferase activity was observed in miR-29b/c, miR-30b, and miR-200b/c mimic-transfected SUM159PT cells compared to control mimic-transfected cells (Figure 2.5A). miR-30d did not produce significant decrease in the luciferase activity. Disruption of the predicted miR-29, miR-30, and miR-200 target sites by site-directed mutagenesis largely diminished the effects of miR-29b/c (Figure 2.5B), miR-30b (Figure 2.5C), and miR-200b/c (Figure 2.5D).

To determine whether miR-29b/c, miR-30b/d, or miR-200b/c might regulate ADAM12 expression in breast cancer *in vivo*, we examined the relationship between these miRNAs and *ADAM12* expression in a cohort of 284 breast cancer patients from The Cancer Genome Atlas (TCGA) [37], using the cBioPortal for Cancer Genomics [38, 39]. *ADAM12* expression data were available as median values from three different mRNA expression platforms (microarrays and RNA-Seq) and they contained contributions from both *ADAM12-L* and *ADAM12-S*. Despite this fact, there was a significant negative correlation between *ADAM12* and each of the six miRNAs tested (Figure 2.6). This result is consistent with a role of the miR-29, miR-30, and miR-200 family members in the regulation of *ADAM12* expression.

Discussion

In this report, we examined whether three miRNA families, miR-29, miR-30, and miR-200, directly target the *ADAM12-L* 3'UTR in human breast cancer cells. Since the *ADAM12-S* 3'UTR lacks predicted target sites for these miRNA families and since miR-29, miR-30, or miR-200 levels are highly variable in breast cancer, selective targeting of the *ADAM12-L* 3'UTR by these miRNAs might explain why *ADAM12-L* and *ADAM12-S* expression patterns in breast tumors *in vivo* and in response to experimental manipulations *in vitro* often differ significantly.

Among the three miRNA families tested, miR-30 elicited the least consistent effects. While miR-30b diminished the *ADAM12-L* 3'UTR reporter activity, the level of *ADAM12-L* mRNA in SUM159PT and SUM1315MO2 cells was not affected upon transfection of miR-30b. In contrast, miR-30d seemed to down-regulate *ADAM12-L* in SUM159PT cells, but this effect was not reproduced in SUM1315MO2 cells, and the *ADAM12-L* 3'UTR reporter activity was not diminished in response to miR-30d. Both miR-30b and miR-30d had only a minor effect on ADAM12-L protein levels in SUM159PT and SUM1315MO2 cells. We conclude that the miR-30 family does not contribute significantly to the regulation of ADAM12-L expression in the two cell lines examined here.

In contrast, miR-29b/c consistently produced strong down-regulation of ADAM12-L expression at the mRNA and protein levels in both SUM159PT and SUM1315MO2 cell lines and decreased the *ADAM12-L* 3'UTR reporter activity. Mutation of the single miR-29 target site in the *ADAM12-L* 3'UTR blunted the effect of miR-29b/c on the reporter activity, confirming direct targeting of the *ADAM12-L* 3'UTR region by miR-29b/c. The levels of the *ADAM12-S* splice variant were not changed by miR-29b/c, consistent with the lack of any predicted miR-29 target sites in the *ADAM12-S* 3'UTR.

The miR-29 family was reported previously to target the *Adam12* transcript in NIH3T3 cells [46]. miR-29 has been also implicated in the regulation of *Adam12* expression in response to transforming growth factor β (TGFβ) in experimental renal fibrosis in mice [47]. *Adam12* is the only splice variant known to exist in mice and, similar to human *ADAM12-L*, it contains a miR-29 target site. In humans, *ADAM12-L* was identified as one of the direct targets of miR-29b in trabecular meshwork cells, and increased expression of *ADAM12-L* in response to oxidative stress-induced down-regulation of miR-29b may contribute to the elevation of intra-ocular pressure in glaucoma [48]. In the context of breast cancer, miR-29b has been recently identified as a part of a GATA3-miR-29b axis, which regulates the tumor microenvironment and inhibits metastasis [33]. Down-regulation of miR-29 members also results in increased expression of the transcription factor KLF4 and expansion of stem-like cell populations *in vitro* and *in vivo* [34]. The miR-29 family is down-regulated in claudin-low cell lines and tumors, in which *ADAM12-L*, but not *ADAM12-S*, is strongly elevated. Thus, increased expression of *ADAM12-L* in claudin-low cell lines and tumors could be facilitated, at least in part, by low levels of miR-29 family members.

The third miRNA family tested here, miR-200, has not been previously reported to regulate ADAM12 expression. We have found that two members of this family, miR-200b and miR-200c, strongly diminished ADAM12-L protein in SUM159PT and SUM1315MO2 cells. Although the decrease in *ADAM12-L* mRNA was more modest, it reached statistical significance in SUM1315MO2 cells. The *ADAM12-L* 3'UTR reporter activity was reduced by miR-200b/c, despite the fact that the two predicted miR-200 target sites present in the *ADAM12-L* 3'UTR are not well conserved between species. Mutations within these two miR-200 target sites abolished the effect of transfected miR-200b/c mimics, suggesting direct interaction between miR-200b/c and the *ADAM12-L* 3'UTR. Similarly to miR-29, the miR-200 family is down-regulated in claudin-low tumors and cell lines. Thus, low expression of miR-200 family members, together with low expression of miR-29, may create permissive conditions for high expression of *ADAM12-L* in claudin-low tumors and cell lines.

Unexpectedly, transfection of miR-200b/c also down-regulated the *ADAM12* promoter, and the most logical explanation of this result is that miR-200b/c targeted a transcription factor (or factors) essential for ADAM12 expression. We tried to test this possibility by knocking-down the expression levels of two candidate transcription factors, ZEB1 and ETS1, which both have predicted binding sites in the *ADAM12* promoter and both are known targets of miR-200b/c [30, 31, 45]. However, we did not observe any changes in ADAM12-L protein levels after ZEB1 or ETS1 knock-down, indicating that either these factors are not involved in transcription of the *ADAM12* gene, or that their function is highly redundant and a loss of ZEB1 or ETS1 is readily compensated by other closely related transcription factors. The mechanism by which miR-200b/c down-regulates the *ADAM12* promoter is currently not known, and further studies are needed to identify transcription factors targeted by miR-200b/c.

By analyzing gene expression profiles of a panel of breast tumors available at the TCGA database and accessed via the cBioPortal, we found significant negative correlations between miR-29b/c, miR-30b/d, miR-200b/c, and *ADAM12* mRNA. This finding strongly supports a role for miR-29, miR-30, and miR-200 families in the regulation of *ADAM12* gene expression. It should be noted, however, that the cBioPortal contains only gene-level data, i.e., data for different splice variants of a given gene are merged together. If miR-29b/c, miR-30b/d, and miR-200b/c regulate *ADAM12-L* at the post-transcriptional level, and *ADAM12-S* is not regulated by these miRNAs post-transcriptionally, then merging the expression data for

ADAM12-L and *ADAM12-S* should make any correlations between miRNAs and *ADAM12-L* less evident. The fact that despite merging *ADAM12-L* and *ADAM12-S* expression data into single *ADAM12* values, significant negative correlations exist between miRNAs and *ADAM12* may indicate that a) the actual correlations between miRNAs and *ADAM12-L* are even higher and/or b) *ADAM12-L* is expressed at much higher levels than *ADAM12-S* in breast tumors and thus contributes more strongly to the merged *ADAM12* values. Since the protein products of *ADAM12-L* and *ADAM12-S* differ in their biochemical properties, cellular localization, and most likely substrate specificity and function, better understanding of the mechanisms controlling expression of each splice variant is an important step in the research on ADAM12 in breast cancer.

Conclusions

The *ADAM12-L* 3'UTR is a direct target of the miR-29 and miR-200 families. As miR-29 and miR-200 play important roles in breast cancer progression, these results may help explain different prognostic and chemopredictive values of *ADAM12-L* and *ADAM12-S* in breast cancer.

References

1. Kveiborg M, Albrechtsen R, Couchman JR, Wewer UM: Cellular roles of ADAM12 in health and disease. *Int J Biochem & Cell Biol* 2008, 40:1685-1702.

2. Nyren-Erickson EK, Jones JM, Srivastava DK, Mallik S: A Disintegrin and Metalloproteinase-12 (ADAM12): function, roles in disease progression, and clinical implications. *Biochim Biophys Acta* 2013, 1830:4445-4455.

3. Kveiborg M, Frohlich C, Albrechtsen R, Tischler V, Dietrich N, Holck P, Kronqvist P, Rank F, Mercurio AM, Wewer UM: A role for ADAM12 in breast tumor progression and stromal cell apoptosis. *Cancer Res* 2005, 65:4754-4761.

4. Frohlich C, Nehammer C, Albrechtsen R, Kronqvist P, Kveiborg M, Sehara-Fujisawa A, Mercurio AM, Wewer UM: ADAM12 produced by tumor cells rather than stromal cells accelerates breast tumor progression. *Mol Cancer Res* 2011, 9:1449-1461.

5. Dyczynska E, Syta E, Sun D, Zolkiewska A: Breast cancer-associated mutations in metalloprotease disintegrin ADAM12 interfere with the intracellular trafficking and processing of the protein. *Int J Cancer* 2008, 122:2634-2640.

6. Stautz D, Wewer UM, Kveiborg M: Functional analysis of a breast cancer-associated mutation in the intracellular domain of the metalloprotease ADAM12. *PLoS One* 2012, 7:e37628.

7. Qi Y, Duhachek-Muggy S, Li H, Zolkiewska A: Phenotypic diversity of breast cancer-related mutations in metalloproteinase-disintegrin ADAM12. *PLoS One* 2014, 9:e92536.

8. Kveiborg M, Albrechtsen R, Couchman JR, Wewer UM: Cellular roles of ADAM12 in health and disease. *Int J Biochem Cell Biol* 2008, 40:1685-1702.

9. Duhachek-Muggy S, Li H, Qi Y, Zolkiewska A: Alternative mRNA splicing generates two distinct ADAM12 pro-domain variants. *PLoS One* 2013, 8:e75730.

10. Prat A, Parker JS, Karginova O, Fan C, Livasy C, Herschkowitz JI, He X, Perou CM: Phenotypic and molecular characterization of the claudin-low intrinsic subtype of breast cancer. *Breast Cancer Res* 2010, 12:R68.

11. Harrell JC, Pfefferle AD, Zalles N, Prat A, Fan C, Khramtsov A, Olopade OI, Troester MA, Dudley AC, Perou CM: Endothelial-like properties of claudin-low breast cancer cells promote tumor vascular permeability and metastasis. *Clin Exp Metastasis* 2014, 31:33-45.

12. Li H, Duhachek-Muggy S, Dubnicka S, Zolkiewska A: Metalloproteinase-disintegrin ADAM12 is associated with a breast tumor-initiating cell phenotype. *Breast Cancer Res Treat* 2013, 139:691-703.

13. Taube JH, Herschkowitz JI, Komurov K, Zhou AY, Gupta S, Yang J, Hartwell K, Onder TT, Gupta PB, Evans KW *et al*: Core epithelial-to-mesenchymal transition interactome gene-expression signature is associated with claudin-low and metaplastic breast cancer subtypes. *Proc Natl Acad Sci USA* 2010, 107:15449-15454.

14. Gupta PB, Onder TT, Jiang G, Tao K, Kuperwasser C, Weinberg RA, Lander ES: Identification of selective inhibitors of cancer stem cells by high-throughput screening. *Cell* 2009, 138:645-659.

15. Onder TT, Gupta PB, Mani SA, Yang J, Lander ES, Weinberg RA: Loss of E-cadherin promotes metastasis via multiple downstream transcriptional pathways. *Cancer Res* 2008, 68:3645-3654.

16. Scheel C, Eaton EN, Li SH, Chaffer CL, Reinhardt F, Kah KJ, Bell G, Guo W, Rubin J, Richardson AL *et al*: Paracrine and autocrine signals induce and maintain mesenchymal and stem cell states in the breast. *Cell* 2011, 145:926-940.

17. Dontu G, Abdallah WM, Foley JM, Jackson KW, Clarke MF, Kawamura MJ, Wicha MS: In vitro propagation and transcriptional profiling of human mammary stem/progenitor cells. *Genes Dev* 2003, 17:1253-1270.

18. Creighton CJ, Li X, Landis M, Dixon JM, Neumeister VM, Sjolund A, Rimm DL, Wong H, Rodriguez A, Herschkowitz JI *et al*: Residual breast cancers after conventional therapy display mesenchymal as well as tumor-initiating features. *Proc Natl Acad Sci USA* 2009, 106:13820-13825.

19. Miller WR, Larionov AA, Renshaw L, Anderson TJ, White S, Murray J, Murray E, Hampton G, Walker JR, Ho S *et al*: Changes in breast cancer transcriptional profiles after treatment with the aromatase inhibitor, letrozole. *Pharmacogenet Genomics* 2007, 17:813-826.

20. Farmer P, Bonnefoi H, Anderle P, Cameron D, Wirapati P, Becette V, Andre S, Piccart M, Campone M, Brain E *et al*: A stroma-related gene signature predicts resistance to neoadjuvant chemotherapy in breast cancer. *Nature Medicine* 2009, 15:68-74.

21. Ayers M, Symmans WF, Stec J, Damokosh AI, Clark E, Hess K, Lecocke M, Metivier J, Booser D, Ibrahim N *et al*: Gene expression profiles predict complete pathologic response to neoadjuvant paclitaxel and fluorouracil, doxorubicin, and cyclophosphamide chemotherapy in breast cancer. *J Clin Oncology* 2004, 22:2284-2293.

22. Popovici V, Chen W, Gallas BG, Hatzis C, Shi W, Samuelson FW, Nikolsky Y, Tsyganova M, Ishkin A, Nikolskaya T *et al*: Effect of training-sample size and classification difficulty on the accuracy of genomic predictors. *Breast Cancer Research* 2010, 12:R5.

23. Wang Y, Klijn JG, Zhang Y, Sieuwerts AM, Look MP, Yang F, Talantov D, Timmermans M, Meijer-van Gelder ME, Yu J *et al*: Gene-expression profiles to predict distant metastasis of lymph-node-negative primary breast cancer. *Lancet* 2005, 365:671-679.

24. Minn AJ, Gupta GP, Padua D, Bos P, Nguyen DX, Nuyten D, Kreike B, Zhang Y, Wang Y, Ishwaran H *et al*: Lung metastasis genes couple breast tumor size and metastatic spread. *Proc Nat Acad Sci USA* 2007, 104:6740-6745.

25. Desmedt C, Piette F, Loi S, Wang Y, Lallemand F, Haibe-Kains B, Viale G, Delorenzi M, Zhang Y, d'Assignies MS *et al*: Strong time dependence of the 76-gene prognostic signature for node-negative breast cancer patients in the TRANSBIG multicenter independent validation series. *Clin Cancer Res* 2007, 13:3207-3214.

26. Li H, Duhachek-Muggy S, Qi Y, Hong Y, Behbod F, Zolkiewska A: An essential role of metalloprotease-disintegrin ADAM12 in triple-negative breast cancer. *Breast Cancer Res Treat* 2012, 135:759-769.

27. Schwarzenbacher D, Balic M, Pichler M: The role of microRNAs in breast cancer stem cells. *Int J Mol Sci* 2013, 14:14712-14723.

28. D'Amato NC, Howe EN, Richer JK: MicroRNA regulation of epithelial plasticity in cancer. *Cancer Letters* 2013, 341:46-55.

29. Shimono Y, Zabala M, Cho RW, Lobo N, Dalerba P, Qian D, Diehn M, Liu H, Panula SP, Chiao E *et al*: Downregulation of miRNA-200c links breast cancer stem cells with normal stem cells. *Cell* 2009, 138:592-603.

30. Gregory PA, Bert AG, Paterson EL, Barry SC, Tsykin A, Farshid G, Vadas MA, Khew-Goodall Y, Goodall GJ: The miR-200 family and miR-205 regulate epithelial to mesenchymal transition by targeting ZEB1 and SIP1. *Nat Cell Biol* 2008, 10:593-601.

31. Gregory PA, Bracken CP, Smith E, Bert AG, Wright JA, Roslan S, Morris M, Wyatt L, Farshid G, Lim YY *et al*: An autocrine TGF-β/ZEB/miR-200 signaling network regulates establishment and maintenance of epithelial-mesenchymal transition. *Mol Biol Cell* 2011, 22:1686-1698.

32. Wright JA, Richer JK, Goodall GJ: microRNAs and EMT in mammary cells and breast cancer. *J Mamm Gland Biology Neoplasia* 2010, 15:213-223.

33. Chou J, Lin JH, Brenot A, Kim JW, Provot S, Werb Z: GATA3 suppresses metastasis and modulates the tumour microenvironment by regulating microRNA-29b expression. *Nature Cell Biol* 2013, 15:201-213.

34. Cittelly DM, Finlay-Schultz J, Howe EN, Spoelstra NS, Axlund SD, Hendricks P, Jacobsen BM, Sartorius CA, Richer JK: Progestin suppression of miR-29 potentiates dedifferentiation of breast cancer cells via KLF4. *Oncogene* 2013, 32:2555-2564.

35. Yu F, Deng H, Yao H, Liu Q, Su F, Song E: Mir-30 reduction maintains self-renewal and inhibits apoptosis in breast tumor-initiating cells. *Oncogene* 2010, 29:4194-4204.

36. Ouzounova M, Vuong T, Ancey PB, Ferrand M, Durand G, Le-Calvez Kelm F, Croce C, Matar C, Herceg Z, Hernandez-Vargas H: MicroRNA miR-30 family regulates non-attachment growth of breast cancer cells. *BMC Genomics* 2013, 14:139.

37. The TCGA Network: Comprehensive molecular portraits of human breast tumours. *Nature* 2012, 490:61-70.

38. Gao J, Aksoy BA, Dogrusoz U, Dresdner G, Gross B, Sumer SO, Sun Y, Jacobsen A, Sinha R, Larsson E *et al*: Integrative analysis of complex cancer genomics and clinical profiles using the cBioPortal. *Science Signaling* 2013, 6:pl1.

39. Cerami E, Gao J, Dogrusoz U, Gross BE, Sumer SO, Aksoy BA, Jacobsen A, Byrne CJ, Heuer ML, Larsson E *et al*: The cBio cancer genomics portal: an open platform for exploring multidimensional cancer genomics data. *Cancer Discov* 2012, 2:401-404.

40. Prat A, Karginova O, Parker JS, Fan C, He X, Bixby L, Harrell JC, Roman E, Adamo B, Troester M *et al*: Characterization of cell lines derived from breast cancers and normal mammary tissues for the study of the intrinsic molecular subtypes. *Breast Cancer Res Treat* 2013, 142:237-255.

41. Neve RM, Chin K, Fridlyand J, Yeh J, Baehner FL, Fevr T, Clark L, Bayani N, Coppe JP, Tong F *et al*: A collection of breast cancer cell lines for the study of functionally distinct cancer subtypes. *Cancer Cell* 2006, 10:515-527.

42. Nygren MK, Tekle C, Ingebrigtsen VA, Makela R, Krohn M, Aure MR, Nunes-Xavier CE, Perala M, Tramm T, Alsner J *et al*: Identifying microRNAs regulating B7-H3 in breast cancer: the clinical impact of microRNA-29c. *British J Cancer* 2014, 110:2072-2080.

43. Iorio MV, Ferracin M, Liu CG, Veronese A, Spizzo R, Sabbioni S, Magri E, Pedriali M, Fabbri M, Campiglio M *et al*: MicroRNA gene expression deregulation in human breast cancer. *Cancer Res* 2005, 65:7065-7070.

44. Riaz M, van Jaarsveld MT, Hollestelle A, Prager-van der Smissen WJ, Heine AA, Boersma AW, Liu J, Helmijr J, Ozturk B, Smid M *et al*: miRNA expression profiling of 51 human breast cancer cell lines reveals subtype and driver mutation-specific miRNAs. *Breast Cancer Res* 2013, 15:R33.

45. Chan YC, Khanna S, Roy S, Sen CK: miR-200b targets Ets-1 and is down-regulated by hypoxia to induce angiogenic response of endothelial cells. *J Biol Chem* 2011, 286:2047-2056.

46. Li H, Solomon E, Duhachek Muggy S, Sun D, Zolkiewska A: Metalloprotease-disintegrin ADAM12 expression is regulated by Notch signaling via microRNA-29. *J Biol Chem* 2011, 286:21500-21510.

47. Ramdas V, McBride M, Denby L, Baker AH: Canonical transforming growth factor-beta signaling regulates disintegrin metalloprotease expression in experimental renal fibrosis via miR-29. *Am J Path* 2013, 183:1885-1896.

48. Luna C, Li G, Qiu J, Epstein DL, Gonzalez P: Role of miR-29b on the regulation of the extracellular matrix in human trabecular meshwork cells under chronic oxidative stress. *Mol Vision* 2009, 15:2488-2497.

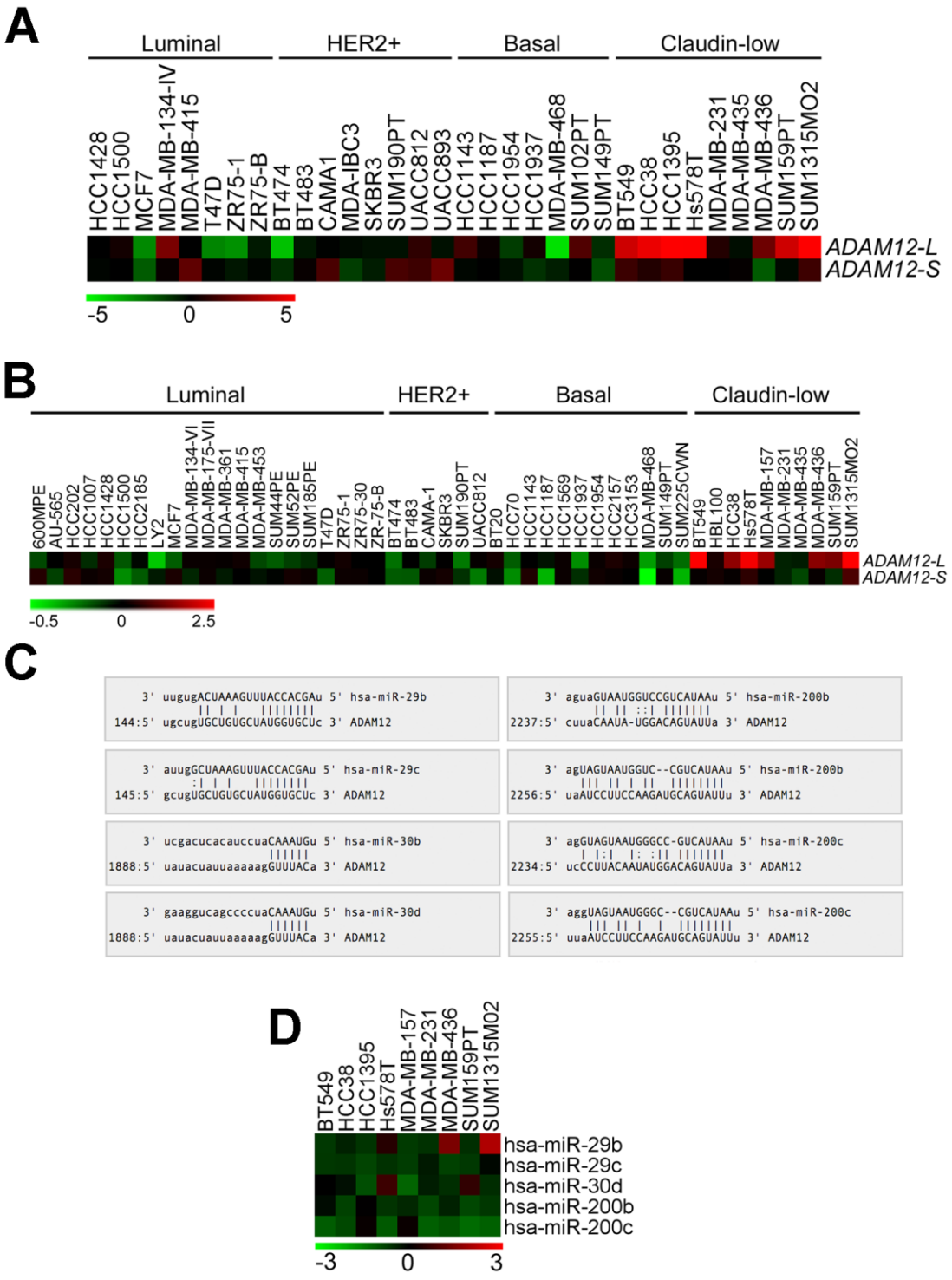

Figure 2.1 Pattern of expression of *ADAM12-L*, *ADAM12-S*, and miRNAs in breast cancer cell lines

(A) Discrepancy between *ADAM12-L* and *ADAM12-S* levels in a panel of human breast cancer cells profiled with the Agilent 4x44K microarray platform, based on ref. [40]. The expression data were retrieved from GEO:GSE50470. Expression values of *ADAM12-L* were

calculated as the average readouts for three probe-sets (A_23_P202327, NM_003474_2_4965, and NM_003474_2_4854). Expression values of *ADAM12-S* are based on the A_23_P350512 probe-set. (B) Discrepancy between *ADAM12-L* and *ADAM12-S* expression levels in a panel of human breast cancer cells profiled with the Affymetrix HG-U133A platform, based on ref. [41]. The expression data were retrieved from ArrayExpress, accession number E-TABM-157. (C) Predicted miR-29b/c, miR-30b/d, and miR-200b/c target sites in the human *ADAM12-L* 3'UTR, based on TargetScan Release 6.2. (D) miR-29b, miR-29c, miR-30d, miR-200b, and miR-200c levels in a panel of claudin-low cell lines, based on ref. [44]. Expression data for miR-30b were not available. In (A),(B), and (D), each colored square in the heatmaps represents the relative transcript abundance, in $\log_2$ space. Expression values were median-centered across all cell lines; in panel (D) only claudin-low cell lines are shown.

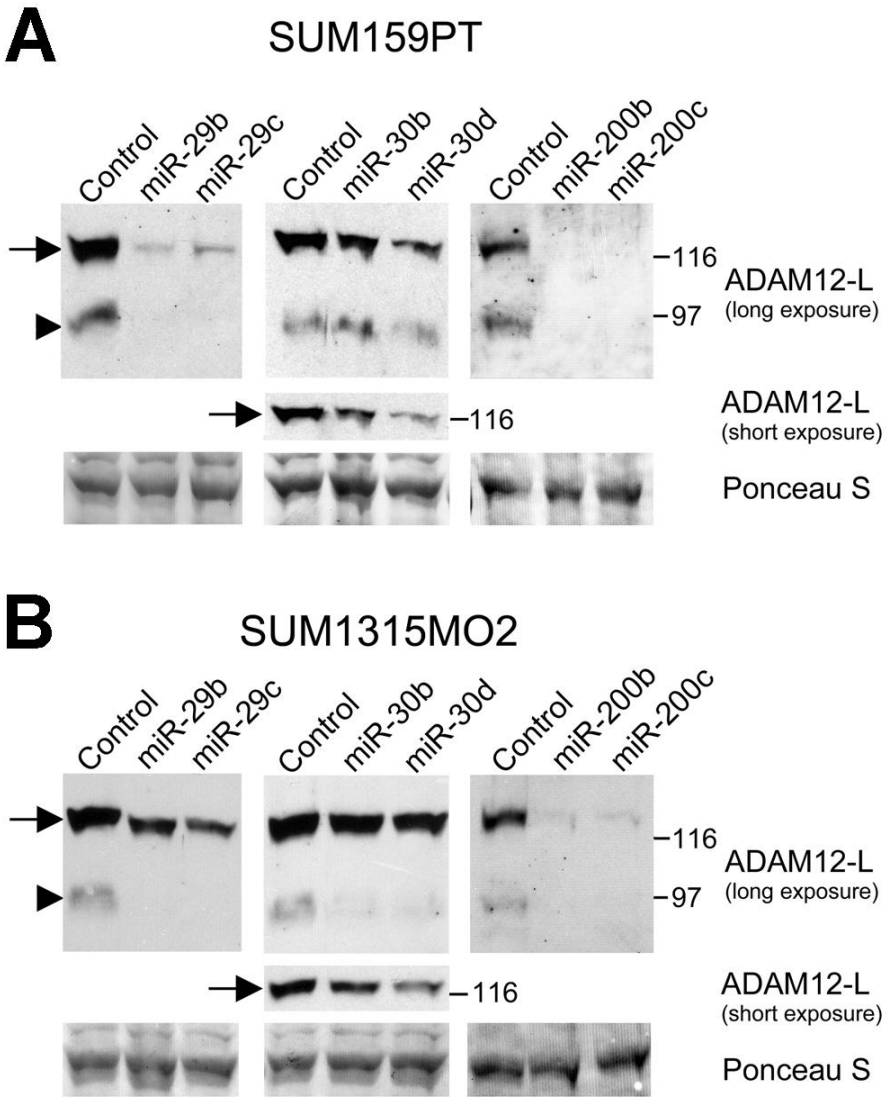

Figure 2.2 The effect of miRNAs on ADAM12-L protein levels

SUM159PT cells (A) or SUM1315MO2 cells (B) were transfected with the indicated miRNA mimics or mimic control. Cell lysates were enriched for glycoproteins and analyzed by Western blotting using an anti-ADAM12-L antibody. The arrow indicates the nascent, inactive ADAM12-L and the arrowhead indicates the processed, active form. For miR-30b/d-transfected cells, both long and short exposures of the Western blots are shown to better visualize the processed and the nascent forms, respectively. A band in the Ponceau S-stained membrane was used as a loading control. The images are representative blots from at least two repeated experiments.

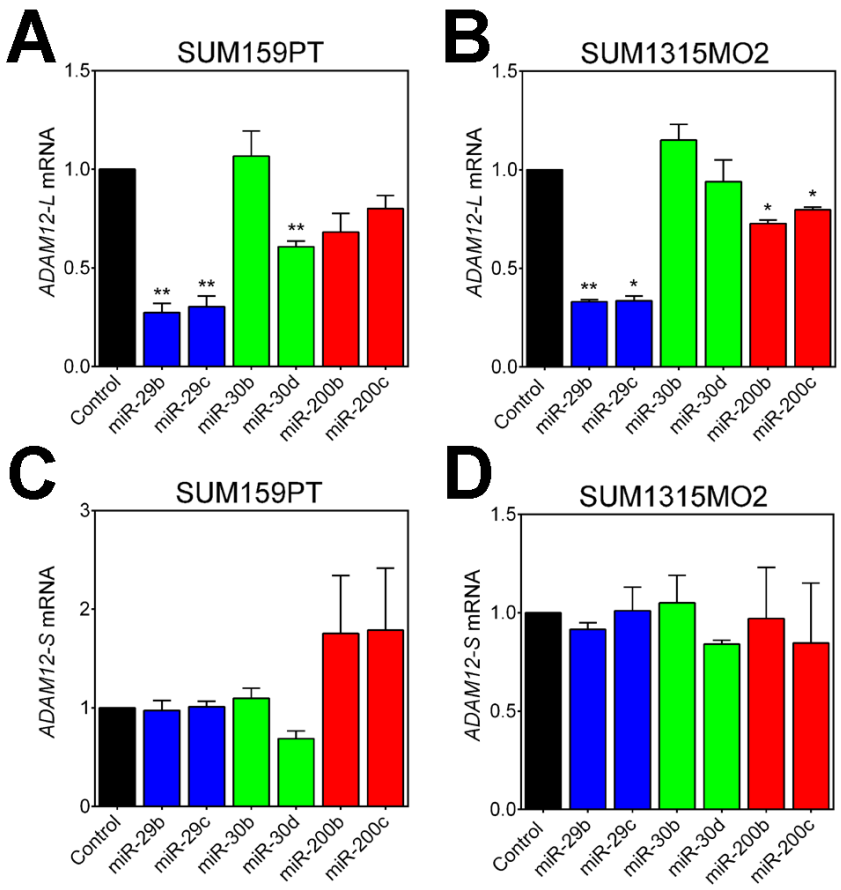

Figure 2.3 The effect of miRNAs on *ADAM12-L* and *ADAM12*-S mRNA levels in breast cancer cells

SUM159PT cells (A,C) or SUM1315MO2 cells (B,D) were transfected with the indicated miRNA mimics or mimic control. *ADAM12-L* (A,B) and *ADAM12-S* (C,D) mRNA levels were measured by qRT-PCR and normalized to β-ACTIN. Fold changes in mRNA levels in miRNA-transfected cells versus control cells were calculated. Graphs represent average values obtained in three (for SUM159PT) or two (for SUM1315MO2) independent experiments, ± SEM. Statistical significance was determined by one-sample t tests. * $P<0.05$ ** $P<0.01$

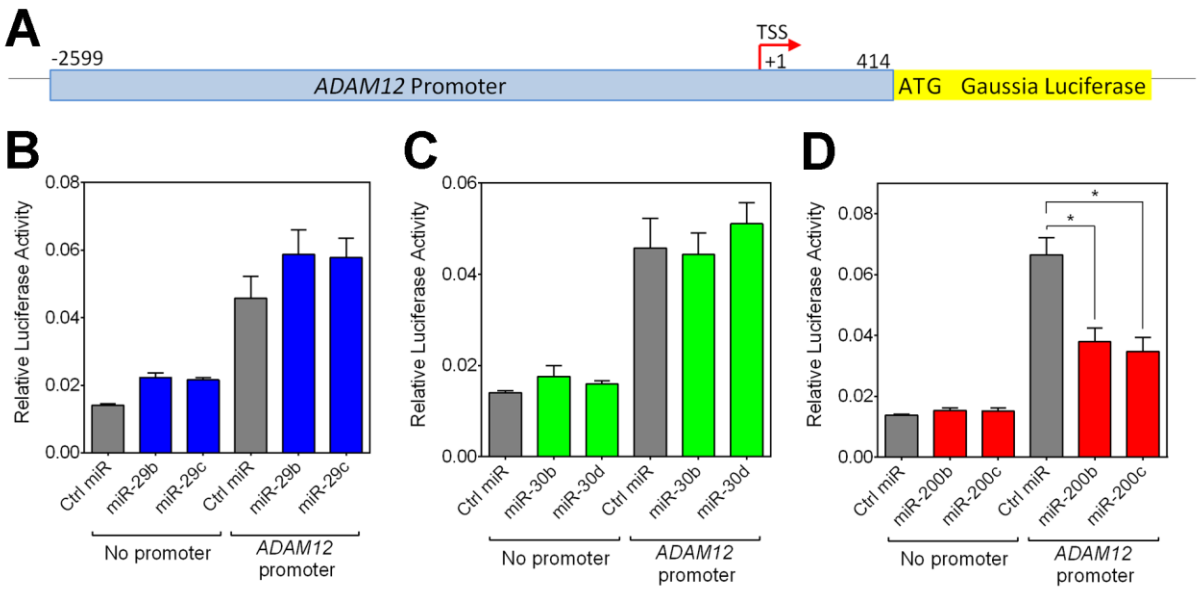

Figure 2.4 miR-200b/c, but not miR-29b/c or miR-30b/d, decrease the activity of the *ADAM12* promoter

(A) Diagram of the *ADAM12* promoter construct. The genomic region extending from -2599 nt to +414 nt, where +1 is the transcriptional start site (TSS), was cloned into the pEZX-PG04 vector upstream of the *Gaussia* luciferase gene. Nucleotides +1-413 represent the entire *ADAM12* 5'UTR. The vector also contained a secreted alkaline phosphatase gene under the control of the CMV promoter for use as an internal transfection control. (B-D) SUM159PT cells were transfected with miR-29b/c (B), miR-30b/d (C), miR-200b/c (D), or mimic control. The cells were then transfected with either the *ADAM12* promoter construct or a promoter-less pEZX-PG04 vector. Secreted luciferase and alkaline phosphatase were allowed to accumulate in the media for 48 hours prior to assaying. Graphs show the average values of *Gaussia* luciferase activity, normalized to alkaline phosphatase activity, ±SEM, obtained in six independent experiments. Significance was determined by Student's t test. * $P<0.05$.

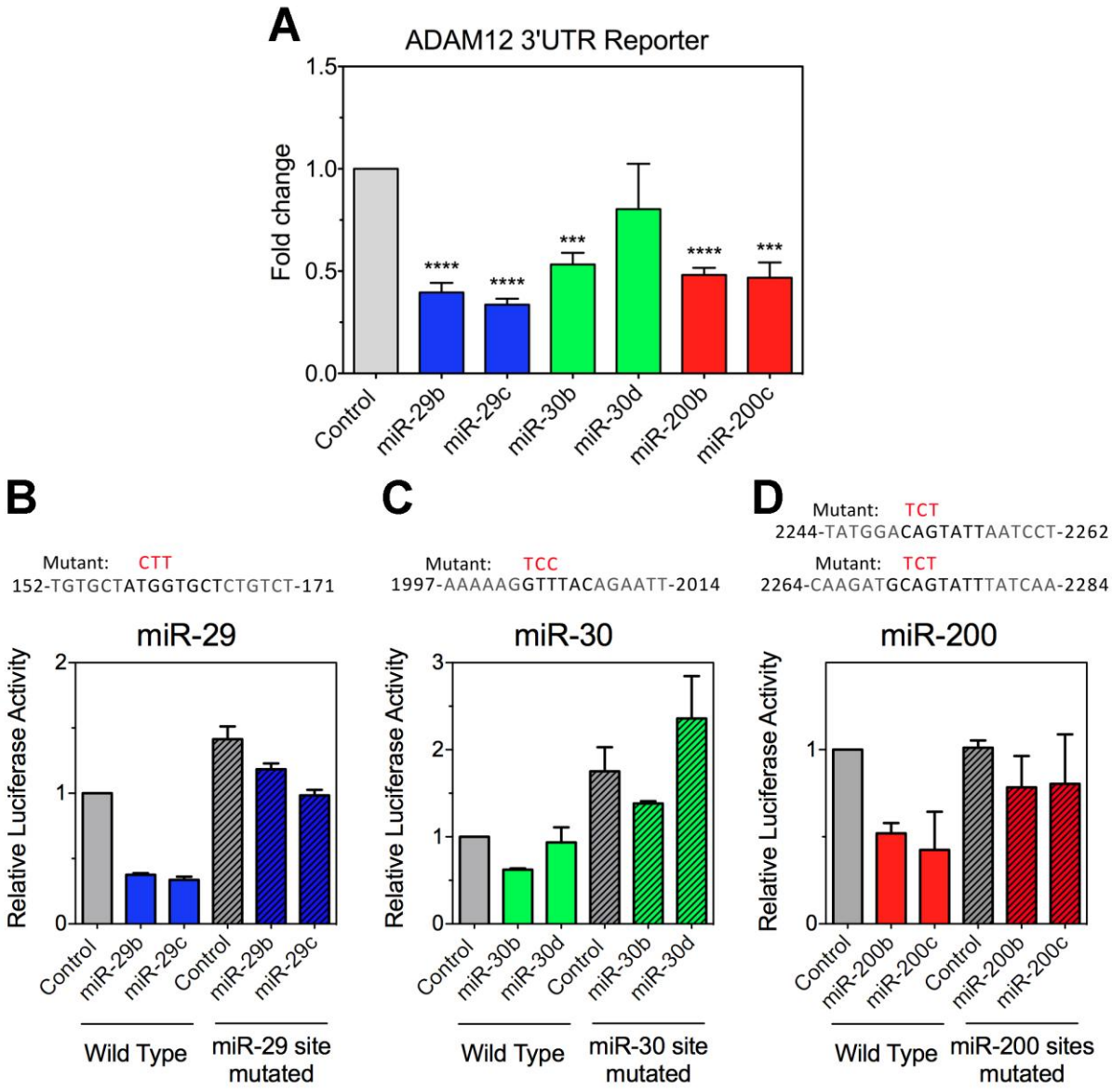

Figure 2.5 *ADAM12-L* 3'UTR is a target for miR-29b/c, miR-30b and miR-200b/c

(A) SUM159PT cells were transfected with the indicated miRNAs, and then with the *ADAM12* 3'UTR reporter or an empty reporter vector, and a *Renilla* luciferase control vector. The firefly luciferase activity was measured after 48 h and was normalized to *Renilla* luciferase and to the empty vector. Graph shows the average values for six independent experiments, ± SEM. Significance was determined by one-sample t-tests. *P<0.05, **P<0.01, ***P<0.001, ****P<0.0001. (B-D) *Upper* Three nucleotides in each putative miRNA target site (shown in black) were mutated to destroy the site. The mutated residues are shown in red above the wild-type sequence. The position in the *ADAM12-L* 3'UTR relative to the stop codon is indicated. *Lower* The effect of miR-29b/c (B), miR-30b/d (C) and miR-200b/c (D) on the wild-type and mutated *ADAM12-L* 3'UTRs. Samples were prepared and analyzed as in panel (A). The average values obtained in two independent experiments, ± SEM, are shown.

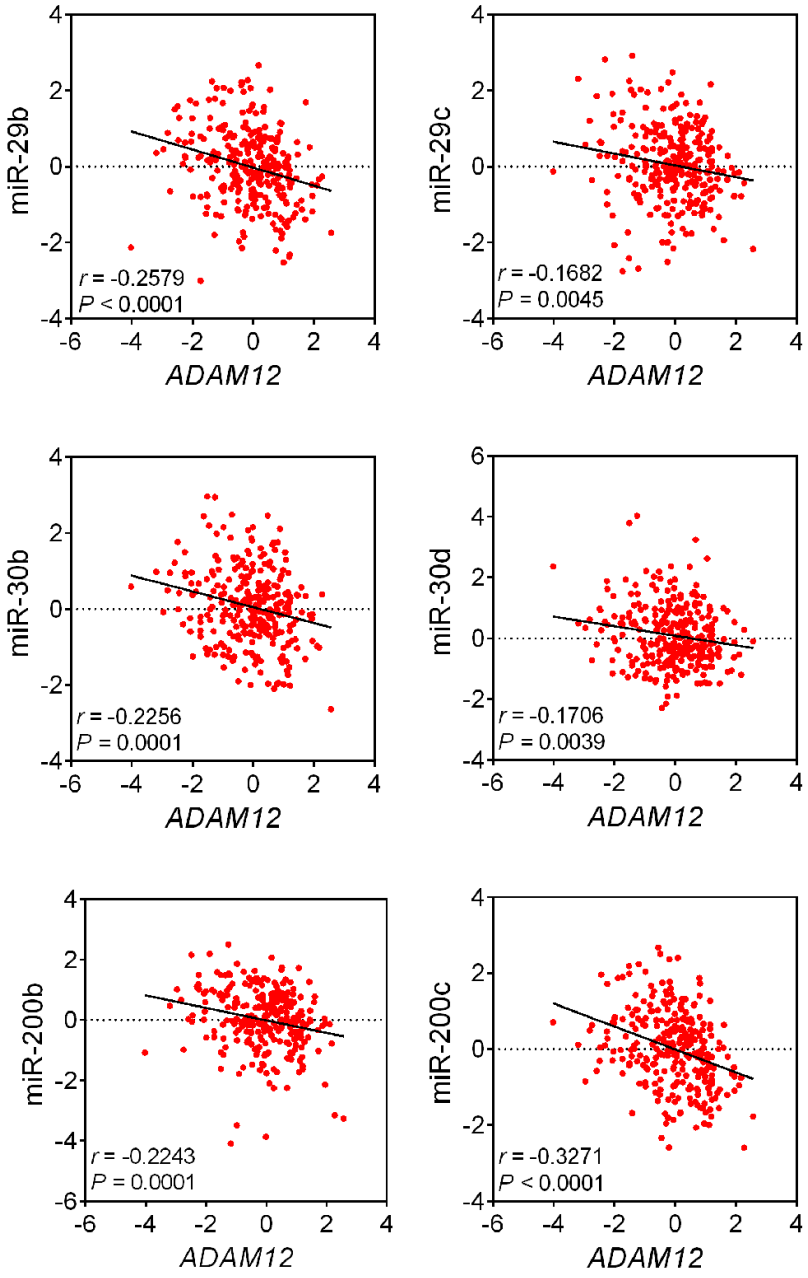

Figure 2.6 *ADAM12* mRNA negatively correlates with miR-29b/c, miR-30b/d and miR-200b/c in breast tumors

Correlation analyses of *ADAM12* mRNA and miR-29b/c, miR-30b/d, and miR-200b/c in 284 breast tumors from the TCGA database. *ADAM12* mRNA and miR29b/c, miR-30b/d or miR-200b/c were downloaded as Z-scores via the cBioPortal and were median-centered. Spearman *r* and P values are shown for each comparison.

Chapter 3 - Alternative mRNA splicing generates two distinct ADAM12 pro-domain variants

This chapter has been published as the following journal article:
Duhachek-Muggy, S., Li, H., Qi, Y., and Zolkiewska, A. (2013). Alternative mRNA splicing generates two distinct ADAM12 pro-domain variants. PLoS ONE 8(10):e75730.

Abstract

Human *ADAM12*, transcript variant 1 (later on referred to as Var1b), present in publicly available databases contains the sequence 5'-GTAATTCTG-3' at the nucleotide positions 340-348 of the coding region, at the 3' end of exon 4. The translation product of this variant, ADAM12-Lb, includes the three amino acid motif ^{114}VIL^{116} in the pro-domain. This motif is not conserved in ADAM12 from different species and is not present in other human ADAMs. Currently, it is not clear whether a shorter variant, Var1a, encoding the protein version without the ^{114}VIL^{116} motif, ADAM12-La, is expressed in human. In this work, we have established that human mammary epithelial cells and breast cancer cells express both Var1a and Var1b transcripts. Importantly, the proteolytic processing and intracellular trafficking of the corresponding ADAM12-La and ADAM12-Lb proteins are different. While ADAM12-La is cleaved and trafficked to the cell surface in a manner similar to ADAM12 in other species, ADAM12-Lb is retained in the EnR and is not proteolytically processed. Furthermore, the relative abundance of ADAM12-La and ADAM12-Lb proteins detected in several breast cancer cell lines varies significantly. We conclude that the canonical form of transmembrane ADAM12 is represented by Var1a/ADAM12-La, rather than Var1b/ADAM12-Lb currently featured in major sequence databases.

Introduction

The Disintegrin and Metalloprotease (ADAM) proteins belong to the M12B adamalysin protease subfamily (http://merops.sanger.ac.uk/, Ref. [1]). Canonical ADAMs are comprised of a pro-domain, a metalloprotease domain, a disintegrin domain, a cysteine-rich domain, an epidermal growth factor-like domain, a transmembrane helix, and a cytoplasmic tail. The human genome contains 21 different *ADAM* genes; however, only 13 of these genes encode functional

proteases [2, 3]. The catalytically active ADAMs contain the HEXXHXXGXXH motif in their metalloprotease domain, with three zinc-binding histidine residues and a catalytic glutamic acid [4]. The proteolytic activity of the metalloprotease is inhibited by the pro-domain. The mechanism of inhibition typically involves a cysteine-switch mechanism, in which a conserved cysteine residue from the pro-domain interacts with the zinc ion in the active site and prevents binding and cleavage of the substrate [5]. During maturation in the Golgi, the pro-domain is cleaved by furin-like enzymes and the metalloprotease is rendered active, although other modes of ADAM activation have also been postulated [6-9].

ADAM12 has an active metalloprotease domain, which has been shown to cleave a range of transmembrane substrate proteins. Depending on a cellular context, substrates include members of the epidermal growth factor (EGF) family of ligands (EGF and heparin-binding-EGF) [10–13], the Notch pathway ligand Delta-like 1 [14], sonic hedgehog [15], receptor tyrosine kinase Tie-2 [12], vascular endothelial (VE) cadherin [12], vascular endothelial growth factor receptor 2, or Flk-1 [12], Kit ligand 1 (Kitl1) [12], Vascular cell adhesion protein 1 (VCAM-1) [12], and ephrin-A1 [16]. In addition, ADAM12 facilitates Transforming Growth Factor β (TGFβ) signaling by a mechanism that is independent of its proteolytic activity and involves the accumulation and stabilization of TGFβ type II receptor in early endosomes [17].

While ADAM12 is transiently expressed during embryonic morphogenesis of skeletal muscles, visceral organs, and bone [18], ADAM12-deficient mice do not show major developmental abnormalities [19]. Post-natal ADAM12 expression in healthy and non-injured organs is low, but it is highly elevated in diseases accompanied by fibrosis, such as liver cirrhosis [20], muscle injury [21], scleroderma [22], chronic wounds [23], and cardiac hypertrophy [24]. Consistently, a recent genetic study in mice has shown that ADAM12 is expressed in mesenchymal perivascular cells (pericytes), which are programmed during vascular wall development, are activated in response to tissue injury, and generate pro-fibrotic myofibroblasts [25]. Furthermore, ADAM12 expression is strongly elevated in many cancers, including breast, head and neck, bone, lung, bladder, prostate, and brain cancers, as well as aggressive fibromatosis [26–39]. Recently, ADAM12 has been shown to be involved in the formation of invadopodia, cellular structures that aid cancer cell invasion, in head and neck, lung, and pancreatic cancer cells [13]. In breast cancers, ADAM12 is selectively up-regulated in the claudin-low subtype of tumors [40], which have aggressive characteristics, molecular signatures

of epithelial-to-mesenchymal transition, and are enriched in gene signatures of breast tumor-initiating cells [41]. By analyzing survival data of a large group of breast cancer patients, we have recently concluded that ADAM12 is the primary protease responsible for the activation of EGF receptor in early stage, lymph node-negative triple negative breast cancer (lacking the expression of estrogen receptor, progesterone receptor, and HER2) [42].

The human *ADAM12* gene is alternatively spliced, resulting in two major protein isoforms: a long, transmembrane form called ADAM12-L and a short, secreted form designated ADAM12-S [43]. The ADAM12-L isoform is encoded by transcript variant 1, or *ADAM12-var1*, which includes exons 1–18 and 20–24. ADAM12-S is encoded by transcript variant 2, or *ADAM12-var2*, which comprises exons 1–19. Furthermore, analysis of human *ADAM12* sequences present in major databases suggests that there are two forms of exon 4, with two alternative 3′ ends. The shorter form will be designated here exon 4a. The longer form, which ends 9 bp further downstream from exon 4a, will be designated exon 4b (Figure 3.1A). The alternative splicing event generating exon 4a and exon 4b is known as alternative 5′ splice site selection [44, 45].

Interestingly, according to the most recent releases of all major sequence databases, alternative splicing at exon 4a/b is present solely in the *ADAM12-var2* transcript, but not in the *ADAM12-var1* transcript. *ADAM12-var1*b and *ADAM12-var2b*, both containing the longer exon 4b, were first described by Gilpin et al. [46] (Figure 3.1B). These variants encode the ADAM12-Lb and ADAM12-Sb protein isoforms, respectively. *ADAM12-var2a*, containing the shorter exon 4a and encoding the ADAM12-Sa isoform, was later identified in a screen for novel secreted proteins [47]. *ADAM12-var1a* transcript and ADAM12-La protein isoform are not featured in any of the DNA/protein databases analyzed (Table 3.1). The 9-bp extension present selectively in exon 4b encodes a highly hydrophobic ^{114}VIL^{116} motif in the ADAM12 pro-domain (Figure 3.1C). This motif is not conserved in ADAM12 from other species or in other human ADAMs (Figure 3.2). Although the ^{114}VIL^{116} sequence is not positioned in a close proximity to the known furin-like cleavage site (^{204}RHKR^{207}) or to the cysteine responsible for the switch mechanism (Cys179), it can potentially affect the structure and/or function of the ADAM12 protein. The high hydrophobicity of this motif might change the stability of structural motifs in the pro-domain or may create a hydrophobic interface for interaction with other proteins.

In this study, we sought to determine whether *ADAM12-var1a* is expressed in human cells and whether any functional differences between the ADAM12-La and ADAM12-Lb protein isoforms exist. We found that breast epithelial cells, as well as breast cancer cells, do express *ADAM12-var1a*. Most importantly, while ADAM12-La protein is proteolytically processed and trafficked to the cell surface, ADAM12-Lb is poorly processed and is retained in the EnR. Furthermore, we show that the relative abundance of the endogenous ADAM12-La and ADAM12-Lb proteins detected in several breast cancer cell lines varies significantly. As the ^{114}VIL^{116} motif is not conserved between species and is not found in other members of the ADAM family, we conclude that the canonical form of ADAM12-L is ADAM12-La and not ADAM12-Lb.

Materials and Methods

Vector Construction

Full-length human *ADAM12var-1a* cDNA was amplified from MCF10DCIS.com cells using two consecutive PCR reactions with nested primers. The first set of primers was: 5′-GGA AAT CCC TCC GGT CGC GAC-3′ (F) and 5′-ACT GAC GGC AGT AGC TCA AAG-3′ (R). The second set of primers was: 5′-TAC CTT CAA TTG TGA AGG CCG GCG ACG ATG GC-3′ (F) and 5′-ACA CGT CGA CTC ACT TAA TAT AGG CGG TGT G-3′ (R). The underlined sequences in the forward and reverse primers of the second set correspond to the beginning and the end of the coding region of human *ADAM12-var1*, respectively. The PCR product was gel-purified, digested with MfeI and SalI, and cloned into the pBABEpuro retroviral expression vector at the EcoRI and the SalI sites. The nine-nucleotide insertion 5′-GTAATTCTG-3′ in exon 4b was generated using the QuickChange Site-Directed Mutagenesis kit (Stratagene). The entire lengths of the coding regions of *ADAM12-var1a* and *ADAM12-var1b* were sequenced to confirm the presence of the insertion and to exclude any PCR errors.

Cell Culture

MCF10DCIS.com cells were obtained from Asterand (Detroit, MI). MCF10A, MDA-MB-231, HEK293, and Hs578T cells were purchased from American Type Culture Collection (Manassas, VA). Phoenix Ampho cells, the retroviral packaging line, were obtained from Dr. Garry P. Nolan (Stanford University). MCF10DCIS.com cells were cultured in 1:1 (v/v)

Dulbecco's Modified Eagle Medium (DMEM)/Ham's F-12 containing 15 mM HEPES and supplemented with 5% horse serum and 29 mM sodium bicarbonate. MCF10A cells were cultured in DMEM/F-12 and supplemented with 5% horse serum, 0.5 µg/mL hydrocortisone, 20 ng/mL human EGF, 10 µg/mL insulin, 100 ng/mL cholera toxin and 1% penicillin/streptomycin. HEK293 and Phoenix Ampho cells were cultured in DMEM supplemented with 10% fetal bovine serum (FBS). Hs578T cells were cultured in DMEM containing 10% FBS and 10 µg/mL insulin. MDA-MB-231 cells were cultured in DMEM/F-12 with 10% FBS. All cells were maintained at 37°C in 5% CO_2.

Antibodies

Polyclonal rabbit anti-ADAM12 antibody (Ab#3394) raised against the cytoplasmic tail of human ADAM12-L [42] was used at a dilution of 1:20,000 for Western blotting and 1:500 for immunofluorescence. Mouse monoclonal anti-ADAM12 antibody (R&D Biosciences; clone 632525) was used for flow cytometric analysis at a dilution of 1:100. Other antibodies were: anti-β-actin (Sigma, clone AC-15; 1:20,000 dilution), anti-α-tubulin (Sigma, clone DM 1A; 1:40,000 dilution), anti-KDEL, an endoplasmic reticulum marker (Enzo Life Sciences, clone 10C3; 1:100 dilution), anti-TGN38, a trans-Golgi marker (BD Biosciences, clone 2; 1:50 dilution), anti-EEA1, an early endosomal marker (BD Biosciences, clone 14; 1:50 dilution), and anti-epidermal growth factor receptor (EGFR) (Cell Signaling Technologies, clone D38B1; 1:5,000 dilution).

Generation of Cells with Stable Overexpression of ADAM12-La or ADAM12-Lb

ADAM12-La and ADAM12-Lb were stably overexpressed in MCF10A cells using retroviral transduction. Phoenix Ampho cells were seeded in 100-mm plates 16 hours prior to transfection. pBabePuro retroviral expression vectors containing *ADAM12-var1a* or *ADAM12-var1b* sequences, or empty pBabePuro vector, were transfected into Phoenix Ampho cells using the calcium phosphate method (15 µg DNA/plate); 25 µM chloroquine was added to the medium prior to adding the DNA/$CaCl_2$ solution. Cells were incubated at 37°C for 24 h, then the medium was changed to fresh DMEM +10% FBS, and cells were incubated for additional 48 h at 32°C. The medium containing retroviruses was then collected and centrifuged at 500×g for 5 min. Supernatants were supplemented with 5 µg/mL polybrene (Sigma), and were added

without further dilution to MCF10A cells. Forty eight hours post-infection, cells with stable overexpression of ADAM12 proteins were selected using 2 µg/mL puromycin for 10 days.

Knock-down of ADAM12 Expression

siRNAs specific for exon 4a and exon 4b were designed using the Thermo Scientific siDESIGN Center. The antisense strand sequence of the exon 4a specific siRNA was 5′-UAG UAA CAG UGA CCC GUG UUU-3′ and was prepared as a regular siRNA. The antisense strand sequence of the exon 4b specific siRNA was 5′-UGA CCC AGA AUU ACC GUG UUU-3′ and was prepared with the proprietary ON-TARGET modifications. The siRNAs were diluted to 20 µM in 1×siRNA buffer (Thermo Scientific) and stored at -20°C. For transfection, siRNAs were used at a final concentration of 50 nM. DharmaFECT 1 transfection reagent was used according to the manufacturer's instructions. Transfection complexes were removed after 24 hours and cell lysates were collected for immunoblotting after 72 hours. In an alternative approach, ADAM12 was knocked-down using MISSION™ Lentiviral shADAM12 Transduction Particles (Sigma, clone ID TRCN0000047037), as described [40]. This shRNA clone targets the sequence GCCTGAATCGTCAATGTCAAA at the nucleotide position 1922–1942 in the ADAM12-var1a coding sequence and 1931–1951 in the ADAM12-var1b coding sequence. Control treatment included cell incubation with MISSION™ Non-Target shRNA Control Transduction Particles (Sigma, SHC002V). Transduction was performed according to the manufacturer's instructions. After one day, media containing lentiviral particles were replaced with fresh media, and after additional 24 h, stably transduced cells were selected with 3 µg/ml of puromycin for 7 days.

Immunoblotting

Cells were treated with lysis buffer (50 mM Tris-HCl pH 7.4, 150 mM NaCl, 1% Triton X-100, 0.5% sodium deoxycholate, 0.1% sodium dodecylsulfate (SDS), 5 mM EDTA, 1 mM 4-(2-Aminoethyl) benzenesulfonyl fluoride hydrochloride (AEBSF), 5 µg/mL pepstatin, 5 µg/mL leupeptin, 5 µg/mL aprotinin, and 10 mM 1,10-phenanthroline). Extracts were centrifuged for 15 minutes at 21,000×g at 4°C. For overexpressed ADAM12, the supernatants were resolved using SDS-PAGE (8%) and transferred to a nitrocellulose membrane. For endogenous ADAM12 detection, supernatants were enriched for glycoproteins by binding to concanavalin A agarose (Sigma; 25 µl resin/500 µl lysate) for 2 hours at 4°C prior to SDS-PAGE. Membranes

were blocked in 5% milk and 0.3% Tween-20 in Dulbecco's Phosphate Buffered Saline (DPBS). Rabbit anti-human ADAM12 (Ab#3394), mouse anti-β-actin, mouse anti-α-tubulin, and rabbit anti-EGFR antibodies were diluted in blocking buffer and incubated with the membranes. Horseradish peroxidase-conjugated anti-rabbit or anti-mouse antibodies were used as secondary antibodies. Signal detection was performed using SuperSignal West Pico Chemiluminescent Substrate (Pierce).

cDNA Preparation and RT-PCR

Total RNA was extracted using the Qiagen RNeasy kit. One microgram of the total RNA was treated with deoxyribonuclease I (Qiagen) and reverse-transcribed using the SuperScript III First Strand Synthesis system for RT-PCR (Invitrogen). A 100-bp fragment of ADAM12 cDNA including the exon 4-exon 5 splice junction was amplified using the following primers: 5′-GGT ACT GAT GTC TCC CTC GCT CG-3′ (F) and 5′-CGT GCT GAG ACT GAC TGC TGA ATC-3′(R). PCR products were resolved in a 2.0% agarose/TAE gel, visualized with ethidium bromide and UV illumination, and then extracted using the Qiaex II kit (Qiagen). DNA sequencing was performed at the Kansas State University DNA Sequencing and Genotyping Facility using the Applied Biosystems 3730 DNA Analyzer. The sequence of the *ADAM12-var1a* has been deposited in GenBank under the accession number KF444157.

Cell Surface Biotinylation

Cells grown in 6 well plates were washed with DPBS, then incubated at 4°C for 60 minutes with 2.5 mM EZ-link *N*-hydroxysuccinimide -PEG_{12}-biotin (Pierce) in DPBS. Remaining free reagent was quenched using 100 mM glycine. After washing cells several times with DPBS, cell lysates were collected as described above, and a fraction was retained as the input sample. The remaining lysate was allowed to adsorb onto Neutravidin agarose resin (Pierce) for 60 minutes at 4°C. The resin was washed three times with cell lysis buffer, followed by elution with SDS sample buffer. Samples were resolved by SDS-PAGE and transferred to a nitrocellulose membrane for immunoblotting.

Endo H Digestion

Cell lysate supernatants were prepared as described above. Supernatants were treated with 10×glycoprotein denaturation buffer (New England Biolabs) and boiled for 10 minutes.

After cooling, 10×G5 buffer (New England Biolabs) was added, and each sample was divided into two parts; each part was treated with or without Endo H (New England Biolabs) at 37°C for 1 hour. The reaction was stopped by adding SDS sample buffer and boiling. Samples were resolved by SDS-PAGE and transferred to a nitrocellulose membrane for immunoblotting.

Immunofluorescence

Cells were plated onto sterile coverslips and allowed to attach overnight. Cells were then washed and treated with 3.7% paraformaldehyde in DPBS for 20 minutes at room temperature. After the fixative was removed, cells were permeabilized with 0.1% Triton X-100 in DPBS for 5 minutes. The blocking step was performed using 1% bovine serum albumin (BSA) and 5% donkey serum in DPBS at for 30 minutes 37°C. Primary antibodies were diluted in 1% BSA in DPBS and incubation was performed for 60 minutes at 37°C. Red X-conjugated anti-rabbit (1:200) and AlexaFluor 488-conjugated anti-mouse (1:200) antibodies were diluted in 1% BSA in DPBS and incubated with the coverslips for 45 minutes at 37°C. After washing, coverslips were mounted onto slides and allowed to dry overnight. Slides were imaged at 63×magnification using a Zeiss Axiovert-200 inverted fluorescent microscope.

Flow Cytometry

Cells were trypsinized into a single cell suspension, washed with DPBS and incubated with monoclonal anti-ADAM12 antibody or isotype control antibody for 30 minutes on ice. Cells were then washed 3 times, incubated with allophycocyanin (APC)-conjugated anti-mouse antibodies (Jackson ImmunoResearch; 1:100) for 30 min on ice, and then with 1 µg/ml propidium iodide (Sigma) for viability. Analysis was performed using a BD FACSCalibur flow cytometer. Only the cells negative for propidium iodide (PI) staining (viable cells) were selected for the ADAM12 analysis.

Results

ADAM12 Transcripts Present in Human Mammary Epithelial Cells Contain Exon 4a and 4b

To determine which forms of exon 4 are present in *ADAM12* transcripts expressed by human mammary cells, we amplified a ~100-bp region surrounding the exon 4-exon 5 splice

junction using cDNA isolated from MCF10A mammary epithelial cell line. After PCR products were resolved by agarose gel electrophoresis, two bands were clearly visualized (Figure 3.3A). The two bands were excised from the gel and subjected to DNA sequencing. The lower band produced a single sequence that was identical to the sequence of the control vector containing a cloned *ADAM12-var1a* insert (Figure 3.3B). The upper band produced two sequences that had identical 5′-ends but then diverged at the site corresponding to the 3′-end of exon 4a, as indicated by the arrow. This might be due to the presence of heteroduplexes containing the 4a and 4b sequences in a non-denaturing gel, as well as unresolved 4a and 4b homoduplexes. Importantly, the chromatogram obtained for the upper band was indistinguishable from the chromatogram obtained for a mixture of *ADAM12-var1a* and *ADAM12-var1b* vector controls. We have concluded that the upper band represented, therefore, a mixture of *ADAM12* variants containing exon 4a and exon 4b.

ADAM12-Lb is Poorly Processed and is Retained in the EnR

Next, we examined the effect of the ^{114}VIL^{116} motif on the proteolytic processing and intracellular trafficking of ADAM12-L. The ADAM12-La and ADAM12-Lb isoforms were stably overexpressed in MCF10A cells, and cell lysates were subjected to immunoblotting using antibody specific for the intracellular domain of ADAM12-L. Cells overexpressing ADAM12-La produced two bands of similar intensities: the ~120-kDa band representing the nascent protein, and the ~90-kDa band corresponding to the processed form, after cleavage of the pro-domain (Figure 3.4A). In contrast, cells overexpressing ADAM12-Lb produced a major band of ~120 kDa, and a very weak band of ~90 kDa (Figure 3.4A). A similar pattern of bands was observed when ADAM12-La and ADAM12-Lb were stably overexpressed in HEK 293 cells. Thus, while ADAM12-La was readily processed in cells, the proteolytic processing of ADAM12-Lb was much less efficient.

Since the proteolytic processing of ADAMs occurs in the Golgi apparatus, we next probed the progression of ADAM12-La and ADAM12-Lb through the secretory pathway using endoglycosidase H (Endo H). Endo H readily cleaves high mannose-type oligosaccharides but cannot remove the complex oligosaccharides that result from modification by Golgi enzymes. As expected, the ~120-kDa form of ADAM12-La was sensitive to Endo H, and thus must have resided in the EnR. The ~90-kDa form of ADAM12-La was more resistant to Endo H and thus

must have been localized to the Golgi or post-Golgi compartments (Figure 3.4B). Importantly, the ~120-kDa ADAM12-Lb form was fully sensitive to Endo H, was not modified by Golgi enzymes, and thus must have been localized to a pre-Golgi compartment.

Next, we performed cell surface biotinylation of ADAM12-La and ADAM12-Lb. Live cells were incubated with an amine-reactive, membrane impermeable biotinylation reagent, biotinylated proteins were then isolated by adsorption to Neutravidin agarose beads and analyzed by Western blotting using anti-ADAM12 antibody. Comparison of the pattern of ~120-kDa and ~90-kDa ADAM12 bands in total cell lysates (inputs) and in eluates showed that the 90-kDa form of ADAM12-La and ADAM12-Lb was the predominant form that was biotinylated (Figure 3.4C). Importantly, the total amount of ADAM12-Lb protein eluted from the Neutravidin beads (the ~120-kDa and the ~90-kDa forms combined) was much lower than that of ADAM12-La. This result indicated that ADAM12-Lb localized to the cell surface more poorly than ADAM12-La.

To directly visualize subcellular localization of ADAM12-La and ADAM12-Lb in cells, immunofluorescence staining was performed using anti-ADAM12-L antibody and three different antibodies marking distinct compartments of the secretory pathway. Using anti-KDEL antibody, a marker of the EnR, we determined that ADAM12-La only partially localized to the EnR, and majority of ADAM12-La protein was found in post-EnR compartments (Figure 3.5A–C). In contrast, anti-ADAM12 staining of ADAM12-Lb-expressing cells fully co-localized with anti-KDEL staining (Figure 3.5D–F). Using anti-TGN38 antibody, a *trans*-Golgi marker, we detected partial co-staining with anti-ADAM12 antibody in ADAM12-La-expressing (Figure 3.5G–I), but not in ADAM12-Lb-expressing cells (Figure 3.5J–L). Finally, we examined co-localization of ADAM12 with EEA1, an early endosomal marker. It was previously shown that ADAM12 is constitutively internalized from the cell surface via the clathrin-dependent pathway and is detected in both early and recycling endosomes [17, 48]. Indeed, we detected partial co-localization of ADAM12-La with EEA1 (Figure 3.5M–O), but no co-localization was observed for ADAM12-Lb and EEA1 (Figure 3.5P–R). In summary, these results confirmed that ADAM12-Lb is efficiently retained in the EnR. To further explore whether ADAM12-Lb might have been misfolded and retained in the EnR by the EnR quality control system, we performed co-immunoprecipitation of ADAM12-Lb with several known EnR chaperones: BiP, ERp44, ERp72, Grp94, PDI and calnexin. None of these chaperones was detected in the anti-ADAM12-

Lb immunoprecipitates (results not shown). This data, together with the relative stability of the ADAM12-Lb protein, implied that the protein was not grossly misfolded.

Breast Cancer Cell Lines Show Different Relative Expression Levels of ADAM12-La and ADAM12-Lb

Next, we analyzed ADAM12-La and ADAM12-Lb expression in three cancer cell lines, Hs578T, MDA-MB-231, and MCF10DCIS.com. Hs578T and MDA-MB-231 cell lines represent claudin-low breast cancer cell lines, in which high levels of *ADAM12* transcript variant 1 were detected by microarray profiling [41]. MCF10DCIS.com is a breast cancer cell line derived from a tumor originating from xenografting premalignant MCF10AT cells into severe combined immunodeficient mice [49, 50]. MCF10DCIS.com cells are frequently used to model early breast cancer, and they express high levels of *ADAM12* transcript variant 1 [40]. First, we amplified a ~100-bp region surrounding the exon 4-exon 5 splice junction in *ADAM12* transcripts using cDNA isolated from Hs578T, MDA-MB-231, and MCF10DCIS.com cells and the same primer set as in Figure 3.3 above. The PCR band pattern was different for each of these three cell lines, with a single band indicative of exon 4a present in Hs578T cells, a predominant band indicative of exon 4b in MDA-MB-231 cells, and two bands detected in MCF10DCIS.com cells (Figure 3.6A). Consistently, Western blotting showed that Hs578T cells express high levels of ADAM12-La, whereas ADAM12-Lb is undetected in these cells (Figure 3.6B). Conversely, MDA-MB-231 express high levels of ADAM12-Lb, while ADAM12-La is below the detection limit. MCF10DCIS.com cells express both ADAM12-La and ADAM12-Lb isoforms. The apparent molecular weight of ADAM12-Lb in MDA-MB-231 and MCF10DCIS.com cells (~125-kDa) was noticeably larger than the molecular weight of the full-length ADAM12-La (~120-kDa) despite only a three-amino acid difference (^{114}VIL^{116}) in their pro-domains, which might be due to different glycosylation or other post-translational modifications. Analysis of live cells by flow cytometry using an antibody specific for the extracellular domain of ADAM12-L demonstrated that Hs578T and MCF10DCIS.com cells both had detectable levels of ADAM12-L at the surface, while MDA-MB-231 did not (Figure 3.6C). Additional immunoprecipitation experiments confirmed that this antibody recognized ADAM12-La and ADAM12-Lb equally well (Figure 3.8). Therefore, the lack of detection of ADAM12-L at the surface of live MDA-MB-231 cells corroborates the notion that these cells express predominantly the ADAM12-Lb

form that is retained in the EnR and not proteolytically processed in the Golgi. In contrast, Hs578T and MCF10DCIS.com cells express sizeable amounts of ADAM12-La that is transported out of the EnR, is proteolytically processed in the Golgi, and is trafficked to the cell surface.

To further confirm the identity of the ADAM12-La and ADAM12-Lb proteins detected in cancer cells, we generated siRNAs selectively targeting each variant (Figure 3.7A). The efficacy and specificity of these siRNAs were tested in HEK293 cells stably overexpressing ADAM12-La or ADAM12-Lb. The exon 4a siRNA efficiently knocked down ADAM12-La and had much lesser effect on ADAM12-Lb (Figure 3.7B). The exon 4b siRNA potently knocked down ADAM12-Lb and, unexpectedly, increased the level of ADAM12-La (Figure 3.7B). Although the mechanism of this increased expression of ADAM12-La by exon 4b siRNA is not clear, we have concluded that both siRNAs efficiently down-regulated the cognate ADAM12-L isoforms and thus were suitable for distinguishing between the endogenous ADAM12-La and ADAM12-Lb isoforms.

We selected Hs578T and MCF10DCIS.com cells for the siRNA analysis, because these cells expressed significantly more ADAM12-L than MDA-MB-231 cells. As expected, the two forms of ~120 kDa and ~90 kDa observed in Hs578T cells were down-regulated by an shRNA construct targeting both ADAM12-La and ADAM12-Lb (Figure 3.7C). When Hs578T cells were transfected with exon 4a-specific siRNA, both ~120-kDa and ~90-kDa isoforms were also reduced. In contrast, exon 4b siRNA did not down-regulate the ~120-kDa or the ~90-kDa form in Hs578T cells (Figure 3.7C). Thus, ADAM12-La represents the major ADAM12-L form in Hs578T cells. In MCF10DCIS.com cells, all three ADAM12-L forms of ~125 kDa, 120 kDa, and ~90 kDa were reduced by an shRNA construct targeting sequences common for both ADAM12-La and ADAM12-Lb (Figure 3.7D). Furthermore, exon 4a siRNA primarily diminished the ~120-kDa and ~90-kDa forms, and exon 4b diminished the ~125-kDa form (Figure 3.7D), indicating that these cells express both the ADAM12-La and ADAM12-Lb isoforms. Collectively, the results presented in Figures 3.6 and 3.7 suggest that both ADAM12-La and ADAM12-Lb are expressed at the endogenous levels in breast cancer cells, but their relative contribution to the overall ADAM12-L expression varies.

Discussion

In this work, we show that two alternative versions of exon 4 in human *ADAM12* transcripts exist, namely exon 4a and 4b. They arise as a result of alternative 5′ (or donor) splice site usage in intron 4-5. The two alternative donor sites are located 9 nt apart and are an example of tandem sites [45]. Both versions of exon 4 can be detected in *ADAM12* transcripts present in cultured human cells. Remarkably, *ADAM12* transcript variant 1 currently featured in all publicly available databases contains exclusively exon 4b. *ADAM12* transcript variant 1 with exon 4a, *ADAM12-var1a*, is not included in any of these databases. The translation products of variant 1 comprising exon 4a or 4b, ADAM12-La and ADAM12-Lb, differ by the sequence ^{114}VIL^{116} in the pro-domain, which is present only in the ADAM12-Lb protein isoform. Since the amino acid sequences of ADAM12 from other species, as well as sequences of other ADAMs, do not contain the VIL motif in their pro-domains, we believe that the ADAM12-La protein isoform (and the corresponding *ADAM12* transcript variant 1a) should be considered the "canonical" form of ADAM12.

We show that the ^{114}VIL^{116} motif has a dramatic impact on the intracellular trafficking and proteolytic processing of ADAM12-L protein. Unlike ADAM12-La, ADAM12-Lb protein containing this motif is retained in the EnR and is not transported to the cell surface. The mechanisms responsible for the retention of ADAM12-Lb in the EnR are not known. ADAM12-Lb does not seem to be grossly misfolded because: (a) it does not interact with major EnR chaperones, (b) it is glycosylated, and (c) it is not rapidly degraded by the EnR-associated protein degradation (ERAD) [51]. The question then arises: Is ADAM12-Lb catalytically active? According to the commonly accepted view of ADAM activation, proteolytic removal of the pro-domain in the Golgi is required for the disruption of the interaction between the inhibitory cysteine in the pro-domain and the zinc ion in the active site. Since ADAM12-Lb contains an intact pro-domain, it is expected to be catalytically inactive. However, according to other unconventional models of ADAM activation, conformational changes or protein-protein interactions involving the pro-domain may be sufficient to disrupt the cysteine-zinc interaction [6-9]. In such case, ADAM12-Lb may be, at least partially, catalytically active. Direct detection of ADAM12-Lb activity might prove challenging, however, since no potential ADAM12 substrates have been identified in the EnR so far. Although we did not study the proteolytic processing and trafficking of ADAM12-S here, we predict that the ^{114}VIL^{116} motif exerts a

similar effect on ADAM12-S as it does on ADAM12-L, i.e., ADAM12-Sa should be processed and secreted, whereas ADAM12-Sb is most likely retained in the EnR and is not processed.

The mechanisms dictating the selection of two alternative donor splice sites in intron 4-5 of the *ADAM12* transcripts are not clear. According to the Splice-Site Analyzer Tool (http://ibis.tau.ac.il/ssat/SpliceSiteFrame.htm, Ref. [52]), the splice site score for the sequence ACG/GTAATT at the donor site of exon 4a is 78.51, for the sequence CTG/GCACTG at the donor site of exon 4b this score is 63.57, and the score for a perfect donor site sequence CAG/GTAAGT is 100 ("/" indicate the exon/intron junction). Thus, the strength of the donor site in exon 4a seems somewhat higher than that in exon 4b. However, apart from the strength of donor sites, splice site selection is regulated by *cis*-acting elements such as exonic splicing enhancers (ESEs) or silencers (ESSs), and intronic splicing enhancers (ISEs) or silencers (ISSs). These splicing regulatory elements (SREs) recruit *trans*-acting splicing factors such as serine-arginine-rich (SR) proteins or heterogeneous nuclear ribonucleoprotein (hnRNPs), which activate or suppress splice site recognition [44, 45]. Indeed, multiple SREs are detected in exon 4 a/b and intron 4-5 by the ESR Research (http://esrsearch.tau.ac.il/) and ACESCAN2 (http://genes.mit.edu/acescan2/) site prediction tools (see also below).

An important question is whether the ratio of splicing at the two tandem sites, eventually translating into the ratio of ADAM12-La and ADAM12-Lb proteins, is maintained at a fixed level or whether it varies. Our examination of three different breast cancer cell lines indicates that the relative abundance of ADAM12-La and ADAM12-Lb is different in these lines. Interestingly, two of these cell lines, Hs578T and MDA-MB-231, have been classified as claudin-low, and all three express high levels of *ADAM12* transcript variant 1 mRNA (*ADAM12-var1a* and/or *ADAM12-var1b*), as determined by microarray profiling [41]. However, the predominant protein isoform in Hs578T cells is ADAM12-La, while MDA-MB-231 cells seem to express mainly the ADAM12-Lb protein isoform. MCF10DCIS.com cells, in contrast, express both ADAM12-La and ADAM12-Lb forms at a comparable level. Thus, individual genetic variations such as single nucleotide polymorphisms (SNPs) may contribute to the differences in the relative abundance of *ADAM12-var1a*/ADAM12-La and *ADAM12-var1b*/ADAM12-Lb.

It has been shown that naturally occurring polymorphisms can lead to the disappearance of a selective splice variant [53]. The donor splice site of exon 4b comprises an intronic SNP

C>T at chr10:127,843,783 (variation name: rs201532694). However, the splice site score for the sequence containing this SNP, CTG/GCATTG, is 64.36, and thus it is similar to the score of the main variant CTG/GCACTG (see above). There are five other intronic SNPs positioned close to the 5′ end of intron 4-5 and three synonymous SNPs in exon 4a (http://uswest.ensembl.org/Homo_sapiens/). Interestingly, these SNPs are located within the predicted SREs and thus they may cause variations in alternative splicing at the exon 4a/4b tandem sites.

Alternative splicing has been previously described for a number of *ADAM* genes. The most common splicing events among *ADAMs* include the inclusion or skipping of entire exons. The alternative use of cytosolic-encoding exons in human *ADAM15* generates ADAM15 protein isoforms with differential propensities to regulatory cytosolic interactions [54, 55]. Interestingly, aberrant patterns of *ADAM15* splice variants have been observed in human breast cancer cells [56]. Tissue specific insertion or skipping of cytosolic-encoding exons has been also reported for *ADAM22* [57, 58]. Furthermore, alternative usage of exons encoding membrane-proximal regions in the extracellular domains of ADAM9, -12, -19, -28, and -33 gives rise to circulating forms of the proteins, which lack the membrane-spanning and cytoplasmic domains [8, 37, 59–64]. Our studies provide for the first time an evidence of alternative 5′ splice site selection in an *ADAM* mRNA that results in variations in the amino acid sequence of the pro-domain, altered intracellular protein trafficking, and most likely an altered enzyme functionality.

Author Contributions

Conceived and designed the experiments: SDM HL AZ. Performed the experiments: SDM HL YQ. Analyzed the data: SDM HL AZ YQ. Wrote the paper: SDM AZ. Reviewed/edited the paper prior to submission: HL YQ.

References

1. Rawlings ND, Morton FR, Kok CY, Kong J, Barrett AJ (2008) MEROPS: the peptidase database. Nucleic Acids Res 36: D320–325. doi: 10.1093/nar/gkm954

2. Weber S, Saftig P (2012) Ectodomain shedding and ADAMs in development. Development 139: 3693–3709. doi: 10.1242/dev.076398

3. Edwards DR, Handsley MM, Pennington CJ (2008) The ADAM metalloproteinases. Mol Aspects Med 29: 258–289. doi: 10.1016/j.mam.2008.08.001

4. Gomis-Ruth FX (2009) Catalytic domain architecture of metzincin metalloproteases. J Biol Chem 284: 15353–15357. doi: 10.1074/jbc.r800069200

5. Van Wart HE, Birkedal-Hansen H (1990) The cysteine switch: a principle of regulation of metalloproteinase activity with potential applicability to the entire matrix metalloproteinase gene family. Proc Natl Acad Sci USA 87: 5578–5582. doi: 10.1073/pnas.87.14.5578

6. Scheller J, Chalaris A, Garbers C, Rose-John S (2011) ADAM17: a molecular switch to control inflammation and tissue regeneration. Trends Immunol 32: 380–387. doi: 10.1016/j.it.2011.05.005

7. Gonzales PE, Solomon A, Miller AB, Leesnitzer MA, Sagi I, et al. (2004) Inhibition of the tumor necrosis factor- α-converting enzyme by its pro-domain. J Biol Chem 279: 31638–31645. doi: 10.1074/jbc.m401311200

8. Sorensen HP, Vives RR, Manetopoulos C, Albrechtsen R, Lydolph MC, et al. (2008) Heparan sulfate regulates ADAM12 through a molecular switch mechanism. J Biol Chem 283: 31920–31932. doi: 10.1074/jbc.m804113200

9. Capasso R, Sambri I, Cimmino A, Salemme S, Lombardi C, et al. (2012) Homocysteinylated albumin promotes increased monocyte-endothelial cell adhesion and up-regulation of MCP1, Hsp60 and ADAM17. PLoS One 7: e31388. doi: 10.1371/journal.pone.0031388

10. Horiuchi K, Le Gall S, Schulte M, Yamaguchi T, Reiss K, et al. (2007) Substrate selectivity of epidermal growth factor-receptor ligand sheddases and their regulation by phorbol esters and calcium influx. Mol Biol Cell 18: 176–188. doi: 10.1091/mbc.e06-01-0014

11. Asakura M, Kitakaze M, Takashima S, Liao Y, Ishikura F, et al. (2002) Cardiac hypertrophy is inhibited by antagonism of ADAM12 processing of HB-EGF: metalloproteinase inhibitors as a new therapy. Nat Med 8: 35–40. doi: 10.1038/nm0102-35

12. Frohlich C, Klitgaard M, Noer JB, Kotzsch A, Nehammer C, et al. (2013) ADAM12 is expressed in the tumour vasculature and mediates ectodomain shedding of several membrane-anchored endothelial proteins. Biochem J 452: 97–109. doi: 10.1042/bj20121558

13. Diaz B, Yuen A, Iizuka S, Higashiyama S, Courtneidge SA (2013) Notch increases the shedding of HB-EGF by ADAM12 to potentiate invadopodia formation in hypoxia. J Cell Biol 201: 279–292. doi: 10.1083/jcb.201209151

14. Dyczynska E, Sun D, Yi H, Sehara-Fujisawa A, Blobel CP, et al. (2007) Proteolytic processing of Delta-like 1 by ADAM proteases. J Biol Chem 282: 436–444. doi: 10.1074/jbc.m605451200

15. Ohlig S, Farshi P, Pickhinke U, van den Boom J, Hoing S, et al. (2011) Sonic hedgehog shedding results in functional activation of the solubilized protein. Dev Cell 20: 764–774. doi: 10.1016/j.devcel.2011.05.010

16. Ieguchi K, Tomita T, Omori T, Komatsu A, Deguchi A, et al.. (2013) ADAM12-cleaved ephrin-A1 contributes to lung metastasis. Oncogene. doi: 10.1038/onc.2013.180.

17. Atfi A, Dumont E, Colland F, Bonnier D, L'Helgoualc'h A, et al. (2007) The disintegrin and metalloproteinase ADAM12 contributes to TGF-β signaling through interaction with the type II receptor. J Cell Biol 178: 201–208. doi: 10.1083/jcb.200612046

18. Kurisaki T, Masuda A, Osumi N, Nabeshima Y, Fujisawa-Sehara A (1998) Spatially- and temporally-restricted expression of meltrin α (ADAM12) and β (ADAM19) in mouse embryo. Mech Dev 73: 211–215. doi: 10.1016/s0925-4773(98)00043-4

19. Kurisaki T, Masuda A, Sudo K, Sakagami J, Higashiyama S, et al. (2003) Phenotypic analysis of Meltrin α (ADAM12)-deficient mice: involvement of Meltrin αin adipogenesis and myogenesis. Mol Cell Biol 23: 55–61. doi: 10.1128/mcb.23.1.55-61.2003

20. Le Pabic H, Bonnier D, Wewer UM, Coutand A, Musso O, et al. (2003) ADAM12 in human liver cancers: TGF-β-regulated expression in stellate cells is associated with matrix remodeling. Hepatology 37: 1056–1066. doi: 10.1053/jhep.2003.50205

21. Borneman A, Kuschel R, Fujisawa-Sehara A (2000) Analysis for transcript expression of meltrin α in normal, regenerating, and denervated rat muscle. J Muscle Res Cell Motil 21: 475–480.

22. Shi-Wen X, Renzoni EA, Kennedy L, Howat S, Chen Y, et al. (2007) Endogenous endothelin-1 signaling contributes to type I collagen and CCN2 overexpression in fibrotic fibroblasts. Matrix Biol 26: 625–632. doi: 10.1016/j.matbio.2007.06.003

23. Harsha A, Stojadinovic O, Brem H, Sehara-Fujisawa A, Wewer U, et al. (2008) ADAM12: a potential target for the treatment of chronic wounds. J Mol Med 86: 961–969. doi: 10.1007/s00109-008-0353-z

24. Wang X, Chow FL, Oka T, Hao L, Lopez-Campistrous A, et al. (2009) Matrix metalloproteinase-7 and ADAM-12 (a disintegrin and metalloproteinase-12) define a signaling axis in agonist-induced hypertension and cardiac hypertrophy. Circulation 119: 2480–2489. doi: 10.1161/circulationaha.108.835488

25. Dulauroy S, Di Carlo SE, Langa F, Eberl G, Peduto L (2012) Lineage tracing and genetic ablation of ADAM12(+) perivascular cells identify a major source of profibrotic cells during acute tissue injury. Nat Med 18: 12621270.

26. Iba K, Albrechtsen R, Gilpin BJ, Loechel F, Wewer UM (1999) Cysteine-rich domain of human ADAM 12 (meltrin α) supports tumor cell adhesion. Am J Pathol 154: 1489–1501. doi: 10.1016/s0002-9440(10)65403-x

27. Bertucci F, Finetti P, Cervera N, Charafe-Jauffret E, Mamessier E, et al. (2006) Gene expression profiling shows medullary breast cancer is a subgroup of basal breast cancers. Cancer Res 66: 4636–4644. doi: 10.1158/0008-5472.can-06-0031

28. Turashvili G, Bouchal J, Baumforth K, Wei W, Dziechciarkova M, et al. (2007) Novel markers for differentiation of lobular and ductal invasive breast carcinomas by laser microdissection and microarray analysis. BMC Cancer 7: 55. doi: 10.1186/1471-2407-7-55

29. Kveiborg M, Frohlich C, Albrechtsen R, Tischler V, Dietrich N, et al. (2005) A role for ADAM12 in breast tumor progression and stromal cell apoptosis. Cancer Res 65: 4754–4761. doi: 10.1158/0008-5472.can-05-0262

30. Lendeckel U, Kohl J, Arndt M, Carl-McGrath S, Donat H, et al. (2005) Increased expression of ADAM family members in human breast cancer and breast cancer cell lines. J Cancer Res Clin Oncol 131: 41–48. doi: 10.1007/s00432-004-0619-y

31. Mitsui Y, Mochizuki S, Kodama T, Shimoda M, Ohtsuka T, et al. (2006) ADAM28 is overexpressed in human breast carcinomas: implications for carcinoma cell proliferation through cleavage of insulin-like growth factor binding protein-3. Cancer Res 66: 9913–9920. doi: 10.1158/0008-5472.can-06-0377

32. Rao VH, Kandel A, Lynch D, Pena Z, Marwaha N, et al. (2012) A positive feedback loop between HER2 and ADAM12 in human head and neck cancer cells increases migration and invasion. Oncogene 31: 2888–2898. doi: 10.1038/onc.2011.460

33. Uehara E, Shiiba M, Shinozuka K, Saito K, Kouzu Y, et al. (2012) Upregulated expression of ADAM12 is associated with progression of oral squamous cell carcinoma. Int J Oncol 40: 1414–1422. doi: 10.3892/ijo.2012.1339

34. Georges S, Chesneau J, Hervouet S, Taurelle J, Gouin F, et al.. (2013) A Disintegrin And Metalloproteinase 12 produced by tumour cells accelerates osteosarcoma tumour progression and associated osteolysis. Eur J Cancer 49: 22532263.

35. Mino N, Miyahara R, Nakayama E, Takahashi T, Takahashi A, et al. (2009) A disintegrin and metalloprotease 12 (ADAM12) is a prognostic factor in resected pathological stage I lung adenocarcinoma. J Surg Oncol 100: 267–272. doi: 10.1002/jso.21313

36. Frohlich C, Albrechtsen R, Dyrskjot L, Rudkjaer L, Orntoft TF, et al. (2006) Molecular profiling of ADAM12 in human bladder cancer. Clin Cancer Res 12: 7359–7368. doi: 10.1158/1078-0432.ccr-06-1066

37. Peduto L, Reuter VE, Sehara-Fujisawa A, Shaffer DR, Scher HI, et al. (2006) ADAM12 is highly expressed in carcinoma-associated stroma and is required for mouse prostate tumor progression. Oncogene 25: 5462–5466. doi: 10.1038/sj.onc.1209536

38. Kodama T, Ikeda E, Okada A, Ohtsuka T, Shimoda M, et al. (2004) ADAM12 is selectively overexpressed in human glioblastomas and is associated with glioblastoma cell proliferation and shedding of heparin-binding epidermal growth factor. Am J Path 165: 1743–1753. doi: 10.1016/s0002-9440(10)63429-3

39. Skubitz KM, Skubitz AP (2004) Gene expression in aggressive fibromatosis. J Lab Clin Med 143: 89–98. doi: 10.1016/j.lab.2003.10.002

40. Li H, Duhachek-Muggy S, Dubnicka S, Zolkiewska A (2013) Metalloproteinase-disintegrin ADAM12 is associated with a breast tumor-initiating cell phenotype. Breast Cancer Res Treat 139: 691–703. doi: 10.1007/s10549-013-2602-2

41. Prat A, Parker JS, Karginova O, Fan C, Livasy C, et al. (2010) Phenotypic and molecular characterization of the claudin-low intrinsic subtype of breast cancer. Breast Cancer Res 12: R68. doi: 10.1186/bcr2635

42. Li H, Duhachek-Muggy S, Qi Y, Hong Y, Behbod F, et al. (2012) An essential role of metalloprotease-disintegrin ADAM12 in triple-negative breast cancer. Breast Cancer Res Treat 135: 759–769. doi: 10.1007/s10549-012-2220-4

43. Kveiborg M, Albrechtsen R, Couchman JR, Wewer UM (2008) Cellular roles of ADAM12 in health and disease. Int J Biochem Cell Biol 40: 1685–1702. doi: 10.1016/j.biocel.2008.01.025

44. Wang Z, Burge CB (2008) Splicing regulation: from a parts list of regulatory elements to an integrated splicing code. RNA 14: 802–813. doi: 10.1261/rna.876308

45. Hiller M, Platzer M (2008) Widespread and subtle: alternative splicing at short-distance tandem sites. Trends Genet 24: 246–255. doi: 10.1016/j.tig.2008.03.003

46. Gilpin BJ, Loechel F, Mattei MG, Engvall E, Albrechtsen R, et al. (1998) A novel, secreted form of human ADAM 12 (meltrin α) provokes myogenesis *in vivo*. J Biol Chem 273: 157–166. doi: 10.1074/jbc.273.1.157

47. Clark HF, Gurney AL, Abaya E, Baker K, Baldwin D, et al. (2003) The secreted protein discovery initiative (SPDI), a large-scale effort to identify novel human secreted and transmembrane proteins: a bioinformatics assessment. Genome Res 13: 2265–2270. doi: 10.1101/gr.1293003

48. Stautz D, Leyme A, Grandal MV, Albrechtsen R, van Deurs B, et al. (2012) Cell-surface metalloprotease ADAM12 is internalized by a clathrin- and Grb2-dependent mechanism. Traffic 13: 1532–1546. doi: 10.1111/j.1600-0854.2012.01405.x

49. Barnabas N, Cohen D (2013) Phenotypic and molecular characterization of MCF10DCIS and SUM breast cancer cell lines. Int J Breast Cancer 2013: 872743. doi: 10.1155/2013/872743

50. Miller FR, Santner SJ, Tait L, Dawson PJ (2000) MCF10DCIS.com xenograft model of human comedo ductal carcinoma in situ. J Natl Cancer Inst 92: 1185–1186. doi: 10.1093/jnci/92.14.1185a

51. Brodsky JL (2012) Cleaning up: ER-associated degradation to the rescue. Cell 151: 1163–1167. doi: 10.1016/j.cell.2012.11.012

52. Carmel I, Tal S, Vig I, Ast G (2004) Comparative analysis detects dependencies among the 5′ splice-site positions. RNA 10: 828–840. doi: 10.1261/rna.5196404

53. Hiller M, Huse K, Szafranski K, Jahn N, Hampe J, et al. (2006) Single-nucleotide polymorphisms in NAGNAG acceptors are highly predictive for variations of alternative splicing. Am J Hum Genet 78: 291–302. doi: 10.1086/500151

54. Kleino I, Ortiz RM, Huovila AP (2007) ADAM15 gene structure and differential alternative exon use in human tissues. BMC Mol Biol 8: 90. doi: 10.1186/1471-2199-8-90

55. Kleino I, Ortiz RM, Yritys M, Huovila AP, Saksela K (2009) Alternative splicing of ADAM15 regulates its interactions with cellular SH3 proteins. J Cell Bioch 108: 877–885. doi: 10.1002/jcb.22317

56. Ortiz RM, Karkkainen I, Huovila AP (2004) Aberrant alternative exon use and increased copy number of human metalloprotease-disintegrin ADAM15 gene in breast cancer cells. Genes, Chromosomes & Cancer 41: 366–378. doi: 10.1002/gcc.20102

57. Sagane K, Hayakawa K, Kai J, Hirohashi T, Takahashi E, et al. (2005) Ataxia and peripheral nerve hypomyelination in ADAM22-deficient mice. BMC Neurosci 6: 33.

58. Godde NJ, D'Abaco GM, Paradiso L, Novak U (2007) Differential coding potential of ADAM22 mRNAs. Gene 403: 80–88. doi: 10.1016/j.gene.2007.07.033

59. Howard L, Maciewicz RA, Blobel CP (2000) Cloning and characterization of ADAM28: evidence for autocatalytic pro-domain removal and for cell surface localization of mature ADAM28. Bioch J 348: 21–27. doi: 10.1042/0264-6021:3480021

60. Roberts CM, Tani PH, Bridges LC, Laszik Z, Bowditch RD (1999) MDC-L, a novel metalloprotease disintegrin cysteine-rich protein family member expressed by human lymphocytes. J Biol Chem 274: 29251–29259. doi: 10.1074/jbc.274.41.29251

61. Powell RM, Wicks J, Holloway JW, Holgate ST, Davies DE (2004) The splicing and fate of ADAM33 transcripts in primary human airways fibroblasts. Am J Resp Cell Mol Biol 31: 13–21. doi: 10.1165/rcmb.2003-0330oc

62. Mazzocca A, Coppari R, De Franco R, Cho JY, Libermann TA, et al. (2005) A secreted form of ADAM9 promotes carcinoma invasion through tumor-stromal interactions. Cancer Res 65: 4728–4738. doi: 10.1158/0008-5472.can-04-4449

63. Hotoda N, Koike H, Sasagawa N, Ishiura S (2002) A secreted form of human ADAM9 has an α-secretase activity for APP. Bioch Biophys Res Comm 293: 800–805. doi: 10.1016/s0006-291x(02)00302-9

64. Kurisaki T, Wakatsuki S, Sehara-Fujisawa A (2002) Meltrin β mini, a new ADAM19 isoform lacking metalloprotease and disintegrin domains, induces morphological changes in neuronal cells. FEBS Lett 532: 419–422. doi: 10.1016/s0014-5793(02)03732-8

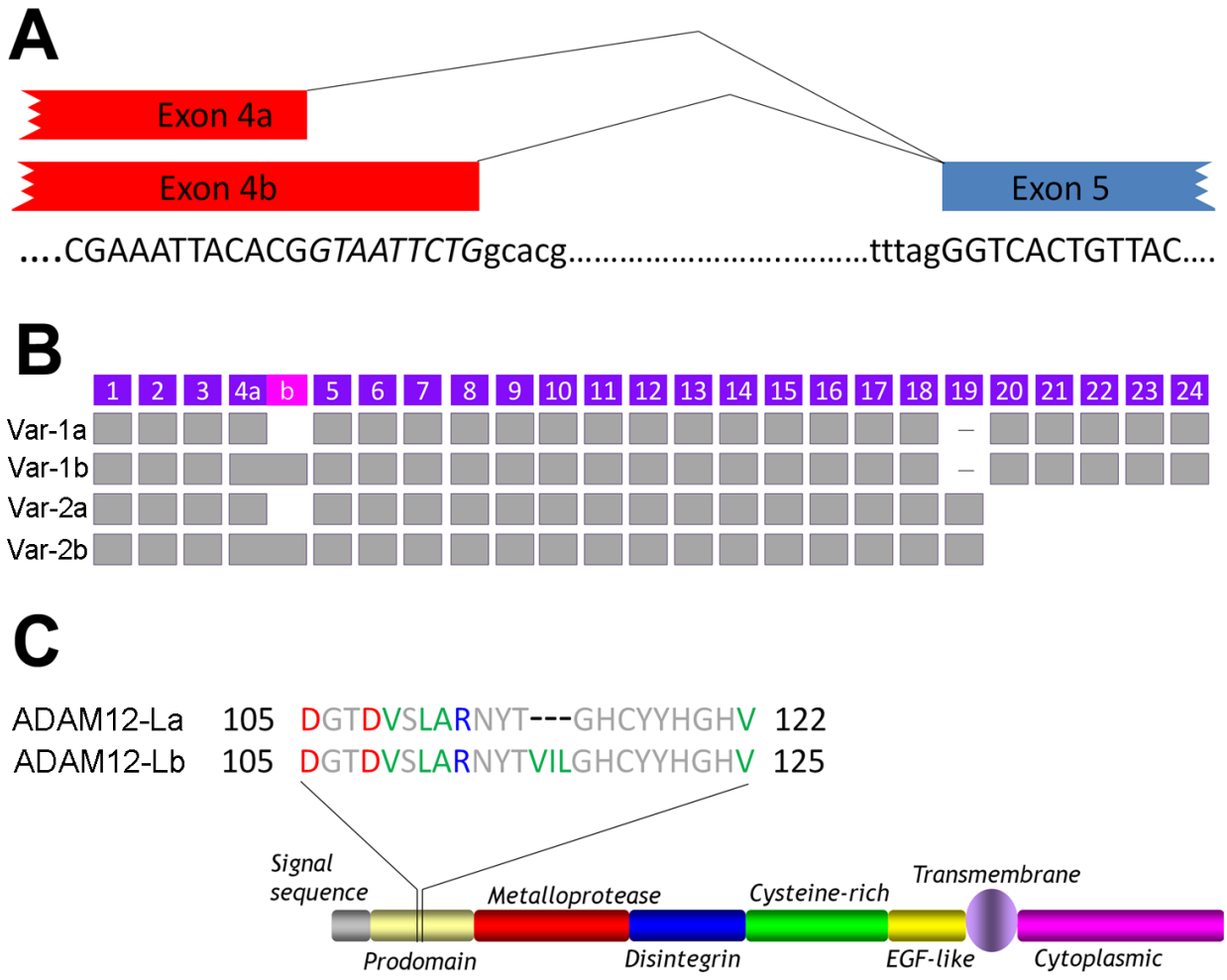

Figure 3.1 Alternative splicing of human *ADAM12* transcripts generates two ADAM12-L isoforms

(A) Diagram of the alternative mRNA splicing event at the exon 4-exon 5 junction. Capital letters represent exons and lower case letters represent the intron. The nine nucleotide sequence 5′-GTAATTCTG-3′ missing in exon 4a and present in exon 4b are shown in *italics*. (B) Exon composition of human *ADAM12* transcripts. The nine-nucleotide extension in exon 4b is shown in magenta. Exons are not drawn to scale. (C) Diagram of the two transmembrane protein isoforms: ADAM12-La, which lacks the ^{114}VIL^{116} motif in the pro-domain, and ADAM12-Lb, which includes this motif.

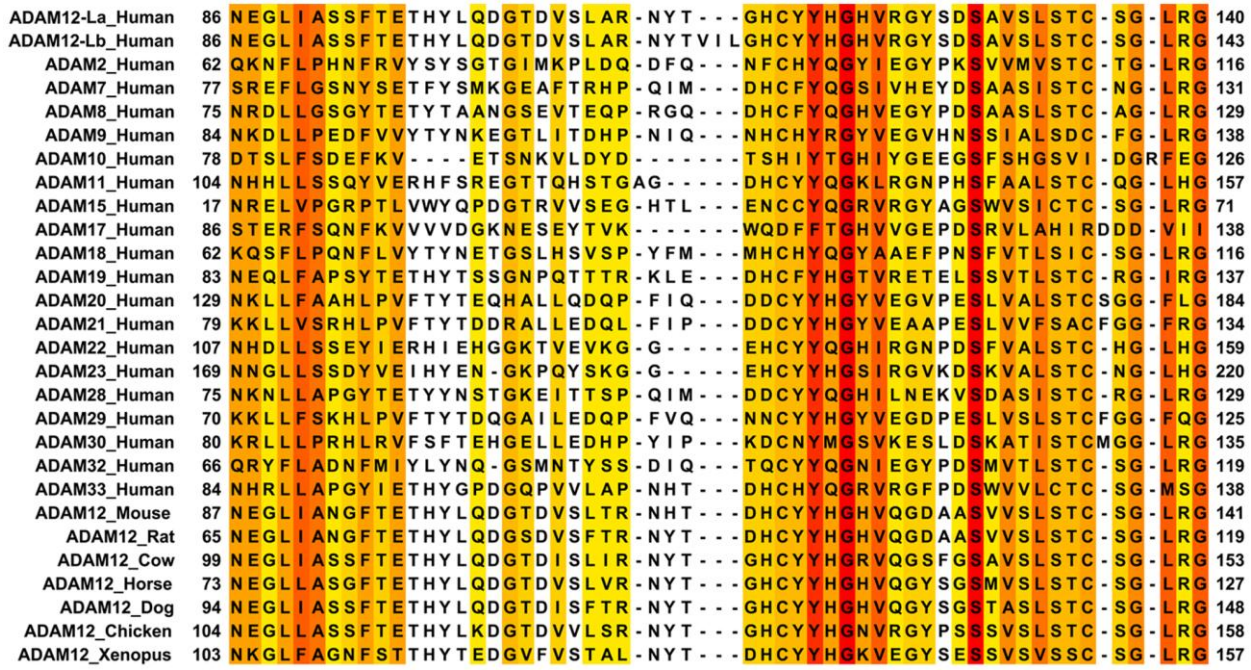

Figure 3.2 The ^{114}VIL^{116} motif is not conserved between different human ADAMs and between ADAM12 from different species

Multiple sequence alignment of the region in ADAM proteins flanking the ^{114}VIL^{116} motif. GenBank accession numbers are: ADAM2, NP_001455; ADAM7, NP_003808; ADAM8, NP_001100; ADAM9, NP_003807; ADAM10, NP_001101; ADAM11, NP_002381; ADAM12, NP_003465; ADAM15, AAS72997; ADAM17, NP_003174; ADAM18, NP_055052; ADAM19, NP_150377; ADAM20, NP_003805; ADAM21, NP_003804; ADAM22, NP_068369; ADAM23, NP_003803; ADAM28, NP_055080; ADAM29, NP_055084; ADAM30, NP_068566; ADAM32, NP_659441; ADAM33, NP_079496; Mouse, NP_031426; Rat, XP_001054670; Cow, NP_001001156; Horse, XP_001490097; Chicken, NP_001136322; Xenopus, NP_00035103. The dog sequence was obtained from e!Ensembl (ENSCAFP00000041414) due to the lack of a signal peptide in the GenBank sequence. Conservation strength is shown in red (high), orange (medium), yellow (poor), and white (no conservation).

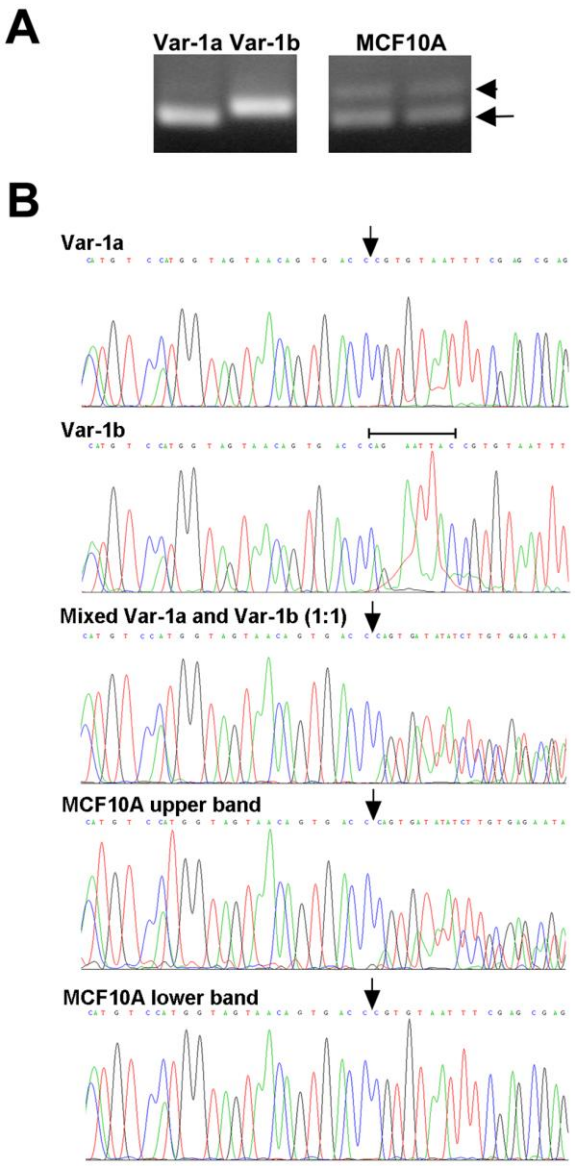

Figure 3.3 Breast epithelial cells express *ADAM12* transcripts containing exon 4a and 4b

(A) PCR amplification of a 100-bp region flanking the exon 4-exon 5 junction was performed using Var1a and Var1b vector controls (left) or cDNA samples from MCF10A cells. PCR products were resolved in a 2.0% agarose gel; two duplicate samples are shown for MCF10A cells. Upper and lower bands observed for MCF10A cells are indicated with arrowhead and arrow, respectively. (B) The PCR products were extracted from the gel and sequenced. The chromatograms of the sequencing reactions are shown for Var1a and Var1b vector controls, a 1:1 mixture of the two vector controls, and the two PCR products (corresponding to the upper or the lower band in panel A) amplified from MCF10A cells. The bar designates the nine-nucleotide region present exclusively in exon 4b, and arrow indicates the 3′ end of exon 4a. In samples containing mixed fragments, this arrow therefore indicates the site where the sequences diverge and the chromatogram begins to show multiple peaks. Notice that the sequencing reaction was performed using a reverse primer, and the sequences shown represent reverse complements of *ADAM12* transcripts.

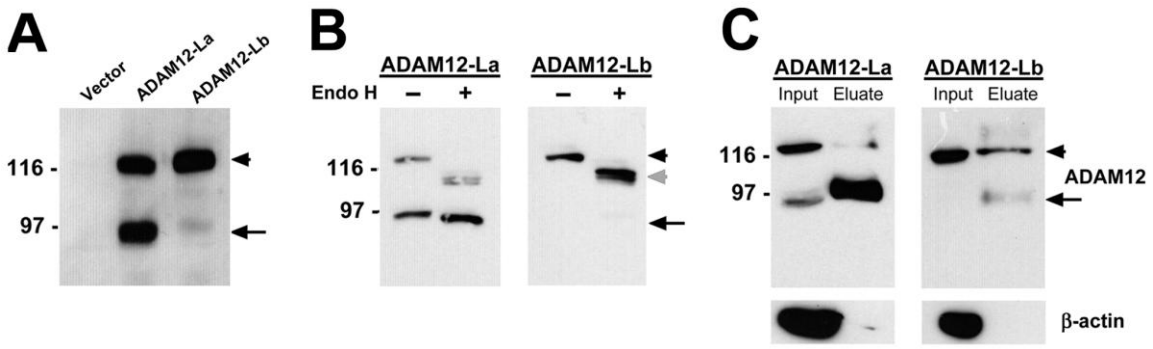

Figure 3.4 ADAM12-Lb is poorly processed and is retained in a pre-Golgi compartment

(A) Proteolytic processing of ADAM12-La and ADAM12-Lb in MCF10A cells. Cells with stable expression of ADAM12 proteins were selected with puromycin after retroviral infection. Total cell lysates were analyzed by Western blotting. The full-length protein is indicated by arrowhead, and the processed form after pro-domain removal is denoted with arrow. (B) Mobility shift analysis of ADAM12-La and ADAM12-Lb after endoglycosidase H (Endo H) treatment. The nascent full-length protein and the processed form are indicated with arrowhead and arrow, respectively. The deglycosylated full-length species is denoted with grey arrow. (C) Cell surface biotinylation of MCF10A cells stably expressing ADAM12-La or ADAM12-Lb. Biotinylated proteins were isolated on Neutravidin agarose and subjected to SDS-PAGE and Western blotting. Input (1/40 of the sample volume) refers to total cell lysates prior to Neutravidin binding, and eluate (1/2 of the sample volume) refers to biotinylated proteins that bound to the resin. β-actin, an intracellular protein, is not biotinylated and does not bind to Neutravidin.

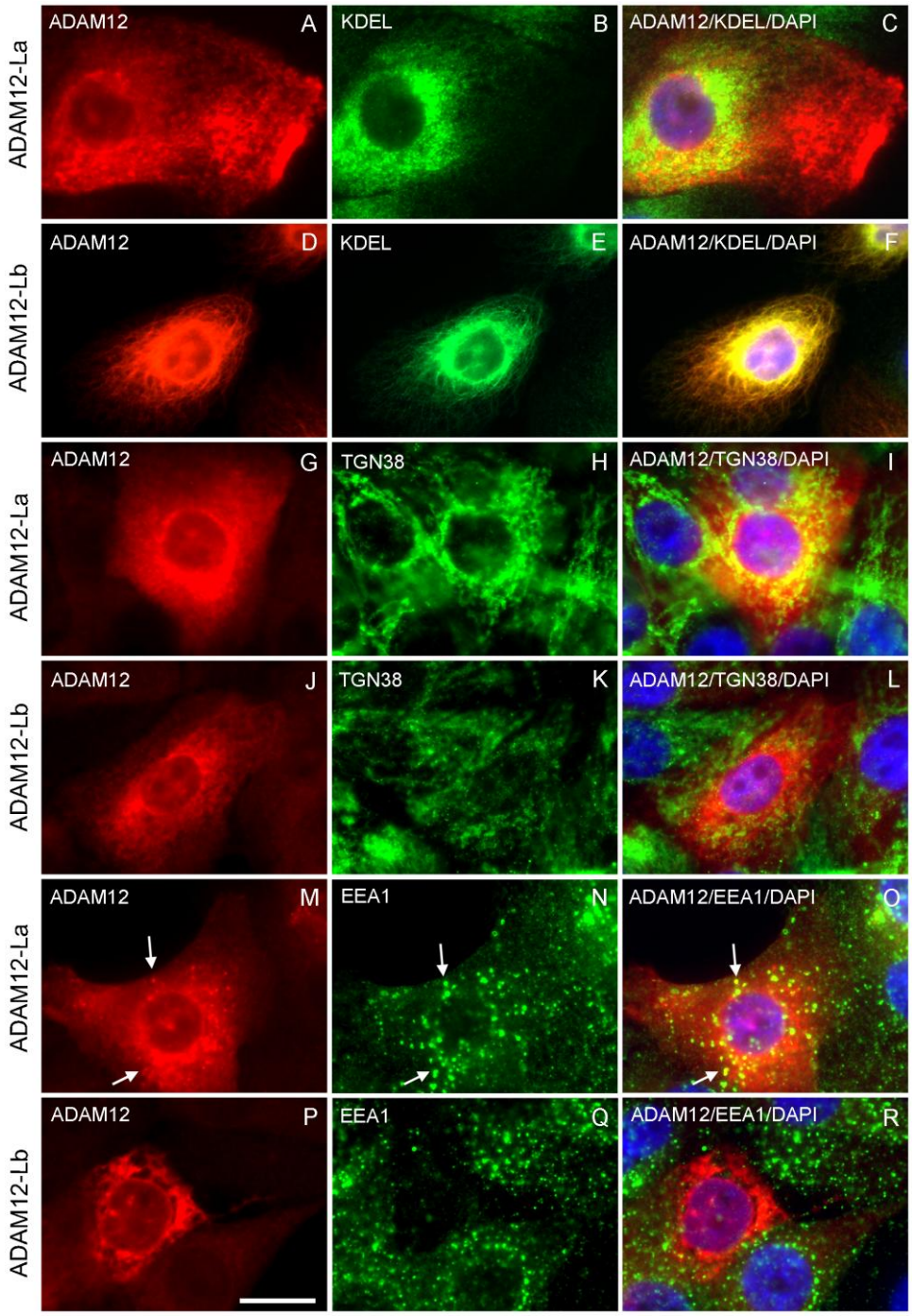

Figure 3.5 ADAM12-Lb is localized to the endoplasmic reticulum

MCF10A cells stably expressing ADAM12-La or ADAM12-Lb were fixed, permeabilized, and stained with anti- ADAM12 antibody (A, D, G, J, M, P), anti-KDEL antibody (an endoplasmic reticulum marker; B, E), anti-TGN38 antibody (a trans-Golgi marker; H, K), anti-EEA1 antibody (an early endosomal marker; N, Q), and DAPI. Overlay images are shown in panels C, F, I, L, O, R. Partial co-localization of ADAM12-La and EEA1 is indicated by white arrows. Bar, 20 µm.

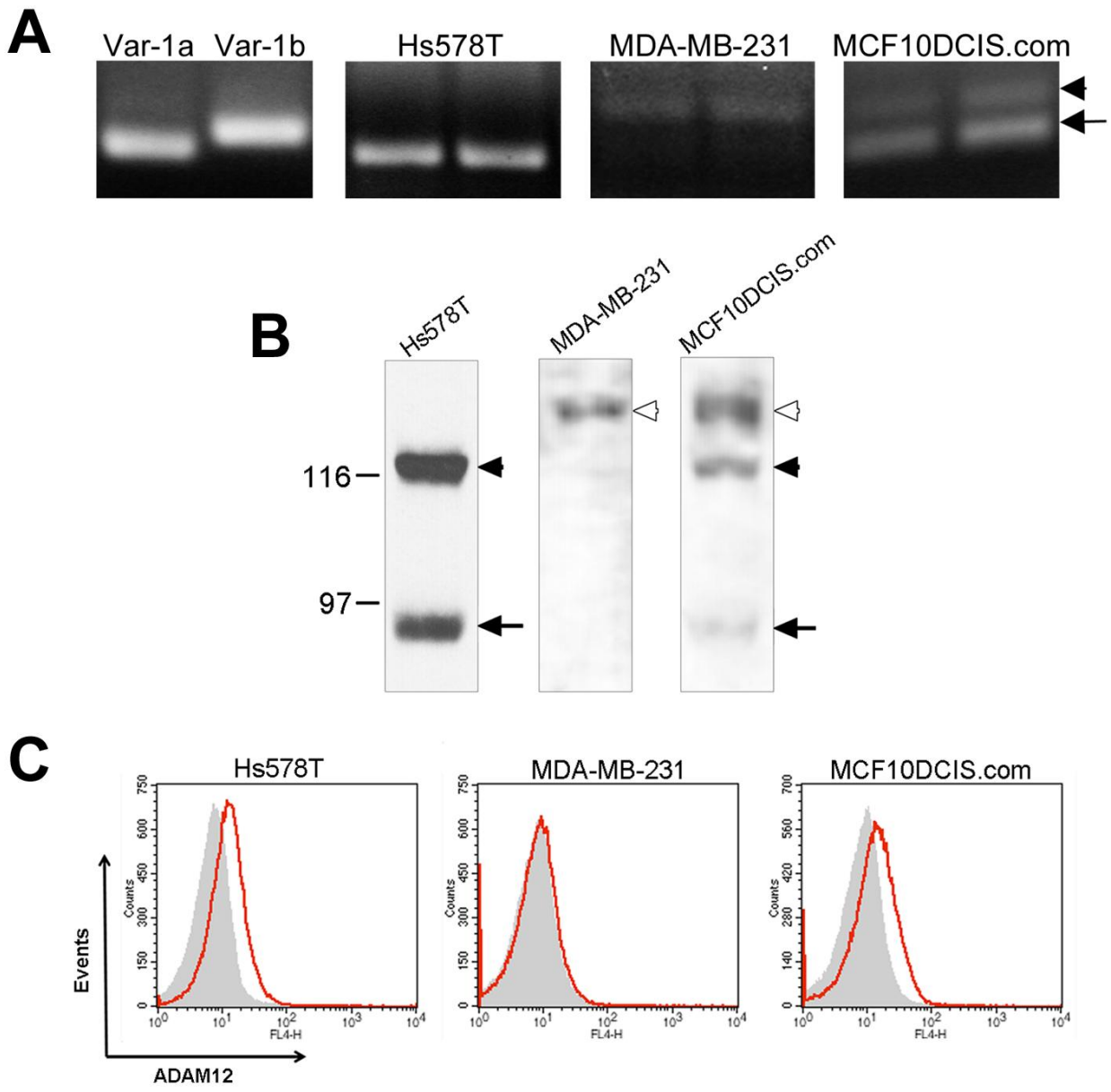

Figure 3.6 Breast cancer cell lines express different levels of ADAM12-La and ADAM12-Lb

(A) A 100-bp region flanking the exon 4-exon 5 junction was PCR-amplified using duplicate cDNA samples isolated from Hs578T, MDA-MB-231, and MCF10DCIS.com cells and analyzed as in Figure 3.3. Var1a and Var1b vectors served as controls. Exon 4a- and exon 4b-related bands are indicated with arrow and arrowhead, respectively. (B) Glycoprotein-enriched fractions from Hs578T, MDA-MB-231, and MCF10DCIS.com cells were analyzed by Western blotting using anti-ADAM12-L antibody. Full length ADAM12-La and ADAM12-Lb are indicated with solid and open arrowheads, respectively. The processed form of ADAM12-La is shown with arrow. (C) Cell surface localization of ADAM12-L was examined by flow cytometry. Live cells were trypsinized and stained with an antibody specific for the extracellular domain of ADAM12-L (red) or with isotype control antibody (grey).

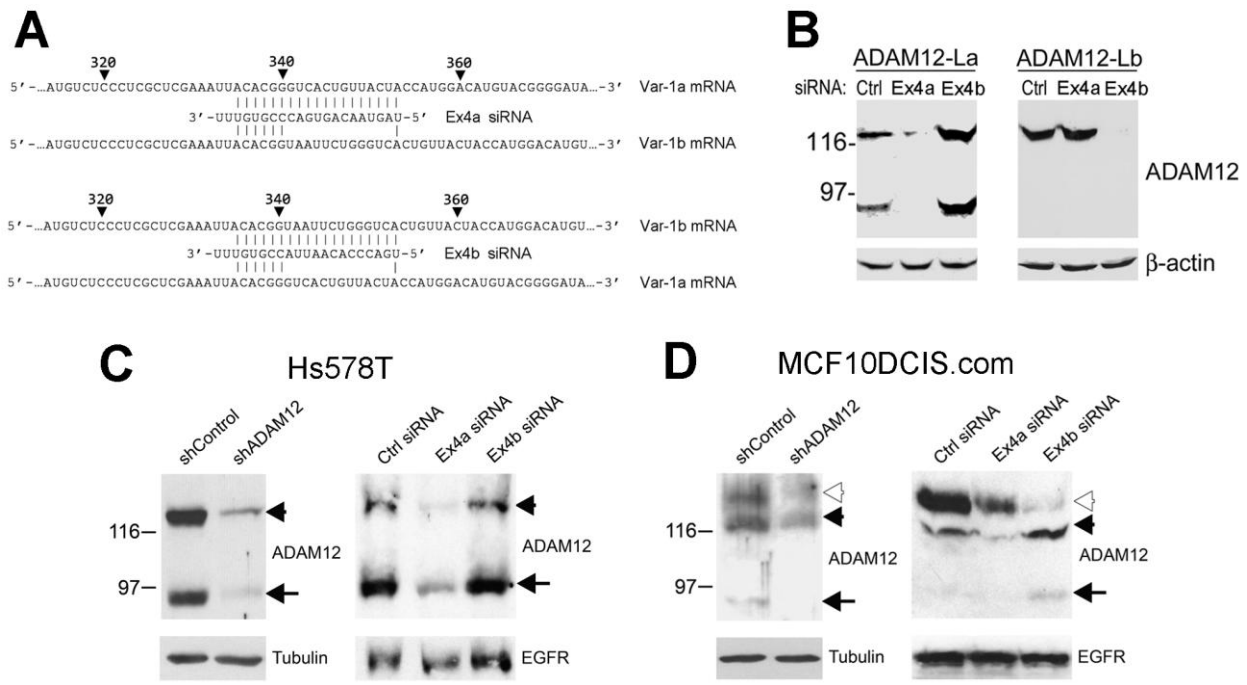

Figure 3.7 Confirmation of the identities of the endogenous ADAM12-La and ADAM12-Lb proteins detected in breast cancer cell lines

(A) Sequences of two siRNAs designed to specifically target *ADAM12* exon 4a (Ex4a) or exon 4b (Ex4b). The siRNA antisense strands are shown, and possible base pairing between each siRNA and Var1a or Var1b mRNA is indicated. The numbers refer to the nucleotide position in the coding sequence for each mRNA variant. (B) Efficacies and specificities of the two siRNAs. HEK293 cells stably expressing ADAM12-La or ADAM12-Lb were transfected with negative control siRNA (Ctrl), Ex4a siRNA, or Ex4b siRNA. Total cell lysates were analyzed by Western blotting using anti-ADAM12 antibody. β-actin is a loading control. (C,D) ADAM12-L knockdown in Hs578T and MCF10DCIS.com cells. Cells were stably transduced with lentiviruses bearing an shRNA construct targeting both *ADAM12-var1a* and *ADAM12-var1b* or control viruses. Alternatively, cells were transiently transfected with Ex4a siRNA, Ex4b siRNA, or negative control siRNA. Total cell lysates in C and D were enriched for glycoproteins on concanavalin A agarose prior to analysis. Full length ADAM12-La and ADAM12-Lb are indicated with solid and open arrowheads, respectively. The processed form of ADAM12-La is indicated with arrow. Epidermal Growth Factor Receptor (EGFR), ß-actin, and tubulin are gel-loading controls.

Table 3.1 Accession numbers of the individual splice variants of human *ADAM12*

	GenBank/EMBL/DDBJ		NCBI RefSeq		Ensembl		Vega		CCDS	UniProt
	mRNA	Translation	mRNA	Translation	mRNA	Translation	mRNA	Translation	mRNA and Translation	Translation
Var-1a	-	-	-	-	-	-	-	-	-	-
Var-1b	AF023476	AAC08702	NM_003474	NP_003465	ENST00000368679	ENSP00000357668	OTTHUMT00000050961	OTTHUMP00000020726	7653	O43184-1
Var-2a	AY358878	AAQ89237	-	-	-	-	-	-	-	O43184-3
Var-2b	AF023477	AAC08703	NM_021641	NP_067673	ENST00000368679	ENSP00000357665	OTTHUMT00000050962	OTTHUMP00000020727	7654	O43184-2

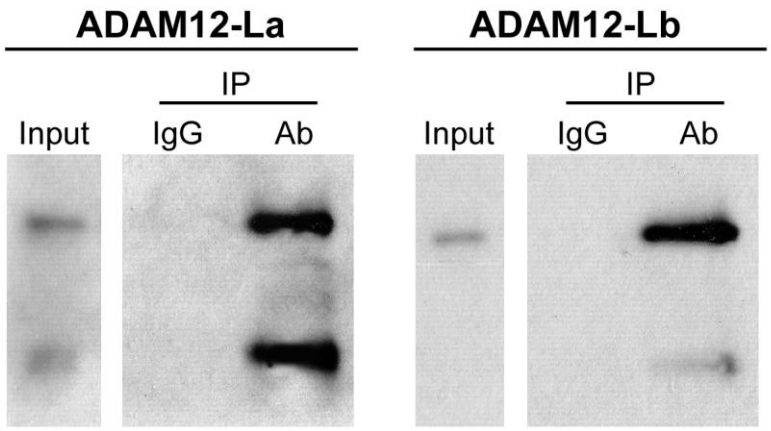

Figure 3.8 The anti-ADAM12 antibody used for flow cytometry recognizes both ADAM12-La and ADAM12-Lb

MCF10A cells stably transduced to express ADAM12-La or ADAM12-Lb were subjected to immunoprecipitation using mouse anti-ADAM12 antibody (R&D Biosciences, clone 632525) and Protein G agarose. IgG isotype control was used as a negative control. Equal volumes of total cell lysates of ADAM12-La- and ADAM-Lb-expressing cells (Inputs), as well as equal volumes of Protein G eluates, were analyzed by Western blotting using rabbit polyclonal anti-ADAM12 antibody #3394.

Chapter 4 - An essential role of metalloprotease-disintegrin ADAM12 in triple negative breast cancer

This chapter has been published as the following journal article:
Li, H., Duhachek-Muggy, S., Qi, Y., Hong, Y., Behbod, F., and Zolkiewska, A.
An essential role of metalloprotease-disintegrin ADAM12 in triple negative breast cancer. Breast Cancer Res Treat (2012) 135:759–769 (doi:10.1007/s10549-012-2220-4).
The final publication is available at link.springer.com.

Abstract

In the absence of HER2 overexpression, triple-negative breast cancers (TNBCs) rely on the signaling by epidermal growth factor receptor (EGFR/ErbB1/HER1) to convey growth signals and stimulate cell proliferation. Soluble EGF-like ligands are derived from their transmembrane precursors by ADAM proteases, but the identity of the ADAM that is primarily responsible for ligand release and activation of EGFR in TNBCs is not clear. Using publicly available gene expression data for patients with lymph node-negative breast tumors who did not receive systemic treatment, we show that ADAM12-L is the only ADAM whose expression level is significantly associated with decreased distant metastasis-free survival times. Similar effect was not observed for patients with ER-negative non-TNBCs. There was a positive correlation between ADAM12-L and HB-EGF and EGFR in TNBCs, but not in ER-negative non-TNBCs. We further demonstrate that ectopic expression of ADAM12-L increased EGFR phosphorylation in a mouse intraductal xenograft model of early breast cancer. Finally, we detect strong correlation between the level of anti-ADAM12-L and anti-phospho-EGFR immunostaining in human breast tumors using tissue microarrays. These studies suggest that ADAM12-L is the primary protease responsible for the activation of EGFR in early stage, lymph node-negative TNBCs. Thus, our results may provide novel insight into the biology of TNBC.

Introduction

Triple-negative breast cancer (TNBC) is an aggressive form of the disease, with poor prognosis, and limited treatment options [1-3]. TNBC, which accounts for ~20% of all breast

cancers, is characterized by the absence of estrogen receptor (ER) and progesterone receptor (PR) expression, and the lack of human epidermal growth factor receptor 2 (HER2) overexpression. Based on their gene expression profiles, the majority of TNBCs fall into the basal-like or claudin-low molecular subtypes [4, 5]. Due to the absence of ER and HER2, established targeted therapies, such as endocrine therapy or anti-HER2 therapy, are not applicable.

HER2 is a member of the ErbB family of receptors that include epidermal growth factor receptor (EGFR/ErbB1/HER1), ErbB2/HER2/Neu, ErbB3/HER3, and ErbB4/HER4 [6]. EGFR requires ligand binding for dimerization, autophosphorylation, and stimulation of its tyrosine kinase activity. HER2 does not bind ligands but exists in an open conformation that is constitutively available for dimerization with other ErbBs. HER3 lacks intrinsic tyrosine kinase activity. Signaling by EGFR, HER2, and HER3 plays fundamental roles in breast tumor cell proliferation, survival, and metastasis [7]. HER4 also binds ligands and possesses tyrosine kinase activity but, unlike EGFR or HER2, it elicits anti-proliferative responses in mammary epithelium [8]. In the absence of HER2 overexpression, TNBCs depend on EGFR to convey growth signals, and ligand-mediated activation of EGFR becomes important for tumor progression. Ligands for EGFR include epidermal growth factor (EGF), tumor growth factor α (TGFα), heparin-binding EGF-like growth factor (HB-EGF), amphiregulin (AREG), epigen (EPGN), epiregulin (EREG), and betacellulin (BTC) [9]. They are all synthesized as transmembrane precursors that need to be shed from the membrane to generate soluble, biologically active agonists. The shedding is mediated by cell surface proteases (sheddases) that belong predominantly to the ADAM (A Disintegrin And Metalloprotease) family. Studies in cells cultured *in vitro* showed that several different ADAMs are capable of generating soluble EGFR ligands [10-13]. ADAM17 has emerged as the primary sheddase of EGF-like ligands in breast cancer [14, 15], although its prognostic value is not limited to TNBC [15].

Whether the expression levels of other ADAMs are linked to breast cancer outcome and whether the potential risk is particularly increased in TNBC has not been investigated. The ADAM family comprises 20 members, 9 out of which are catalytically active and expressed beyond the reproductive system: ADAM8, -9, -10, -12, -15, -17, -19, -28, and -33 [16]. ADAM12 is strongly up-regulated in breast tumors and it has been previously implicated in breast cancer [17-20]. ADAM12 mRNA is alternatively spliced, giving rise to two different

protein isoforms: ADAM12-L (a transmembrane form) and ADAM12-S (a secreted form) [17]. Recently, ADAM12-S was reported to enhance tumor cell migration and invasion through Matrigel *in vitro* and to increase metastasis in mice *in vivo* [20]. It is currently unknown whether these pro-tumor roles of ADAM12 observed in laboratory settings translate into increased patient risk in clinical settings. Furthermore, despite the fact that ADAM12 was shown to be a potent sheddase of at least two different EGF-like ligands, EGF and BTC, in cultured cells [10], it is not clear whether it plays any role in the activation of EGFR in breast tumors *in vivo*.

The goal of this study was to examine whether ADAM12-L plays a role in activation of EGFR in TNBC. Our results suggest that ADAM12-L is the primary protease responsible for the activation of EGFR in an early stage, lymph node-negative TNBC.

Materials and Methods

Cell culture

MCF10DCIS.com cells (Asterand) were grown in Dulbecco's modified Eagle's medium (DMEM)/F12 nutrient mixture (1:1) supplemented with 5% horse serum and 29 mM $NaHCO_3$, at 37˚C in the presence of 5% CO_2 under a humidified atmosphere. Retroviral packaging cell line Phoenix Ampho (G. P. Nolan, Stanford University) was grown in DMEM supplemented with 10% FBS. Phoenix Ampho cells were transfected with hADAM12-L-pBABEpuro or empty pBABEpuro retroviral vector (15 µg plasmid DNA per 100-mm plate) using the calcium phosphate precipitation method. Viral supernatants were harvested 48 hours later, supplemented with 5 µg/ml polybrene, and used without further dilution for infection of MCF10DCIS.com cells. After one day, media containing retroviral particles were replaced with fresh media, and after an additional 24 h, stably transduced cells were selected with 3 µg/ml of puromycin for 7 days. For the EGF dose-response experiment, cells were starved in serum-free medium for 16 h, and then incubated for 30 min with the indicated concentrations of human EGF (R&D Systems).

Antibodies

Rabbit polyclonal anti-phospho-EGFR (Y1173) antibody was obtained from R&D Systems and it was used at a 1:5,000 dilution for Western blotting and 1:20 for IHC. Rabbit monoclonal anti-EGFR antibody (clone D38B1) XP® (Cell Signaling) was used at a 1:1,000 dilution for Western blotting. Mouse monoclonal anti-ADAM12 antibody (clone #632525)

recognizing the extracellular domain of human ADAM12 was purchased from R&D Systems and it was used at a 1:20 dilution for flow cytometry. Rabbit polyclonal anti-ADAM12 antibody (Ab #3394) was raised against the recombinant cytoplasmic domain of human ADAM12-L (amino acids 730-909). The recombinant protein was expressed in E. coli as a 6xHis-tagged protein, was purified using preparative SDS-PAGE, and was submitted to Open Biosystems for custom generation of the antibody. Rabbit anti-ADAM12 Ab (whole serum) was used at a dilution 1:20,000 for Western blotting and 1:500 for IHC; pre-immune serum at the same dilution was used as a negative control for IHC.

Western blotting

Cells were incubated in extraction buffer (50 mM Tris-HCl, pH 7.4, 150 mM NaCl, 5 mM EDTA, 1% Triton X-100, 0.5% sodium deoxycholate, 0.1% SDS, 1 mM 4-(2-aminoethyl)-benzene-sulfonyl fluoride hydrochloride (AEBSF), 10 µg/ml aprotinin, 10 µg/ml leupeptin, 10 µg/ml pepstatin A, 10 mM 1,10-phenanthroline) for 15 minutes at 4˚C. In the experiment in which EGFR phosphorylation was analyzed, the extraction buffer included 50 mM NaF, 2 mM Na_3VO_4, and 10 mM $Na_4P_2O_7$. Cell extracts were centrifuged at 21,000x g for 15 min, supernatants were resolved by SDS-PAGE and transferred to a nitrocellulose membrane. The membrane was blocked in DPBS containing 3% (w/v) dry milk and 0.3% (v/v) Tween 20, then incubated with primary antibodies in blocking buffer, followed by incubation with horseradish peroxidase-labeled secondary antibodies and detection using the West Pico chemiluminescence kit (Pierce).

Flow cytometry

Cells were trypsinized into single cell suspension, washed with PBS, and incubated with anti-ADAM12 monoclonal antibody or with isotype control for 30 min on ice. Cells were then washed 3 times, incubated with anti-mouse IgG antibody conjugated to FITC, and analyzed on a BD FACSCalibur flow cytometer.

Intraductal transplantation of cells

Intraductal transplantation of MCF10DCIS.com cells into NOD-SCID IL2 receptor γ knockout (NSG) mice was performed as described earlier [29]. Briefly, cells were trypsinized into single cells and resuspended in PBS at the 5,000 cells/µl density. Eight to twelve week-old

female mice were anesthetized, and 2 µl of cell suspension were injected into the ducts, using a 50-µl Hamilton syringe, with a blunt-ended 1/2-inch 30-gauge needle inserted directly through the nipple of the fourth inguinal gland. After 6 weeks, mice were sacrificed and the mammary tissue was collected for histological and immunohistochemical examination. All animal experiments were conducted by following protocols approved by the Animal Care and Use and Human Subjects Committee at the University of Kansas Medical Center.

Tissue Microarrays

Breast cancer tissue microarrays (BR1503a) were purchased from US Biomax. These arrays contained consecutive 4-µm sections of paraffin-embedded tissue samples from 3 cases of breast fibroadenoma, 2 cases of cystosarcoma phyllodes, 7 cases of intraductal carcinoma, 60 cases of invasive ductal carcinoma and 3 cases of normal adjacent breast tissue. Each case was represented by two different cores. Two cores out of the total 144 tumor cores were not suitable for staining. The ER-, PR- and HER2-status of each core had been previously determined by immunohistochemistry. Test arrays (T086b) were also purchased from US Biomax, Inc. and used to assess specificity of staining.

Immunohistochemistry

Samples were de-paraffinized in xylene and rehydrated in an ethanol gradient (100%-50%). Antigen retrieval was performed by boiling slides for 10 minutes in Acidic Antigen Retrieval buffer (R&D Systems). Slides were stained using HRP-DAB Cell and Tissue Staining Kit (R&D Systems) according to the manufacturer's protocol. Incubation with primary antibodies was performed overnight at 4°C. Samples were counterstained with hematoxylin prior to mounting with Permount solution (Fisher).

Quantification of immunohistochemical staining

All samples to be quantified were stained simultaneously using the same staining conditions and were analyzed with Axiovert-200 Zeiss microscope using a 10x (for mouse xenografts) or a 4x objective (for tissue microarrays). Samples were photographed with a RGB color camera using the same illumination conditions and a fixed exposure time. The images were viewed using a linear display characteristic curve, and were exported as TIFF files. The TIFF files were processed and analyzed by ImageJ software, version 1.46m. First, the brown

and blue colors were separated using the color deconvolution plug-in and the hematoxylin/DAB built-in vector. This color deconvolution plug-in implements stain separation algorithm developed by Ruifrok and Johnston [60] and it was downloaded from the following website: http://www.dentistry.bham.ac.uk/landinig/software/cdeconv/cdeconv.html. Next, the 8-bit monochromatic image representing DAB staining was inverted, and a region of interest (ROI) was selected using a polygon tool (for xenograft sections) or a circle tool (for tissue microarrays). For xenograft sections, ROIs either included the entire duct sections or, if a duct section was larger than the size of the image, the largest area of the duct captured in the image. This was followed by measuring the mean gray value within the ROI (i.e., the sum of the gray values of all the pixels in the ROI, divided by the number of pixels). As most of the carcinomas formed inside mouse ducts contained irregular areas of comedo-like necrosis that were visible as hollow spaces within the ducts, a threshold value was set prior to the measurement to exclude all pixels that did not correspond to cancer cells. The threshold value was the same for all analyzed images. An example of quantification of DAB staining in a xenograft section is shown in Figure 4.9. A similar approach was used to quantify DAB staining in tissue microarrays. For each core in the array, the entire area of the core was included in the ROI. Since DAB staining method is not stoichiometric and since DAB does not follow the Beer-Lambert law, the relationship between the optical density of the brown color developed during the HRP-DAB reaction and the amount of antigen is not linear [61]. Nevertheless, quantification of DAB staining using the approach described here provided an objective, albeit qualitative, estimate of the amount of antigen in tissue sections.

Patient populations

We used four datasets that are publicly available at Gene Expression Omnibus (GEO, http://www.ncbi.nlm.nih.gov/geo/): EMC286 (GSE2034) [21,22], Erasmus (GSE5327) [22], TRANSBIG (GSE7390) [23], and Mainz (GSE11121) [24]. We applied the following criteria for dataset selection: (a) patients with lymph-node negative tumors, (b) patients did not receive systemic adjuvant treatment, (c) distant metastasis free survival times (DMFS) were available, (d) gene expression profiling was performed using Affymetrix HG-U133A platform, and (e) the number of TNBCs identified by gene expression profiling (ref. [25], see below) was greater than 15. Patient clinical characteristics are reported in Table 4.1.

Data analysis

The EMC286, Erasmus, and TRANSBIG datasets contained information on the ER, but not PR or HER2 status. The Mainz dataset lacked information on ER, PR, and HER2. To identify TNBCs, we have adopted tumor classification based on bimodal filtering on ER, PR, and HER2 expression determined by Lehman et al. [25]. Previous studies have shown that microarray-based readout of ER, PR, and HER2 correlates well with immunohistochemical (IHC) determination of the ER, PR, and HER2 status [26, 27]. Overall, 53 tumors in the EMC286 dataset were classified as TNBCs. Nine tumors that were originally categorized as ER-positive based on IHC, but were classified as TNBC based on ER/PR/HER2 mRNA expression, were considered TNBC in our analyses. Consistently, the set of ER-negative tumors comprised 77 tumors that were called ER-negative by IHC, plus 9 ER-positive tumors that were classified as TNBC based on gene expression profiling. The remaining 200 tumors were considered ER-positive. Erasmus, TRANSBIG and Mainz datasets contained 16, 29, and 19 TNBCs, respectively. To evaluate the prognostic value of ADAM12-L in the combined set TNBCs from the fours cohorts, ADAM12-L expression data were merged. Data were first $\log_2$-transformed, median-centered, and Z-score transformed [28] to normalize ADAM12-L expression across all samples in each cohort. The flowchart of data analysis is shown in Figure 4.1. The list of Affymetrix probes used to retrieve gene expression profiles is provided in Table 4.3.

Statistical analyses

All data analyses were performed using GraphPad Prism version 5.0d. Survival curves were calculated using the Kaplan-Meier method and compared by the log-rank (Mantel-Cox) test. All reported P values are two-sided.

Results

High expression level of ADAM12-L is associated with poor prognosis in lymph node-negative TNBC without systemic therapy

We assessed the prognostic value of ADAM12-L and ADAM12-S in 286 early stage breast cancer patients treated at the Erasmus Medical Center (the EMC286 dataset) [21]. All tumors were lymph node-negative, and patients did not receive neoadjuvant or adjuvant systemic

therapy. Patients were divided into two groups with low and high expression of ADAM12-L (Figure 4.2A) or ADAM12-S (Figure 4.2B), with cut-offs set as median expression values. When all 286 tumors were analyzed together, the group with high expression of ADAM12-L had worse prognosis than the group with low expression of ADAM12-L, but the difference was not statistically significant. When ER-negative and ER-positive tumors were considered separately, a striking difference in the prognostic value of ADAM12-L became evident. In ER-negative tumors, high expression of ADAM12-L was associated with significantly lower distant metastasis-free survival (DMFS) rates (hazard ratio (HR) 2.154, 95% confidence interval (CI) 1.071 to 4.332, P = 0.0314). In ER-positive tumors, there was no difference in survival rates for patients with high or low levels of ADAM12-L. Most importantly, within ER-negative tumors, poor prognosis associated with high ADAM12-L was restricted to TNBCs (HR 2.492, 95% CI 1.047 to 5.933, P = 0.0391). Remarkably, in ER-negative non-TNBC, high expression of ADAM12-L was not linked to poor outcome. Assuming that the difference between TNBC and ER-negative non-TNBC was mainly due to HER2 overexpression (the mean expression level of HER2 in TNBC was indeed ~12-fold lower than in ER-negative non-TNBC, P<0.0001, data not shown), this result indicates that the poor prognostic value of ADAM12-L was manifested only in the absence of HER2 overexpression. Interestingly, although TNBCs overlap to a large extent with basal cancers (a majority of basal cancer are triple-negative, and 60-80% of TNBCs are basal tumors [1-4]), the prognostic value of ADAM12-L in basal cancers was lower than in TNBCs (Figure 4.7). Thus, decreased DMFS in TNBC expressing high ADAM12-L were not a simple consequence of poor prognostic value of ADAM12-L in basal cancers. Given the fact that the mean values of ADAM12-L were not statistically different between TNBCs and other tumor groups (Figure 4.8), these results suggest that ADAM12-L may activate EGFR via the cleavage of EGF-like ligands, and this function is masked or irrelevant in the presence of HER2 overexpression. In a marked contrast to ADAM12-L, ADAM12-S did not have a significant prognostic value in any of the tumor groups examined (Figure 4.2B).

Efficient activation of the EGFR pathway requires three components: the receptor, a ligand, and a sheddase that generates the soluble ligand. While the expression of these components may be regulated by entirely separate mechanisms, it is clear that increased levels of all three components create a particular advantage for tumor cells. Therefore, we examined the correlation between ADAM12-L, EGF-like ligand mRNAs and EGFR. We observed no positive

correlation in all 286 tumors or in ER-positive cancers (Table 4.2). In contrast, in ER-negative tumors, there was a positive correlation between ADAM12-L and HB-EGF (Pearson r = 0.3038, P = 0.0045; Table 4.2). Most importantly, this positive correlation between ADAM12-L and HB-EGF (Pearson r = 0.3632, P = 0.0075) and EGFR (Pearson r = 0.2728, P = 0.0481) was retained in the TNBC subset of ER-negative tumors. In the remaining ER-negative non-TNBCs, ADAM12-L was not significantly correlated with any of the mRNAs tested. Interestingly, despite their correlation with ADAM12-L, high expression of HB-EGF or EGFR mRNA alone was not significantly associated with decreased DMFS in TNBC (Figure 4.7). This is not surprising, since high HB-EGF or EGFR protein levels do not inevitably lead to the activation of EGFR unless a sheddase, i.e., ADAM12-L, is also expressed at high level.

Next, we asked whether other transmembrane, catalytically active ADAMs also contribute to poor prognosis in TNBCs. Out of eight other catalytically active ADAMs whose expression is not limited to the reproductive system, the following seven were represented on the Affymetrix U133A array: ADAM8, -9, -10, -15, -17, -19, and -28. Among TNBC patients from the EMC286 cohort, ADAM12-L was the only ADAM that was significantly associated with poor prognosis (Figure 4.3).

In order to extend our investigations beyond the EMC286 cohort, we combined ADAM12-L expression profiles in TNBCs from the EMC286 dataset and from three other cohorts, Erasmus [22], TRANSBIG [23], and Mainz [24]. All tumors were node-negative and patients did not receive adjuvant chemotherapy. In this combined dataset of 117 TNBCs, ADAM12-L levels were significantly higher in patients with distant metastases than in patients without metastasis (Figure 4.4A). Patients with high expression of ADAM12-L had significantly lower survival rates than patients with low expression of ADAM12-L (HR 2.030, 95% CI 1.136 to 3.628, P = 0.0168; Figure 4.4B).

ADAM12-L augments EGFR phosphorylation in vivo

Next, we examined whether there is a cause-and-effect relationship between the level of expression of ADAM12-L protein and the extent of EGFR phosphorylation *in vivo* in a mouse model of an early ER-negative breast cancer. We used the MIND (mouse intraductal) transplantation model, in which ER-negative MCF10DCIS.com breast tumor cells are transplanted directly into the mammary ducts [29]. MCF10DCIS.com cells express high levels

of EGFR [29]. We confirmed that this receptor is fully functional, as it became readily phosphorylated at Tyr1173, one of the major autophosphorylation sites [30], in response to added EGF (Figure 4.5A). The endogenous expression level of ADAM12-L protein in MCF10DCIS.com cells was low and poorly detected by immunoblotting (Figure 4.5B). Using a retroviral delivery system and selection with puromycin, we established cells with stable overexpression of ADAM12-L. The ectopically expressed ADAM12-L produced two bands in Western blots (Figure 4.5B). The ~120-kDa band represented the inactive intracellular ADAM12-L, and the ~90-kDa band represented the processed, active form that resides at the cell surface [31]. Flow cytometry using live cells further demonstrated surface expression of ADAM12-L in stably transduced cells (Figure 4.5B).

ADAM12-L overexpressing cells and control cells transduced with vector only were transplanted into mammary ducts. Six weeks later, the extent of EGFR phosphorylation in intraductal lesions was examined by immunohistochemistry. As reported earlier, most of the lesions at this time point were DCIS-like, with some lesions already progressing to invasion [29]. Figure 4.5C shows examples of anti-phospho-EGFR (Y1173) staining in the intraductal lesions. To assess the effect of ADAM12-L on the extent of EGFR phosphorylation, the intensity of anti-phospho-EGFR staining was quantified, as described in Methods. Analysis of 76 different intraductal lesions (38 lesions per each cell type, 6 mice total) showed significantly higher anti-phospho-EGFR staining in lesions generated by ADAM12-L-overexpressing cells than control cells (Figure 4.5D). This result suggested that ADAM12-L was capable of inducing EGFR phosphorylation in the MIND model *in vivo*. As MCF10DCIS.com cells express oncogenic H-RasG12V [32], it was not feasible to study downstream effects of EGFR activation.

EGFR phosphorylation in human breast tumors strongly correlates with ADAM12-L expression level

To assess an association between EGFR phosphorylation and the level of ADAM12-L protein in human breast tumors, we performed IHC analysis of tissue microarrays. We analyzed 142 samples of 72 different breast tumors, using anti-ADAM12-L and anti-phospho-EGFR (Y1173) antibodies (Figure 4.6A,B). The results show a strong correlation between staining intensities for ADAM12-L and for phospho-EGFR (Pearson $r = 0.8353$, $P < 0.0001$) (Figure 4.6C). Interestingly, this strong correlation was not limited just to TNBC, as a similar degree of

correlation was observed when only TNBC samples were included in the analysis (Pearson r = 0.7663, P < 0.0001) (Figure 4.6C). Thus, ADAM12-L may be a universal modulator of EGFR activation in all breast tumors, but this activity of ADAM12-L becomes biologically relevant only in the context of TNBC, where the EGFR pathway controls cell proliferation.

Discussion

Due to the absence of ER and HER2 in TNBC, anti-estrogen or anti-HER2 therapies are not possible. The only remaining option for systemic treatment is conventional chemotherapy. However, as chemotherapy typically aims at basic cellular processes such as cell division, it is non-specific and harmful to normal dividing cells. Furthermore, many TNBCs acquire chemoresistance after prolonged exposure to cytotoxic drugs, compromising the efficacy of the treatment. Thus, finding new molecular targets in TNBC and identifying novel predictive markers are of the utmost urgency.

The ongoing clinical trials for patients with TNBC include novel cytotoxic drugs, poly(ADPribose) polymerase (PARP) inhibitors, antiangiogenic agents, Src and Abl kinase inhibitors, and EGFR-targeting agents [33]. EGFR seems to be a logical target in TNBC for several reasons. First, in the absence of HER2-overexpression, TNBCs depend on signaling by EGFR to stimulate tumor cell proliferation and survival. Second, 60-70% of all TNBCs show increased expression of EGFR [34-37]. Third, KRAS mutations are infrequent in TNBC [38], making the tumors amenable to EGFR inhibition. Current EGFR-targeting agents being evaluated in clinical trials include small molecule inhibitors of the EGFR tyrosine kinase, as well as monoclonal antibodies (Cetuximab) [3, 39]. However, so far these strategies have produced limited success [1, 39]. One possible reason could be that the clinical studies involving EGFR inhibitors were conducted in unselected TNBC patients, and were not directed by any mechanistic hypotheses. Since ligand binding is an absolute requirement for EGFR activation, and since activating mutations in EGFR that would nullify this requirement are rare [40, 41], limiting ligand availability represents another logical approach to block the EGFR pathway. Furthermore, one can postulate that TNBC patients with the highest sheddase activity, in which soluble EGF-like ligands are produced with the highest efficiency, are the best candidates for the existing anti-EGFR therapies. This approach requires, however, precise knowledge of the sheddase responsible for the release of EGF-like ligands and activation of EGFR.

In this study, we demonstrate that high levels of ADAM12-L are associated with decreased DMFS in TNBC and we link this effect to the activation of EGFR. Importantly, ADAM12-L was the only ADAM encoding a transmembrane, catalytically active protease whose expression level was significantly linked to poor prognosis in TNBC patients. We further used an *in vivo* model to confirm a causal role of ADAM12-L protein in tyrosine phosphorylation of EGFR, which often serves as a read-out of the activation status of the receptor. Importantly, we uncovered a strong correlation between ADAM12-L protein level and the extent of EGFR phosphorylation using tissue arrays.

Although the significance of ADAM-mediated shedding of EGF-like ligands in breast cancer biology has been well recognized [42-44], the identity of the "perpetrator" ADAM that is actually responsible for ligand cleavage and activation of EGFR has not been conclusively determined. To our best knowledge, the current study represents the first evaluation of the prognostic values of all catalytically active ADAMs in systemically untreated TNBCs. This is also the first report that specifically links ADAM12-L to the activation of EGFR in TNBC. This function of ADAM12-L has not been previously revealed by cell biology approaches or by mouse models. Interestingly, the two breast cancer-associated loss-of-function mutations in ADAM12, i.e., D301H and G479E, were not found in TNBC [45, 46]. The third mutation, L792F, was found in TNBC, but this mutation does not alter the proteolytic activity of ADAM12-L (ref. [47] and our unpublished observations). Thus, it appears that TNBCs express the active form of ADAM12-L, which is consistent with its role in EGFR activation in TNBC described here.

One unexpected result of our survival analyses is the discrepancy between the prognostic values of ADAM12-L and ADAM12-S. The distinction between ADAM12-L and ADAM12-S is important, because these two mRNAs encode transmembrane and secreted proteases, respectively, with potentially diverse biological functions during tumor progression and metastasis. Recently, ADAM12-S has been recently shown to be more potent than ADAM12-L in inducing metastasis in an orthotopic mouse xenograft model [20]. This result does not agree with the results of our survival analyses presented here, but the discrepancy may be explained by the fact that the model used in the referenced study did not mimic human TNBC.

Finally, an important question remains: what is the functional mechanism by which ADAM12-L promotes metastasis in node-negative TNBC, despite complete removal of the

primary tumor? One possibility is that the ADAM12-L/EGFR axis increases the chance of an early dissemination of a small number of cancer cells prior to surgery, and these cells go undetected in the node analysis. EGFR activation has been shown to promote epithelial-to-mesenchymal-like transition (EMT), down-regulation of E-cadherin, tumor cell migration, and invasion [48-53], and these functions fit the proposed model of ADAM12-L/EGFR enhancing tumor cell dissemination. Another possibility is that ADAM12-L-mediated activation of the EGFR pathway might enhance tumor cell colonization at a metastatic site. Recent studies have shown that shedding of EGF-like ligands from tumor cells modulates in a paracrine manner the bone microenvironment and promotes osteolytic metastasis [54]. The sheddases implicated in this process are ADAMTS1 (a disintegrin and metalloproteinase with thrombospondin motifs1) and MMP1 (matrix metalloprotease 1). These two proteases are not linked to poor prognosis in TNBCs from the EMC286 cohort (results not shown). However, as the pattern of metastatic spread in TNBC is different from other types of breast cancer, with brain and liver metastases being more frequent than metastasis to bone or lung [55-57], the identity of the sheddases and the spectrum of EGF-like ligands involved may also be different. Recently, HB-EGF has been shown to be a mediator of cancer cell passage through the blood-brain barrier [58]. Our preliminary examination of the gene expression data suggested that the expression level of ADAM12-L might be indeed higher in TNBCs that metastasized to the brain than in other TNBCs, but because of the limited number of cases available, the difference did not reach statistical significance (results not shown).

The discovery of ADAM12-L as a prognostic factor in TNBC and linking its function to the EGFR pathway may have at least two potential implications. First, it should promote further studies to establish whether ADAM12-L may serve as a novel therapeutic target in TNBC. It should also encourage a quest for highly specific inhibitors that would effectively discriminate between ADAM12-L and other catalytically active ADAMs. Second, stratification of TNBC patients based on the expression level of ADAM12-L may identify a group that could benefit the most from inhibition of EGFR and thus it may increase the efficacy of anti-EGFR treatment.

Acknowledgements

This work was supported by NIH grant 1R15CA151065 and Innovative Research Award from Terry C. Johnson Center for Basic Cancer Research at KSU to AZ, and by NIH grant

5R00CA127462 to FB. This is contribution 12-470-J from Kansas Agricultural Experiment Station.

References

1. Carey L, Winer E, Viale G, Cameron D, Gianni L (2010) Triple-negative breast cancer: disease entity or title of convenience? Nat Rev Clin Oncol 7 (12):683-692. doi:10.1038/nrclinonc.2010.154

2. Foulkes WD, Smith IE, Reis-Filho JS (2010) Triple-negative breast cancer. New Engl J Med 363 (20):1938-1948. doi:10.1056/NEJMra1001389

3. Pal SK, Childs BH, Pegram M (2011) Triple negative breast cancer: unmet medical needs. Breast Cancer Res Treat 125 (3):627-636. doi:10.1007/s10549-010-1293-1

4. Sotiriou C, Pusztai L (2009) Gene-expression signatures in breast cancer. New Engl J Med 360 (8):790-800. doi:10.1056/NEJMra0801289

5. Prat A, Parker JS, Karginova O, Fan C, Livasy C, Herschkowitz JI, He X, Perou CM (2010) Phenotypic and molecular characterization of the claudin-low intrinsic subtype of breast cancer. Breast Cancer Res 12 (5):R68. doi:10.1186/bcr2635

6. Hynes NE, MacDonald G (2009) ErbB receptors and signaling pathways in cancer. Curr Opin Cell Biol 21 (2):177-184. doi:10.1016/j.ceb.2008.12.010

7. Foley J, Nickerson NK, Nam S, Allen KT, Gilmore JL, Nephew KP, Riese DJ, 2nd (2010) EGFR signaling in breast cancer: bad to the bone. Semin Cell Dev Biol 21 (9):951-960. doi:10.1016/j.semcdb.2010.08.009

8. Muraoka-Cook RS, Feng SM, Strunk KE, Earp HS, 3rd (2008) ErbB4/HER4: role in mammary gland development, differentiation and growth inhibition. J Mammary Gland Biol Neoplasia 13 (2):235-246. doi:10.1007/s10911-008-9080-x

9. Wilson KJ, Gilmore JL, Foley J, Lemmon MA, Riese DJ, 2nd (2009) Functional selectivity of EGF family peptide growth factors: implications for cancer. Pharmacol Ther 122 (1):1-8. doi:10.1016/j.pharmthera.2008.11.008

10. Horiuchi K, Le Gall S, Schulte M, Yamaguchi T, Reiss K, Murphy G, Toyama Y, Hartmann D, Saftig P, Blobel CP (2007) Substrate selectivity of epidermal growth factor-receptor ligand sheddases and their regulation by phorbol esters and calcium influx. Mol Biol Cell 18 (1):176-188. doi:10.1091/mbc.E06-01-0014

11. Sunnarborg SW, Hinkle CL, Stevenson M, Russell WE, Raska CS, Peschon JJ, Castner BJ, Gerhart MJ, Paxton RJ, Black RA, Lee DC (2002) Tumor necrosis factor-α converting enzyme (TACE) regulates epidermal growth factor receptor ligand availability. J Biol Chem 277 (15):12838-12845. doi:10.1074/jbc.M112050200

12. Sternlicht MD, Sunnarborg SW, Kouros-Mehr H, Yu Y, Lee DC, Werb Z (2005) Mammary ductal morphogenesis requires paracrine activation of stromal EGFR via ADAM17-dependent shedding of epithelial amphiregulin. Development 132 (17):3923-3933. doi:10.1242/dev.01966

13. Sahin U, Weskamp G, Kelly K, Zhou HM, Higashiyama S, Peschon J, Hartmann D, Saftig P, Blobel CP (2004) Distinct roles for ADAM10 and ADAM17 in ectodomain shedding of six EGFR ligands. J Cell Biol 164 (5):769-779. doi:10.1083/jcb.200307137

14. Kenny PA, Bissell MJ (2007) Targeting TACE-dependent EGFR ligand shedding in breast cancer. J Clin Invest 117 (2):337-345. doi:10.1172/JCI29518

15. McGowan PM, McKiernan E, Bolster F, Ryan BM, Hill AD, McDermott EW, Evoy D, O'Higgins N, Crown J, Duffy MJ (2008) ADAM-17 predicts adverse outcome in patients with breast cancer. Annals of oncology 19 (6):1075-1081. doi:10.1093/annonc/mdm609

16. Edwards DR, Handsley MM, Pennington CJ (2008) The ADAM metalloproteinases. Mol Aspects Med 29 (5):258-289. doi:10.1016/j.mam.2008.08.001

17. Kveiborg M, Albrechtsen R, Couchman JR, Wewer UM (2008) Cellular roles of ADAM12 in health and disease. Int J Biochem Cell Biol 40 (9):1685-1702. doi:10.1016/j.biocel.2008.01.025

18. Kveiborg M, Frohlich C, Albrechtsen R, Tischler V, Dietrich N, Holck P, Kronqvist P, Rank F, Mercurio AM, Wewer UM (2005) A role for ADAM12 in breast tumor progression and stromal cell apoptosis. Cancer Res 65 (11):4754-4761. doi:10.1158/0008-5472.CAN-05-0262

19. Frohlich C, Nehammer C, Albrechtsen R, Kronqvist P, Kveiborg M, Sehara-Fujisawa A, Mercurio AM, Wewer UM (2011) ADAM12 produced by tumor cells rather than stromal cells accelerates breast tumor progression. Mol Cancer Res 9 (11):1449-1461. doi:10.1158/1541-7786.MCR-11-0100

20. Roy R, Rodig S, Bielenberg D, Zurakowski D, Moses MA (2011) ADAM12 transmembrane and secreted isoforms promote breast tumor growth: a distinct role for ADAM12-S protein in tumor metastasis. J Biol Chem 286 (23):20758-20768. doi:10.1074/jbc.M110.216036

21. Wang Y, Klijn JG, Zhang Y, Sieuwerts AM, Look MP, Yang F, Talantov D, Timmermans M, Meijer-van Gelder ME, Yu J, Jatkoe T, Berns EM, Atkins D, Foekens JA (2005) Gene-expression profiles to predict distant metastasis of lymph-node-negative primary breast cancer. Lancet 365 (9460):671-679. doi:10.1016/S0140-6736(05)17947-1

22. Minn AJ, Gupta GP, Padua D, Bos P, Nguyen DX, Nuyten D, Kreike B, Zhang Y, Wang Y, Ishwaran H, Foekens JA, van de Vijver M, Massague J (2007) Lung metastasis genes couple breast tumor size and metastatic spread. Proc Nat Acad Sci USA 104 (16):6740-6745. doi:10.1073/pnas.0701138104

23. Desmedt C, Piette F, Loi S, Wang Y, Lallemand F, Haibe-Kains B, Viale G, Delorenzi M, Zhang Y, d'Assignies MS, Bergh J, Lidereau R, Ellis P, Harris AL, Klijn JG, Foekens JA, Cardoso F, Piccart MJ, Buyse M, Sotiriou C (2007) Strong time dependence of the 76-gene prognostic signature for node-negative breast cancer patients in the TRANSBIG multicenter independent validation series. Clin Cancer Res 13 (11):3207-3214. doi:10.1158/1078-0432.CCR-06-2765

24. Schmidt M, Bohm D, von Torne C, Steiner E, Puhl A, Pilch H, Lehr HA, Hengstler JG, Kolbl H, Gehrmann M (2008) The humoral immune system has a key prognostic impact in node-negative breast cancer. Cancer Res 68 (13):5405-5413. doi:10.1158/0008-5472.CAN-07-5206

25. Lehmann BD, Bauer JA, Chen X, Sanders ME, Chakravarthy AB, Shyr Y, Pietenpol JA (2011) Identification of human triple-negative breast cancer subtypes and preclinical models for selection of targeted therapies. J Clin Invest 121 (7):2750-2767. doi:10.1172/JCI45014

26. Press MF, Finn RS, Cameron D, Di Leo A, Geyer CE, Villalobos IE, Santiago A, Guzman R, Gasparyan A, Ma Y, Danenberg K, Martin AM, Williams L, Oliva C, Stein S, Gagnon R, Arbushites M, Koehler MT (2008) HER-2 gene amplification, HER-2 and epidermal growth factor receptor mRNA and protein expression, and lapatinib efficacy in women with metastatic breast cancer. Clin Cancer Res 14 (23):7861-7870. doi:10.1158/1078-0432.CCR-08-1056

27. Roepman P, Horlings HM, Krijgsman O, Kok M, Bueno-de-Mesquita JM, Bender R, Linn SC, Glas AM, van de Vijver MJ (2009) Microarray-based determination of estrogen receptor, progesterone receptor, and HER2 receptor status in breast cancer. Clin Cancer Res 15 (22):7003-7011. doi:10.1158/1078-0432.CCR-09-0449

28. Cheadle C, Vawter MP, Freed WJ, Becker KG (2003) Analysis of microarray data using Z score transformation. J Mol Diagn 5 (2):73-81. doi:10.1016/S1525-1578(10)60455-2

29. Behbod F, Kittrell FS, LaMarca H, Edwards D, Kerbawy S, Heestand JC, Young E, Mukhopadhyay P, Yeh HW, Allred DC, Hu M, Polyak K, Rosen JM, Medina D (2009) An intraductal human-in-mouse transplantation model mimics the subtypes of ductal carcinoma in situ. Breast Cancer Res 11 (5):R66. doi:10.1186/bcr2358

30. Olayioye MA, Neve RM, Lane HA, Hynes NE (2000) The ErbB signaling network: receptor heterodimerization in development and cancer. EMBO J 19 (13):3159-3167. doi:10.1093/emboj/19.13.3159

31. Cao Y, Kang Q, Zhao Z, Zolkiewska A (2002) Intracellular processing of metalloprotease disintegrin ADAM12. J Biol Chem 277 (29):26403-26411. doi:10.1074/jbc.M110814200

32. Miller FR, Santner SJ, Tait L, Dawson PJ (2000) MCF10DCIS.com xenograft model of human comedo ductal carcinoma in situ. J Natl Cancer Inst 92 (14):1185-1186

33. Carey LA (2011) Directed therapy of subtypes of triple-negative breast cancer. Oncologist 16 Suppl 1:71-78. doi:10.1634/theoncologist.2011-S1-71

34. Shien T, Tashiro T, Omatsu M, Masuda T, Furuta K, Sato N, Akashi-Tanaka S, Uehara M, Iwamoto E, Kinoshita T, Fukutomi T, Tsuda H, Hasegawa T (2005) Frequent overexpression of epidermal growth factor receptor (EGFR) in mammary high grade ductal carcinomas with myoepithelial differentiation. J Clin Pathol 58 (12):1299-1304. doi:10.1136/jcp.2005.026096

35. Arnes JB, Begin LR, Stefansson I, Brunet JS, Nielsen TO, Foulkes WD, Akslen LA (2009) Expression of epidermal growth factor receptor in relation to BRCA1 status, basal-like markers and prognosis in breast cancer. J Clin Pathol 62 (2):139-146. doi:10.1136/jcp.2008.056291

36. Viale G, Rotmensz N, Maisonneuve P, Bottiglieri L, Montagna E, Luini A, Veronesi P, Intra M, Torrisi R, Cardillo A, Campagnoli E, Goldhirsch A, Colleoni M (2009) Invasive ductal carcinoma of the breast with the "triple-negative" phenotype: prognostic implications of EGFR immunoreactivity. Breast Cancer Res Treat 116 (2):317-328. doi:10.1007/s10549-008-0206-z

37. Corkery B, Crown J, Clynes M, O'Donovan N (2009) Epidermal growth factor receptor as a potential therapeutic target in triple-negative breast cancer. Annals Oncol 20 (5):862-867. doi:10.1093/annonc/mdn710

38. Sanchez-Munoz A, Gallego E, de Luque V, Perez-Rivas LG, Vicioso L, Ribelles N, Lozano J, Alba E (2010) Lack of evidence for KRAS oncogenic mutations in triple-negative breast cancer. BMC Cancer 10:136. doi:10.1186/1471-2407-10-136

39. Peddi PF, Ellis MJ, Ma C (2012) Molecular basis of triple negative breast cancer and implications for therapy. Int J Breast Cancer 2012:217185. doi:10.1155/2012/217185

40. Bhargava R, Gerald WL, Li AR, Pan Q, Lal P, Ladanyi M, Chen B (2005) EGFR gene amplification in breast cancer: correlation with epidermal growth factor receptor mRNA and protein expression and HER-2 status and absence of EGFR-activating mutations. Modern Pathol 18 (8):1027-1033. doi:10.1038/modpathol.3800438

41. Reis-Filho JS, Pinheiro C, Lambros MB, Milanezi F, Carvalho S, Savage K, Simpson PT, Jones C, Swift S, Mackay A, Reis RM, Hornick JL, Pereira EM, Baltazar F, Fletcher CD, Ashworth A, Lakhani SR, Schmitt FC (2006) EGFR amplification and lack of activating mutations in metaplastic breast carcinomas. J Pathol 209 (4):445-453. doi:10.1002/path.2004

42. Blobel CP, Carpenter G, Freeman M (2009) The role of protease activity in ErbB biology. Exp Cell Res 315 (4):671-682. doi:10.1016/j.yexcr.2008.10.011

43. Duffy MJ, McKiernan E, O'Donovan N, McGowan PM (2009) Role of ADAMs in cancer formation and progression. Clin Cancer Res 15 (4):1140-1144. doi:10.1158/1078-0432.CCR-08-1585

44. Duffy MJ, Mullooly M, O'Donovan N, Sukor S, Crown J, Pierce A, McGowan PM (2011) The ADAMs family of proteases: new biomarkers and therapeutic targets for cancer? Clin Proteomics 8 (1):9. doi:10.1186/1559-0275-8-9

45. Sjoblom T, Jones S, Wood LD, Parsons DW, Lin J, Barber TD, Mandelker D, Leary RJ, Ptak J, Silliman N, Szabo S, Buckhaults P, Farrell C, Meeh P, Markowitz SD, Willis J, Dawson D, Willson JK, Gazdar AF, Hartigan J, Wu L, Liu C, Parmigiani G, Park BH, Bachman KE, Papadopoulos N, Vogelstein B, Kinzler KW, Velculescu VE (2006) The consensus coding sequences of human breast and colorectal cancers. Science 314 (5797):268-274. doi:10.1126/science.1133427

46. Dyczynska E, Syta E, Sun D, Zolkiewska A (2008) Breast cancer-associated mutations in metalloprotease disintegrin ADAM12 interfere with the intracellular trafficking and processing of the protein. Int J Cancer 122 (11):2634-2640. doi:10.1002/ijc.23405

47. Stautz D, Wewer UM, Kveiborg M (2012) Functional Analysis of a Breast Cancer-Associated Mutation in the Intracellular Domain of the Metalloprotease ADAM12. PLoS One 7 (5):e37628. doi:10.1371/journal.pone.0037628

48. Lu Z, Jiang G, Blume-Jensen P, Hunter T (2001) Epidermal growth factor-induced tumor cell invasion and metastasis initiated by dephosphorylation and downregulation of focal adhesion kinase. Mol Cell Biol 21 (12):4016-4031. doi:10.1128/MCB.21.12.4016-4031.2001

49. Lu Z, Ghosh S, Wang Z, Hunter T (2003) Downregulation of caveolin-1 function by EGF leads to the loss of E-cadherin, increased transcriptional activity of beta-catenin, and enhanced tumor cell invasion. Cancer Cell 4 (6):499-515

50. Hager MH, Morley S, Bielenberg DR, Gao S, Morello M, Holcomb IN, Liu W, Mouneimne G, Demichelis F, Kim J, Solomon KR, Adam RM, Isaacs WB, Higgs HN, Vessella RL, Di Vizio D, Freeman MR (2012) DIAPH3 governs the cellular transition to the amoeboid tumour phenotype. EMBO Mol Med. doi:10.1002/emmm.201200242

51. Nie F, Yang J, Wen S, An YL, Ding J, Ju SH, Zhao Z, Chen HJ, Peng XG, Wong ST, Zhao H, Teng GJ (2012) Involvement of epidermal growth factor receptor overexpression in the promotion of breast cancer brain metastasis. Cancer. doi:10.1002/cncr.27553

52. Samanta S, Sharma VM, Khan A, Mercurio AM (2012) Regulation of IMP3 by EGFR signaling and repression by ERbeta: implications for triple-negative breast cancer. Oncogene. doi:10.1038/onc.2011.620

53. Jin W, Chen BB, Li JY, Zhu H, Huang M, Gu SM, Wang QQ, Chen JY, Yu S, Wu J, Shao ZM (2012) TIEG1 inhibits breast cancer invasion and metastasis by inhibition of epidermal growth factor receptor (EGFR) transcription and the EGFR signaling pathway. Mol Cell Biol 32 (1):50-63. doi:10.1128/MCB.06152-11

54. Lu X, Wang Q, Hu G, Van Poznak C, Fleisher M, Reiss M, Massague J, Kang Y (2009) ADAMTS1 and MMP1 proteolytically engage EGF-like ligands in an osteolytic

signaling cascade for bone metastasis. Genes & development 23 (16):1882-1894. doi:10.1101/gad.1824809

55. Fulford LG, Reis-Filho JS, Ryder K, Jones C, Gillett CE, Hanby A, Easton D, Lakhani SR (2007) Basal-like grade III invasive ductal carcinoma of the breast: patterns of metastasis and long-term survival. Breast Cancer Res 9 (1):R4. doi:10.1186/bcr1636

56. Hicks DG, Short SM, Prescott NL, Tarr SM, Coleman KA, Yoder BJ, Crowe JP, Choueiri TK, Dawson AE, Budd GT, Tubbs RR, Casey G, Weil RJ (2006) Breast cancers with brain metastases are more likely to be estrogen receptor negative, express the basal cytokeratin CK5/6, and overexpress HER2 or EGFR. Am J Surg Pathol 30 (9):1097-1104. doi:10.1097/01.pas.0000213306.05811.b9

57. Dent R, Hanna WM, Trudeau M, Rawlinson E, Sun P, Narod SA (2009) Pattern of metastatic spread in triple-negative breast cancer. Breast Cancer Res Treat 115 (2):423-428. doi:10.1007/s10549-008¬0086-2

58. Bos PD, Zhang XH, Nadal C, Shu W, Gomis RR, Nguyen DX, Minn AJ, van de Vijver MJ, Gerald WL, Foekens JA, Massague J (2009) Genes that mediate breast cancer metastasis to the brain. Nature 459 (7249):1005-1009. doi:10.1038/nature08021

59. McShane LM, Altman DG, Sauerbrei W, Taube SE, Gion M, Clark GM (2005) Reporting recommendations for tumor marker prognostic studies (REMARK). J Nat Cancer Inst 97 (16):1180¬1184. doi:10.1093/jnci/dji237

60. Ruifrok AC, Johnston DA (2001) Quantification of histochemical staining by color deconvolution. Anal Quant Cytol Histol 23:291-299

61. van der Loos CM (2008) Multiple immunoenzyme staining: methods and visualizations for the observation with spectral imaging. J Hist Cytochem 56:313-328. doi:10.1369/jhc.2007.950170

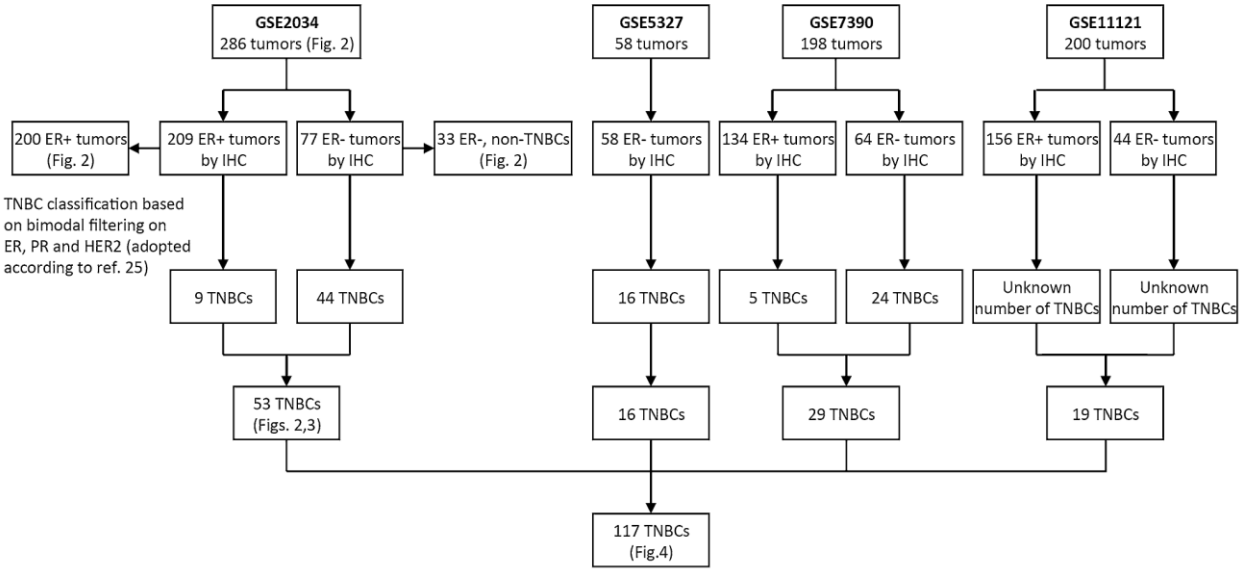

Figure 4.1 Flowchart of analysis according to REMARK criteria

Flowchart of analysis as required by the REMARK criteria [59].

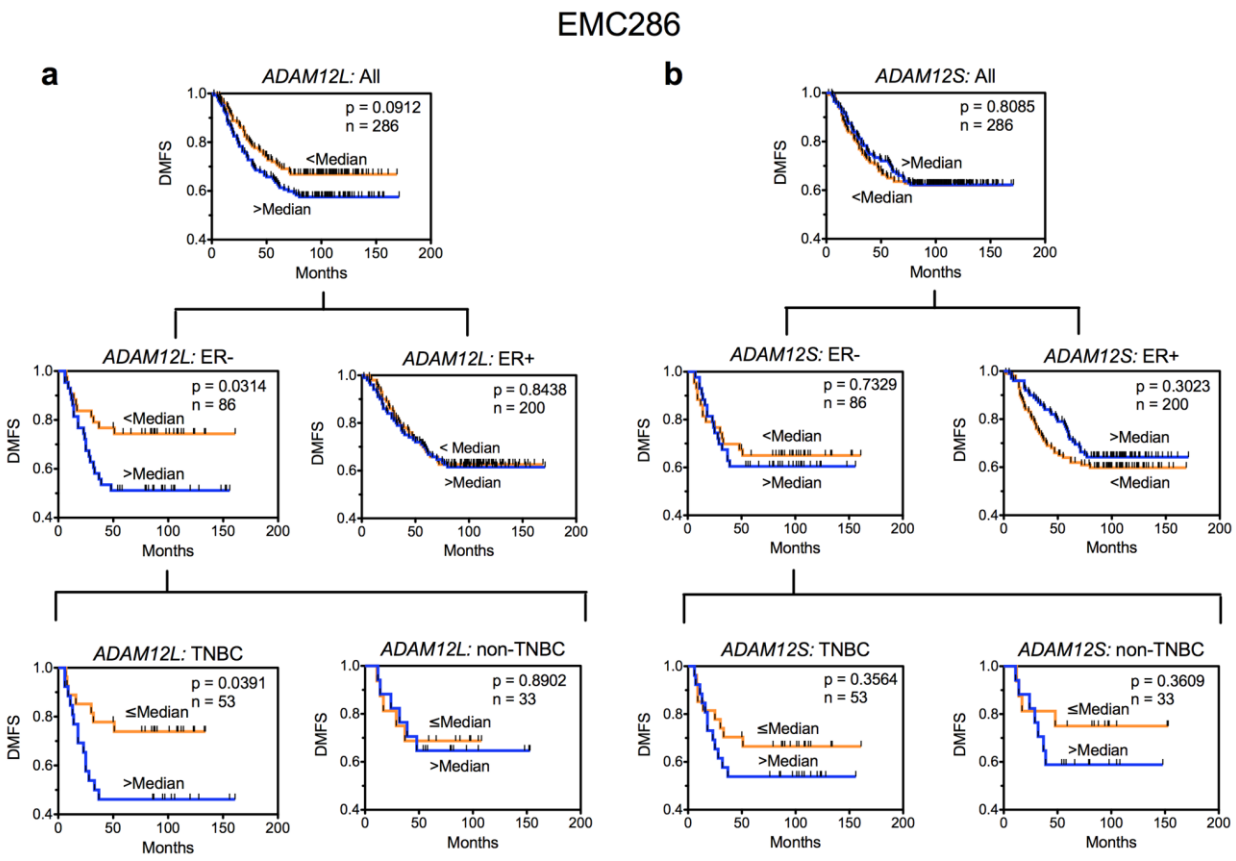

Figure 4.2 High expression of ADAM12-L is associated with poor prognosis in TNBC patients from the EMC286 cohort

Kaplan-Meier analysis of distant metastasis-free survival fractions for all patients (top), patients with ER-negative or ER-positive tumors (middle), and patients with TNBC or ER-negative non-TNBC (bottom). Patients were rank-ordered according to the expression of ADAM12-L (a) or ADAM12-S (b) and divided into two groups with mRNA expression levels below or above the median values.

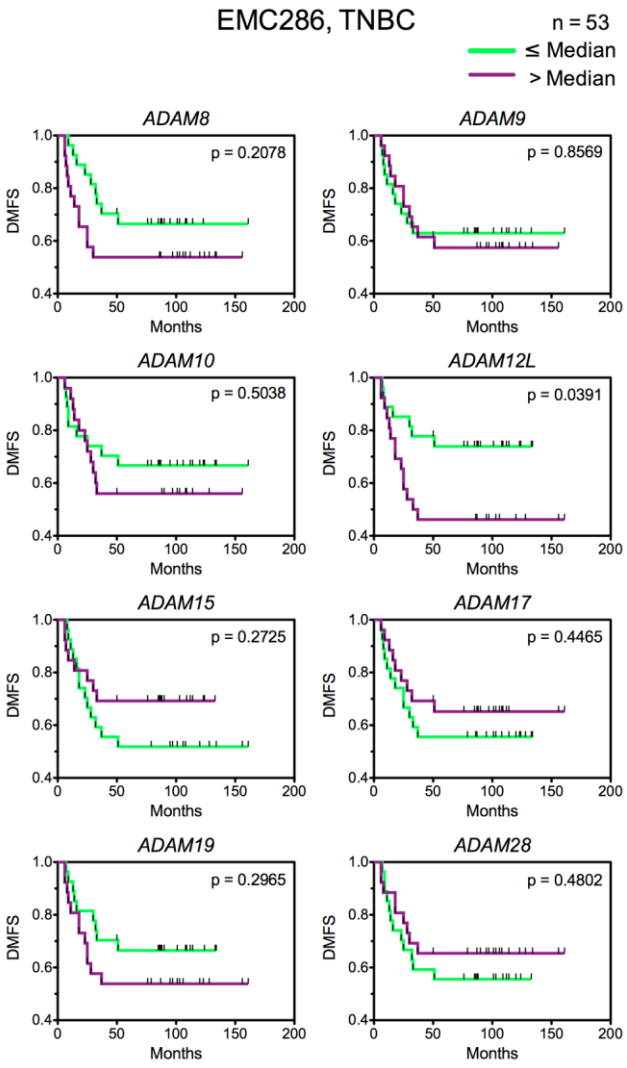

Figure 4.3 The prognostic value of ADAM12-L in TNBCs from the EMC286 dataset is the highest among other ADAMs encoding membrane-anchored, catalytically-active ADAM proteases

Kaplan-Meier plots of distant metastasis-free survival fractions for TNBC patients from the EMC286 cohort are shown.

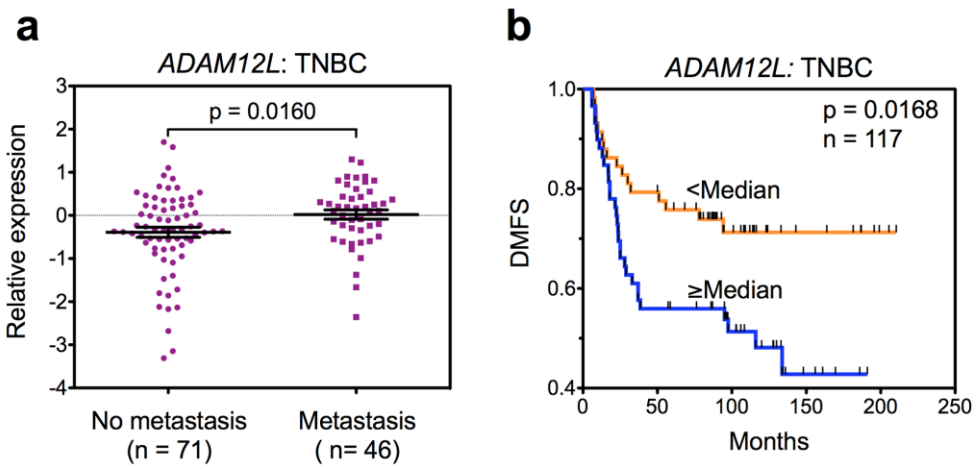

Figure 4.4 High expression of ADAM12-L is associated with poor prognosis in a combined set of node-negative TNBCs without chemotherapy

Gene expression profiles obtained in four independent studies (GEO accession numbers GSE2034, GSE5327, GSE7390, and GSE11121) were merged, as described in Methods. (a) Log_2-transformed, median-centered ADAM12-L expression values in TNBC patients without vs with distant metastasis. Mean expression values ± SEM are indicated. (b) Kaplan-Meier plots of distant metastasis-free survival fractions are shown.

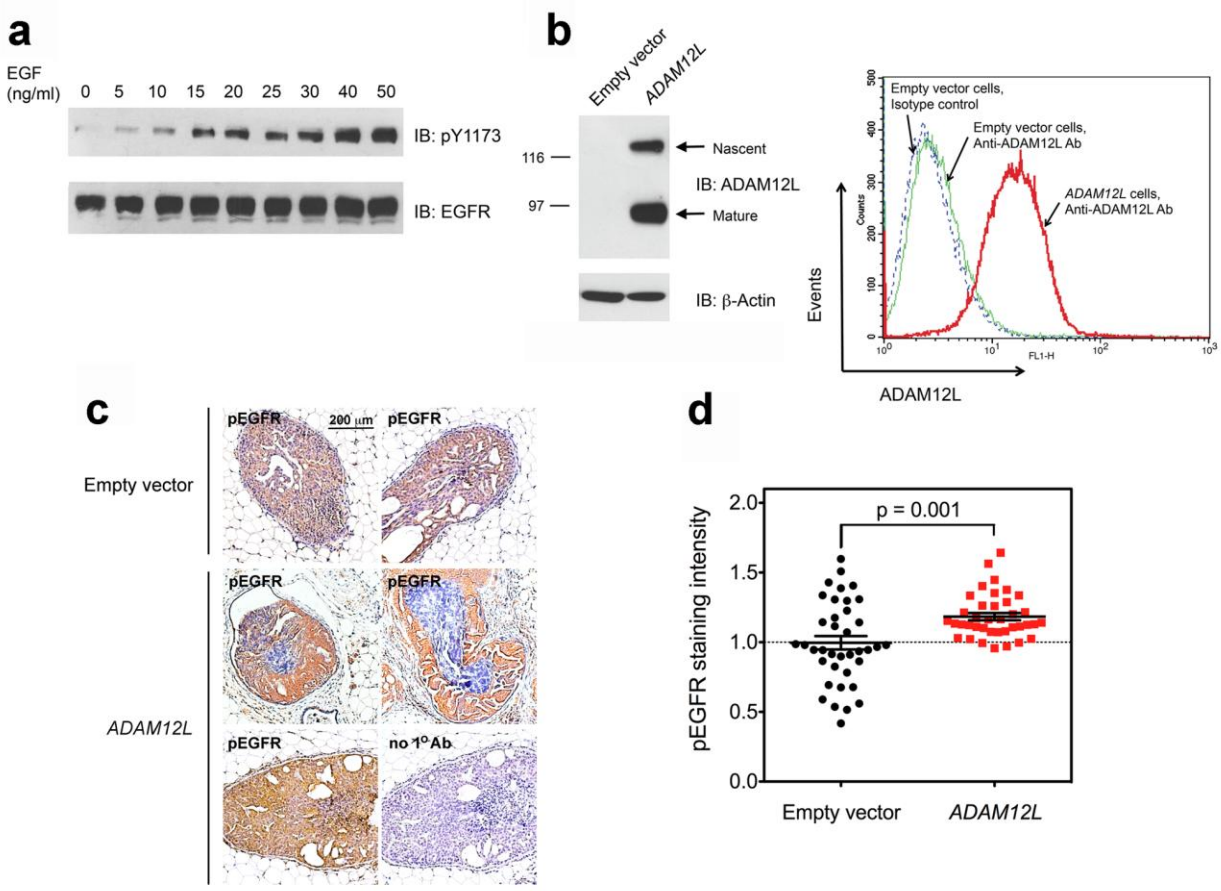

Figure 4.5 Increased expression of ADAM12-L augments EGFR phosphorylation in a mouse-intraductal (MIND) xenograft model of basal breast cancer

(a) Detection of a functional EGFR in MCF10DCIS.com cells. Cells were serum-starved for 16 h and then incubated for 30 min with indicated concentrations of EGF. The extent of EGFR phosphorylation (pY1173) was examined by Western blotting. (b) Stable expression of ADAM12-L in MCF10DCIS.com cells. Cells stably transduced with ADAM12-L or with empty vector were analyzed by Western blotting using an antibody against the cytoplasmic tail of ADAM12-L (left). The nascent form represents the full-length, catalytically inactive, intracellular form of ADAM12-L. The mature form represents ADAM12-L lacking its N-terminal pro-domain, which is catalytically active and resides predominantly at the cell surface. Cell surface localization of the mature form of ADAM12-L was confirmed by flow cytometry after staining of live cells with an antibody recognizing the extracellular domain of ADAM12-L. (c) Immunohistochemical detection of phosphorylated EGFR in mouse intraductal xenografts. MCF10DCIS.com cells stably transduced with ADAM12-L or with empty vector were injected into mammary ducts of NSG mice. Six weeks after injection, paraffin-embedded mammary tissue sections were stained with anti-phospho-EGFR (Y1173) antibody, visualized with DAB (brown), and counterstained with hematoxylin (blue). Four representative images are shown in the top and middle rows, respectively. The specificity of staining was confirmed by incubation of duplicate sections with or without primary antibody (bottom row). (d) Comparison of anti-phospho-EGFR staining intensities in intraductal xenografts of MCF10DCIS.com cells stably

transduced with empty vector or ADAM12-L. For each cell type, 38 tissue sections from three different mice were analyzed. Quantification was performed as described in Methods. All staining intensity values (in arbitrary units) were normalized to the mean value obtained for cells transduced with empty vector.

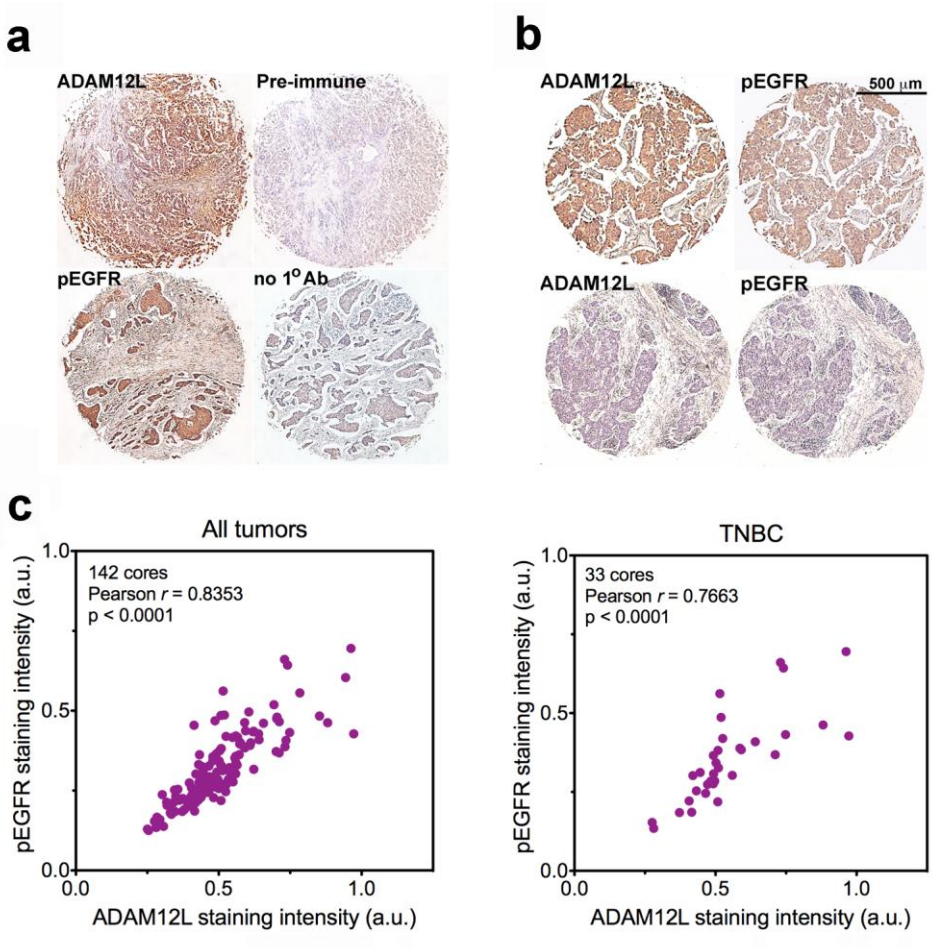

Figure 4.6 Positive correlation between the level of ADAM12-L expression and the extent of EGFR phosphorylation in human breast cancer tissue microarrays

(a) Validation of the specificities of the antibodies used for IHC staining of tissue microarrays. Two cores of the same tumor were stained with anti-ADAM12-L antibody or with pre-immune serum (top). Similarly, two cores of the same tumor were stained with anti-pEGFR (Y1173) or with the secondary antibody only (bottom). Positive staining was observed mostly in epithelial cells, with much weaker staining in the stromal compartment. (b) Two examples of duplicate sections in which epithelial cells stained strongly (top) or weakly (bottom) for both ADAM12-L and pEGFR. (c) Correlation analysis of ADAM12-L staining versus pEGFR staining intensities in 142 cores, including 33 cores of TNBC. Staining intensities (in arbitrary units) were quantified as described in Methods.

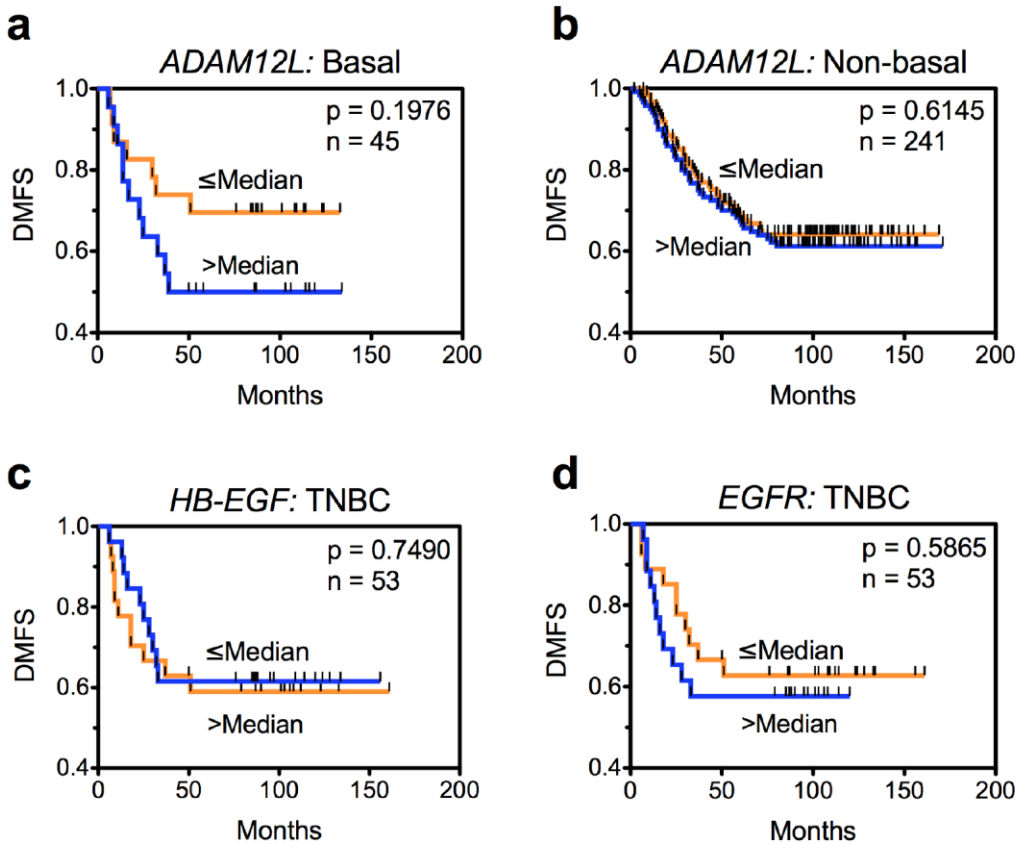

Figure 4.7 Kaplan-Meier survival curves based on median cutoffs for *ADAM12-L*, *HB-EGF*, and *EGFR*

Kaplan-Meier survival curves based on below-the-median and above-the-median *ADAM12-L* expression are shown for patients with basal (a) and non-basal tumors (b) from the EMC286 cohort. Tumors were classified into the basal subtype according to Harrell et al. (2012) Breast Cancer Res Treat 132(2):523-535. (c, d) Kaplan-Meier plots based on below-the-median and above-the-median HB-EGF (c) and EGFR (d) expression levels in TNBCs from the EMC286 cohort.

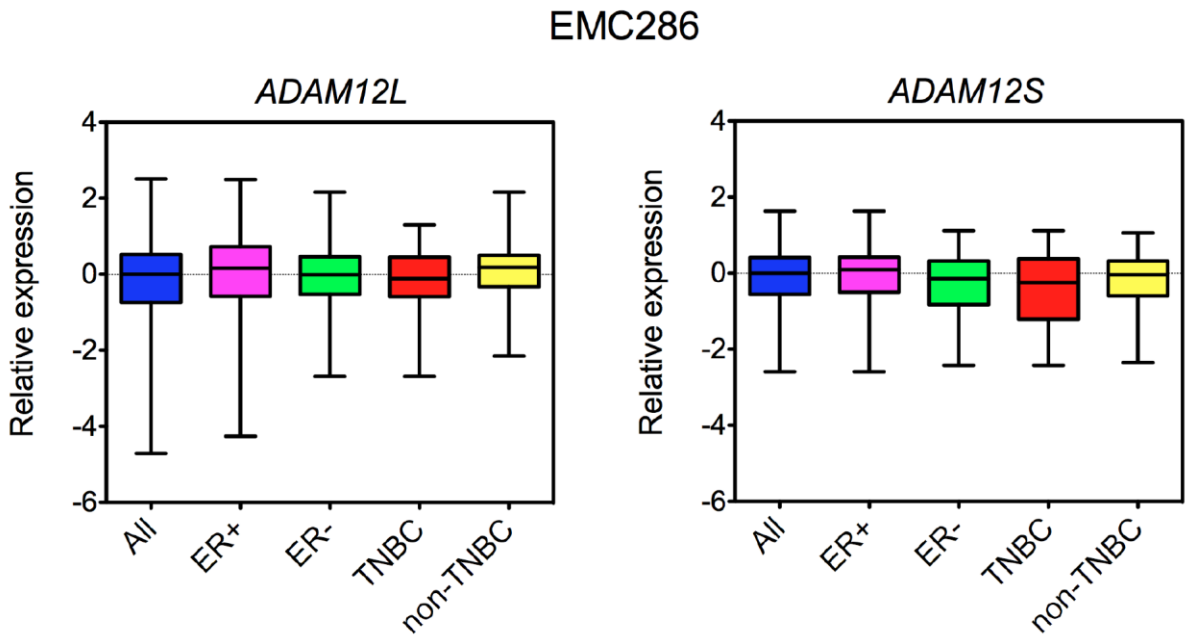

Figure 4.8 Expression levels of *ADAM12-L* and *ADAM12-S* mRNA in breast tumors from the EMC286

All tumors were divided into ER-positive and ER-negative tumors, and the ER-negative group was further divided into TNBC and the remaining non-TNBC. Box-and-whisker plots of log_2-tranformed, median centered values are shown.

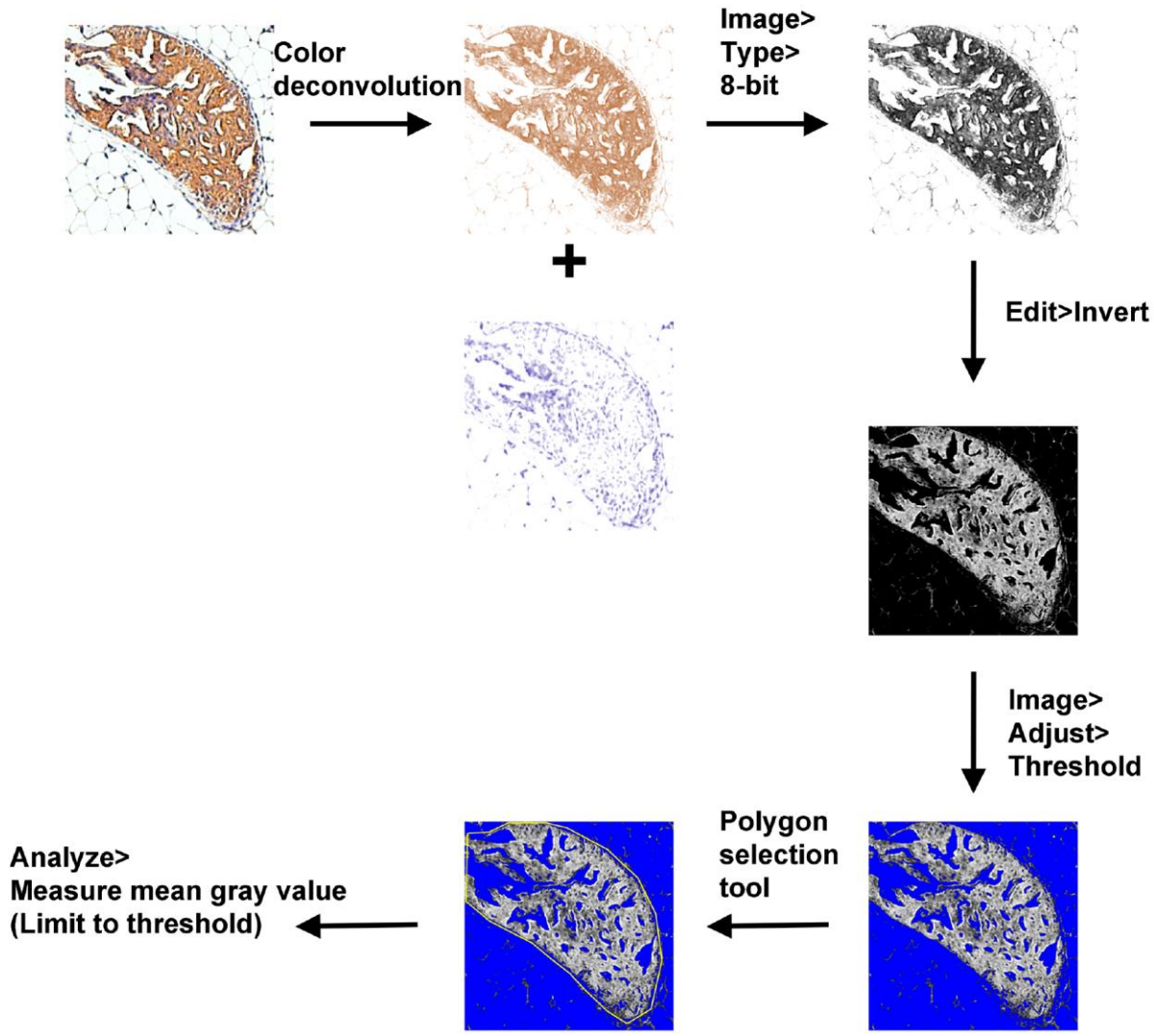

Figure 4.9 Flowchart of the procedure for quantification of the immunohistochemical staining

An example of an image showing pEGFR (DAB, brown) and nuclei (hematoxylin, blue) staining in a mouse xenograft is shown. The consecutive steps were performed using ImageJ software.

Table 4.1 Patient characteristics

	EMC286	Erasmus	TRANSBIG	Mainz
GEO Accession Number	GSE 2034	GSE5327	GSE7390	GSE11121
No. of patients	286	58	198	200
Age (y)				
Median	Unknown	Unknown	46	60
Range	Unknown	Unknown	24-60	34-89
T Stage				
T1	0	0	102	111
T2	0	0	96	81
T3/T4	0	0	0	8
Unknown	286	58	0	0
Tumor grade				
Grade 1	0	0	30	29
Grade 2	0	0	83	136
Grade 3	0	0	83	35
Unknown	286	58	2	0
Lymph node status				
Positive	0	0	0	0
Negative	286	58	198	200
Unknown	0	0	0	0
ER status				
Positive	209	0	134	156
Negative	77	58	64	44
Unknown	0	0	0	0
PR status				
Positive	0	0	0	130
Negative	0	0	0	70
Unknown	286	58	198	0
HER2 status				
Positive	0	0	0	0
Negative	0	0	0	0
Unknown	286	58	198	200
Endocrine Therapy	0	0	0	0
Chemotherapy	0	0	0	0
Median follow-up (y)	7.2	7.2	13.6	7.7
Distant metastasis	107	11	62	46
Reference	21	22	23	24

Table 4.2 Correlation analysis of ADAM12-L, EGF-like ligands, and EGFR in breast tumors from the EMC286 cohort. Values represent Pearson *r*

All

	EGF	**HB-*EGF***	***TGFα***	***AREG***	***BTC***	***EREG***	***EGFR***
ADAM12-L	-0.0525	0.0603	-0.0781	0.0432	-0.1097	0.0278	0.0067
	(P=0.3766)	(P=0.3095)	(P=0.1877)	(P=0.4463)	(P=0.0640)	(P=0.6392)	(P=0.9104)

ER+

	EGF	**HB-*EGF***	***TGFα***	***AREG***	***BTC***	***EREG***	***EGFR***
ADAM12-L	-0.0520	-0.0068	-0.1431	0.0019	-0.1141	0.0258	0.0203
	(P=0.4646)	(P=0.9243)	(P=0.0432)	(P=0.9784)	(P=0.1077)	(P=0.7174)	(P=0.7750)

ER-

	EGF	**HB-*EGF***	***TGFα***	***AREG***	***BTC***	***EREG***	***EGFR***
ADAM12-L	-0.08296	0.3038	-0.0214	0.1193	-0.0497	0.0006	0.1703
	(P=0.4476)	(P=0.0045)	(P=0.8446)	(P=0.2738)	(P=0.6493)	(P=0.9954)	(P=0.1703)

TNBC

	EGF	**HB-*EGF***	***TGFα***	***AREG***	***BTC***	***EREG***	***EGFR***
ADAM12-L	-0.1004	0.3632	0.0504	02246	-0.1060	-0.0276	0.2728
	(P=0.4744)	(P=0.0075)	(P=0.7202)	(P=0.1060)	(P=0.4500)	(P=0.8445)	(P=0.0481)

non-TNBC

	EGF	**HB-*EGF***	***TGFα***	***AREG***	***BTC***	***EREG***	***EGFR***
ADAM12-L	-0.1030	0.2593	-0.2398	0.0735	0.1051	0.1093	0.1751
	(P=0.5685)	(P=0.1450)	(P=0.1789)	(P=0.6843)	(P=0.5605)	(P=0.5448)	(P=0.3297)

Table 4.3 List of Affymetrix probes used to retrieve gene expression profiles

Gene	Affymetrix probe
ADAM8	205180_s_at
ADAM9	202381_at
ADAM10	202604_x_at
ADAM12-L	202952_s_at
ADAM12-S	204943_at
ADAM15	217007_s_at
ADAM17	205746_s_at
ADAM19	209765_at
ADAM28	205997_at
EGF	206254_at
HB-EGF	38037_at
TGFα	205016_at
AREG	205239_at
BTC	207326_at
EREG	205767_at
EGFR	201983_s_at

Chapter 5 - Final Conclusions

I have shown in this dissertation that the major *ADAM12* transcripts are differentially regulated in breast cancer by miRNAs. I have also demonstrated the existence of a novel *ADAM12* splice variant that encodes a protein isoform with a unique pro-domain that results in impaired trafficking of ADAM12 to the cell surface. Finally, I showed that the two major isoforms have distinct prognostic values in early stage TNBC. Collectively, these studies demonstrate that the different splice variants/protein isoforms of ADAM12 vary in their regulation of expression and their biological roles within breast cancer cells.

In Chapter 2, I determined that members of the miR-29 and miR-200 families selectively target the mRNA transcript encoding the transmembrane isoforms of ADAM12 causing mRNA degradation and reduced levels of ADAM12-L protein. The miR-29 and miR-200 miRNA families are important in breast tumor biology because they are involved in metastasis and tumor recurrence. The miR-200 family is a "master regulator" of the epithelial phenotype and loss of these miRNAs induces EMT [1]. Similarly, loss of miR-29 family members are associated with increased risk of metastasis [2]. Both of these miRNA families directly target the *ADAM12-L* transcript and cause degradation of the mRNA, whereas *ADAM12-S* transcript levels are unaffected. The selective regulation of ADAM12-L by miRNAs explains the highly dissimilar patterns of expression between these two isoforms (See Figure 2.1A,B and ref [3]).

However, regulation by miRNAs does not exclude the possibility that variant-specific regulation occurs during the splicing event as well. Thus far, the splicing mechanisms that are responsible for generating the *ADAM12-L* and *ADAM12-S* variants have not been elucidated, nor has any study conclusively shown regulation of these two variants by modulating splicing factors directly. A greater understanding of the molecular mechanisms involved in this particular splicing event and, perhaps, any regulation of these splicing factors/enhancers is critical to determining the major method of cellular regulation of the *ADAM12* variants. I have shown that loss of the miR-29 and miR-200 family members is, at least partially, responsible for the dramatic up-regulation of *ADAM12-L* in claudin-low cells lines and tumors. However, cellular splicing factors such as ESRP1, ESRP2 and Fox2 are differentially regulated across the different subtypes of breast cancer [4–7] and, therefore, the splicing event itself may also be regulated.

One of the interesting questions raised by the targeted regulation of *ADAM12-L* by miR-29 and miR-200 families is whether the association of ADAM12-L with claudin-low tumors, poor prognosis, and increased risk of metastasis is passive, or due to the loss of miR-29 and miR-200, or whether ADAM12-L is a driving force in breast tumor metastasis and recurrence. Assessing whether ADAM12-L is directly involved in tumor progression or if it serves as a marker for cells that have undergone EMT and/or the loss of miR-29 expression is critical to determining how to utilize ADAM12 in clinical applications.

In Chapter 3, I demonstrated the presence of a novel splice variant of *ADAM12* in breast epithelial and breast cancer cell lines. The new variant, *ADAM12-var1b*, is quite similar to the canonical long variant, *ADAM12-var1a*, and these two variants are indistinguishable in most common assays and in curated datasets like the Gene Expression Omnibus (GEO) and The Cancer Genome Atlas (TCGA). Many GEO studies were performed using microarrays and they recognize only the unique 3' regions of the *ADAM12-L* and *ADAM12-S* transcripts since these were the only known variants at the time. TCGA analyses include both microarray data and RNA-Seq data which may show the relative levels of exon 4a and exon 4b inclusion in total *ADAM12* transcripts. However, because these RNA-Seq sequence reads are short, usually 50-100 nt, and the distance between the exon 4 splicing event and the *ADAM12-L/ADAM12-S* splicing events is quite long, ~1700 nt, RNA-Seq will not be able to determine the relative abundance of all 4 splice variants. Yet, detailed analysis of the RNA-Seq raw data could provide information about the relative abundance of *ADAM12* transcripts that include exon 4a versus exon 4b in patient samples. Unfortunately, the cBioPortal for Cancer Genomics that I used to access and the TCGA data only reports gene level expression data, therefore, transcript-specific data and and raw sequence data could not be obtained. In Chapter 2, I analyzed the expression of the 2 major *ADAM12* variants, *ADAM12-L* and *ADAM12-S* in breast cancer cell lines, but because the original data were collected using microarray profiling, I could not assess the inclusion of exon 4b.

Interestingly, the inclusion of exon 4b in the *ADAM12-L* transcript generated a protein isoform, ADAM12-Lb, with unique properties. ADAM12-Lb is retained intracellularly, in the endoplasmic reticulum which often implies that a protein is misfolded. However, ADAM12-Lb is heavily glycosylated, does not interact with a number of major chaperone proteins and is not rapidly degraded. Therefore, ADAM12-Lb is most likely not grossly misfolded. Because it is

retained in the endoplasmic reticulum, ADAM12-Lb does not proceed to the Golgi apparatus and is not proteolytically processed to remove the pro-domain. Traditionally, ADAMs are considered active only once their pro-domains have been cleaved, however, some non-canonical methods of ADAM activation have been described [8–11]. Therefore, it is possible that ADAM12-Lb is active inside the lumen of the endoplasmic reticulum. Activation of ADAM12-Lb would require displacement of the pro-domain from the active site, presumably via an interaction with another endoplasmic reticulum lumenal protein that would pull the pro-domain away from the metalloprotease domain. To test for proteolytic activity, the potential activating conditions must be met, in addition to providing a suitable substrate. However, all of the currently known ADAM12-L substrates are localized at the cell surface. Another method of testing for proteolytic activity of ADAMs and the related matrix metalloproteases is using in gel zymography. In this technique a native PAGE gel is run with a substrate, such as gelatin, embedded in the polyacrylamide gel. The detergents are removed from the gel by soaking and the enzymes are allowed to cleave the gelatin during incubation in an appropriate buffer. Staining the gel with Coomassie brilliant blue will show voids where active proteases cleaved the gelatin substrate. Unfortunately, this method is not appropriate for studying ADAM12-Lb since the protein most likely requires an interactor to remove the autoinhibitory pro-domain from the active site. At this time, any potential activity of ADAM12-Lb and its role in the biology of breast cancer cells are unknown.

Another important portion of my analyses is the identification of the presence or absence of ADAM12-La and ADAM12-Lb in a number of breast cancer cell lines that express high levels of *ADAM12* mRNA. The goal of these investigations of the ADAM12-L isoforms in breast cancer cell lines was to determine which cell lines are most appropriate for studying the role of the different ADAM12-L isoforms. For example, the MDA-MB-231 cell line expresses high levels of the *ADAM12-L* transcript; however, it is mostly the *ADAM12-var1b*/ADAM12-Lb variant/isoform and should not be used to determine the cell surface roles of ADAM12-L in breast cancer. I determined that other cell lines, especially Hs578T and SUM159PT, express very high levels of ADAM12-L and that they almost exclusively express *ADAM12*-var1a/ADAM12-La. Therefore, these cell lines are more appropriate for investigating the cell surface role of ADAM12-L in breast cancer. The special considerations as to which cell line is

most appropriate for the investigation of the ADAM12-L physiological roles are critically important when performing RNAi/knockdown studies.

In Chapter 4, I showed the importance of ADAM12-L in TNBC progression. ADAM12-L, but not ADAM12-S, has prognostic value in early stage TNBC patients, since patients with high ADAM12-L levels are more likely to develop metastases. Interestingly, ADAM12 is the only ADAM for which prognostic value exists in TNBCs. Since TNBCs rely on EGFR signaling, I assessed the relationship between ADAM12-L expression and EGFR activation in 142 tumor biopsy cores and determined that ADAM12-L expression strongly correlated with EGFR activation in patients. In a mouse xenograft model using cells exogenously expressing ADAM12-La or an empty vector, the tumors formed from the ADAM12-La-expressing cells also exhibited increased EGFR activation when compared to tumors formed from control cells. These data show that ADAM12-L, but not ADAM12-S, is important in TNBC progression and that ADAM12-L works to activate EGFR in tumors. Consequently, ADAM12-L may represent a good druggable target for the treatment of TNBC, or may be a good marker for selecting tumors that will respond to anti-EGFR therapies that have already made it to clinical trials and can be deployed more rapidly [12, 13]. Anti-EGFR therapy alone has failed to offer a clinical benefit in TNBC patients [14], and in metastatic TNBC patients who were treated with anti-EGFR therapy and chemotherapy, only 17% of patients responded well to therapy [12]. In cases where anti-EGFR therapy failed, the failure is presumably due to the tumor's lack of dependence on EGFR rather than failure of the drug to inhibit EGFR activity, since efficacy of the EGFR inhibition was verified according to study designs. Therefore, determining molecular markers that indicate which tumors rely upon EGFR signaling and, as a result, would benefit from anti-EGFR therapy, is an important step in generating effective therapies for TNBC tumors. ADAM12-L may be a good marker for tumors which are dependent on EGFR signaling and more studies should be done to assess this possibility.

Additionally, ADAM12-L may make a good target for direct therapeutic intervention in TNBCs and, potentially, claudin-low tumors. Both of these tumor subtypes have high rates of recurrence and metastasis as well as high expression of ADAM12-L. The two major options for directly targeting ADAM12-L would involve using a small molecule inhibitor (SMI) of the metalloprotease domain or using a monoclonal antibody (mAb). Both SMIs to the tyrosine kinase domain and mAbs have been utilized clinically to target HER2 and EGFR and therapies

of these types, i.e. trastuzubmab and lapatanib, are currently being used to treat the HER2+ and HER2-enriched subtypes of breast cancer.

An SMI would target ADAM12-L and ADAM12-S equally since the metalloprotease domain is identical between these two isoforms. The major benefit of SMIs over antibody therapies is ease of administration. Many SMIs are specifically designed to be orally dosed, which allows patients to self-administer. The major drawback to developing an SMI for ADAM12 is that the drug would most likely be ineffective in preventing the non-catalytic functions of the ADAM12 molecule. For example, stabilization of the TGFβ receptor does not require an active metalloprotease and would be uninhibited by this method of treatment [15].

A number of SMIs for ADAM12 currently exist, however, all of these seem to exhibit some non-specific targeting of other ADAM proteins [16]. This highlights one of the major problems with utilizing SMIs to target ADAM proteolytic activity, the high level of conservation of the ADAM metalloprotease active sites. Developing a specific inhibitor has proved challenging but not impossible, in the case of ADAM17, a number of specific inhibitors have been generated as potential drugs [17]. However, due to the high degree of structural and sequence similarity between the metalloprotease domains of ADAMs, it may be more promising to develop other therapies.

Using mAbs to target ADAM12 in breast cancer is also a potentially promising treatment option. Since the extracellular region of ADAM12-L and ADAM12-S are so similar in sequence and, presumably, structure, any mAb designed to target ADAM12-L will probably also target ADAM12-S. The major benefits to using mAbs to target ADAM12 is that they are quite specific and that mAbs are capable of blocking the types of protein-protein interactions that are important for non-proteolytic activities. This blocking may be accomplished directly by covering the regions on ADAM12 that interact with other proteins, like the TGFβ receptor, or by inducing ADAM12 internalization which diminishes the amount of ADAM12 available on the cell surface. Either way, the mAb is able to prevent more potential activities of ADAM12 in breast cancer cells than the SMI.

Some of the drawbacks to employing anti-ADAM12 mAbs as potential therapies stem from difficulties in generating good quality, high specificity antibodies with strong ADAM12 affinity. The selection of commercially available antibodies for biochemical analyses is poor and our lab generated our own antibody for such purposes. This poor selection may be due to

external factors such as low demand or poor quality control, or it may reflect that ADAM12 is a poor epitope or is too similar to other ADAMs to generate a specific antibody. However, a mAb that is suitable for flow cytometric analyses is available commercially. In our analyses, this antibody is specific for ADAM12 but we have only used it on breast cancer cells and not other cell types or in *in vivo* applications. Additionally, we have not tested if this antibody blocks the ADAM12 proteolytic activity or interactions between ADAM12 and other cellular proteins. Yet, this mAb indicates that it is possible to develop the kind of antibody required as a therapeutic, high specificity and high affinity to the extracellular portion of ADAM12. A lesser drawback is that mAb therapies need to be administered intravenously and will require visits to medical clinics for dosing. Since ADAM12 therapy is potentially beneficial in only the more aggressive subtypes of breast cancer, these patients will probably also be on chemotherapy and will need to visit medical clinics regularly for administering both treatments.

Both methods for targeting ADAM12 in breast cancer assume that ADAM12 plays an active role in tumor progression. In the event that ADAM12 emerges as a marker for BTICs but is not required for the survival and proliferation of these cells, it may still be worthy to investigate mAb targeting of ADAM12 as a treatment option. Recently, a new therapy, T-DM1, was approved by the FDA for the treatment of HER2+ tumors [18, 19]. This therapy is an antibody-drug conjugate (ADC) in which a drug that is too toxic for systemic use is conjugated to a mAb, in this case, trastuzumab. By conjugating the drug to the trastuzumab antibody, the drug is targeted only to HER2+ cells where the cytotoxic effects of the drug are concentrated, limiting the exposure of healthy cells to the chemotherapy. Similar to ADCs, radioimmunotherapies are being developed where a radionuclide is conjugated to the antibody to effectively deliver a continuous source of radiation directly to the targeted cell [20]. Both ADCs and radioimmunotherapies may be adapted to targeting ADAM12 in TNBC, claudin-low tumors or BTIC populations. ADC and radioimmunotherapy approaches can be also be used when the target molecule is both a marker and active in promoting tumor cell growth and survival. In the case of T-DM1, HER2 is known to be critical to the growth and progression of these tumors but is also useful as a targeting molecule and the clinical success of this therapy may result from both HER2 inhibition and effects of the cytotoxic drug. ADAM12 may represent a good candidate for this type antibody-conjugate therapy specifically for treating tumor subtypes like TNBC and claudin-low tumors that currently have no targeted therapies.

Considering all of these data and treatment options, I believe a biologic approach to targeting ADAM12 in breast cancer is feasible. This conclusion is predominantly due to the ability of mAbs to target both the proteolytic activity of ADAM12 and any non-catalytic roles ADAM12 may play in tumor development. SMIs may be helpful, but the fact that, even under treatment, cells may still have non-proteolytic ADAM12 activity is concerning, especially considering that the role of ADAM12 in stabilizing the TGFβ receptor could have negative effects on patient prognosis. Additionally, the possibility for increasing efficacy of anti-ADAM12 mAbs by conjugating to cytotoxic drugs or radionuclides makes this option more versatile and adjustable as additional information about ADAM12 and its role in breast cancers emerges.

References

1. Park S-M, Gaur AB, Lengyel E, Peter ME (2008) The miR-200 family determines the epithelial phenotype of cancer cells by targeting the E-cadherin repressors ZEB1 and ZEB2. Genes Dev 22:894–907. doi: 10.1101/gad.1640608

2. Chou J, Lin JH, Brenot A, et al. (2013) GATA3 suppresses metastasis and modulates the tumour microenvironment by regulating microRNA-29b expression. Nat Cell Biol 15:201–213. doi: 10.1038/ncb2672

3. Li H, Duhachek-Muggy S, Dubnicka S, Zolkiewska A (2013) Metalloproteinase-disintegrin ADAM12 is associated with a breast tumor-initiating cell phenotype. Breast Cancer Res Treat 139:691–703.

4. Lapuk A, Marr H, Jakkula L, et al. (2010) Exon-level microarray analyses identify alternative splicing programs in breast cancer. Mol Cancer Res 8:961–74. doi: 10.1158/1541-7786.MCR-09-0528

5. Warzecha CC, Shen S, Xing Y, Carstens RP (2009) The epithelial splicing factors ESRP1 and ESRP2 positively and negatively regulate diverse types of alternative splicing events. RNA Biol 6:546–562. doi: 10.4161/rna.6.5.9606

6. Horiguchi K, Sakamoto K, Koinuma D, et al. (2012) TGF-β drives epithelial-mesenchymal transition through δEF1-mediated downregulation of ESRP. Oncogene 31:3190–201. doi: 10.1038/onc.2011.493

7. Warzecha CC, Carstens RP (2012) Complex changes in alternative pre-mRNA splicing play a central role in the epithelial-to-mesenchymal transition (EMT). Semin Cancer Biol 22:417–27. doi: 10.1016/j.semcancer.2012.04.003

8. Scheller J, Chalaris A, Garbers C, Rose-John S (2011) ADAM17: a molecular switch to control inflammation and tissue regeneration. Trends Immunol 32:380–7. doi: 10.1016/j.it.2011.05.005

9. Capasso R, Sambri I, Cimmino A, et al. (2012) Homocysteinylated albumin promotes increased monocyte-endothelial cell adhesion and up-regulation of MCP1, Hsp60 and ADAM17. PLoS One 7:e31388. doi: 10.1371/journal.pone.0031388

10. Gonzales PE, Solomon A, Miller AB, et al. (2004) Inhibition of the tumor necrosis factor-alpha-converting enzyme by its pro domain. J Biol Chem 279:31638–45. doi: 10.1074/jbc.M401311200

11. Sørensen HP, Vivès RR, Manetopoulos C, et al. (2008) Heparan sulfate regulates ADAM12 through a molecular switch mechanism. J Biol Chem 283:31920–32. doi: 10.1074/jbc.M804113200

12. Carey L a, Rugo HS, Marcom PK, et al. (2012) TBCRC 001: randomized phase II study of cetuximab in combination with carboplatin in stage IV triple-negative breast cancer. J Clin Oncol 30:2615–23. doi: 10.1200/JCO.2010.34.5579

13. Nabholtz JM, Abrial C, Mouret-Reynier M a, et al. (2014) Multicentric neoadjuvant phase II study of panitumumab combined with an anthracycline/taxane-based chemotherapy in operable triple-negative breast cancer: identification of biologically defined signatures predicting treatment impact. Ann Oncol 25:1570–7. doi: 10.1093/annonc/mdu183

14. Baselga J, Albanell J, Ruiz A, et al. (2005) Phase II and tumor pharmacodynamic study of gefitinib in patients with advanced breast cancer. J Clin Oncol 23:5323–33. doi: 10.1200/JCO.2005.08.326

15. Atfi A, Dumont E, Colland F, et al. (2007) The disintegrin and metalloproteinase ADAM12 contributes to TGF-beta signaling through interaction with the type II receptor. J Cell Biol 178:201–208. doi: 10.1083/jcb.200612046

16. Nyren-Erickson EK, Jones JM, Srivastava DK, Mallik S (2013) A disintegrin and metalloproteinase-12 (ADAM12): function, roles in disease progression, and clinical implications. Biochim Biophys Acta 1830:4445–4455. doi: 10.1016/j.bbagen.2013.05.011

17. Arribas J, Esselens C (2009) ADAM17 as a therapeutic target in multiple diseases. Curr Pharm Des 15:2319–2335.

18. Teicher B a, Doroshow JH (2012) The promise of antibody-drug conjugates. N Engl J Med 367:1847–8. doi: 10.1056/NEJMe1211736

19. LoRusso PM, Weiss D, Guardino E, et al. (2011) Trastuzumab emtansine: a unique antibody-drug conjugate in development for human epidermal growth factor receptor 2-positive cancer. Clin Cancer Res 17:6437–47. doi: 10.1158/1078-0432.CCR-11-0762

20. Al-Ejeh F, Shi W, Miranda M, et al. (2013) Treatment of triple-negative breast cancer using anti-EGFR-directed radioimmunotherapy combined with radiosensitizing chemotherapy and PARP inhibitor. J Nucl Med 54:913–21. doi: 10.2967/jnumed.112.111534

Appendix A - Copyright Permissions

This appendix contains the copyright permissions required to include in this dissertation material that was previously published.

PLoS One Open Access Policy:

Open-Access License
No Permission Required

PLOS applies the Creative Commons Attribution (CC BY) license to all works we publish (read the human-readable summary or the full license legal code). Under the CC BY license, authors retain ownership of the copyright for their article, but authors allow anyone to download, reuse, reprint, modify, distribute, and/or copy articles in PLOS journals, so long as the original authors and source are cited. **No permission is required from the authors or the publishers.**

In most cases, appropriate attribution can be provided by simply citing the original article (e.g., Kaltenbach LS et al. (2007) Huntingtin Interacting Proteins Are Genetic Modifiers of Neurodegeneration. *PLOS Genet* 3(5): e82. doi:10.1371/journal.pgen.0030082). If the item you plan to reuse is not part of a published article (e.g., a featured issue image), then please indicate the originator of the work, and the volume, issue, and date of the journal in which the item appeared. For any reuse or redistribution of a work, you must also make clear the license terms under which the work was published.

Springer Copyright Information:

Copyright Information

For Authors

Submission of a manuscript implies: that the work described has not been published before (except in form of an abstract or as part of a published lecture, review or thesis); that it is not under consideration for publication elsewhere; that its publication has been approved by all co-authors, if any, as well as – tacitly or explicitly – by the responsible authorities at the institution where the work was carried out.

Author warrants (i) that he/she is the sole owner or has been authorized by any additional copyright owner to assign the right, (ii) that the article does not infringe any third party rights and no license from or payments to a third party is required to publish the article and (iii) that the article has not been previously published or licensed. The author signs for and accepts responsibility for releasing this material on behalf of any and all co-authors. Transfer of copyright to Springer (respective to owner if other than Springer) becomes effective if and when a Copyright Transfer Statement is signed or transferred electronically by the corresponding author. After submission of the Copyright Transfer Statement signed by the corresponding author, changes of authorship or in the order of the authors listed will not be accepted by Springer.

The copyright to this article, including any graphic elements therein (e.g. illustrations, charts, moving images), is assigned for good and valuable consideration to Springer effective if and when the article is accepted for publication and to the extent assignable if assignability is restricted for by applicable law or regulations (e.g. for U.S. government or crown employees).

The copyright assignment includes without limitation the exclusive, assignable and sublicensable right, unlimited in time and territory, to reproduce, publish, distribute, transmit, make available and store the article, including abstracts thereof, in all forms of media of expression now known or developed in the future, including pre- and reprints, translations, photographic reproductions and microform. Springer may use the article in whole or in part in electronic form, such as use in databases or data networks for display, print or download to stationary or portable devices. This includes interactive and multimedia use and the right to alter the article to the extent necessary for such use.

Authors may self-archive the Author's accepted manuscript of their articles on their own websites. Authors may also deposit this version of the article in any repository, provided it is only made publicly available 12 months after official publication or later. He/she may not use the publisher's version (the final article), which is posted on SpringerLink and other Springer websites, for the purpose of self-archiving or deposit. Furthermore, the Author may only post his/her version provided acknowledgement is given to the original source of publication and a